SOME INVESTIGATIONS OF THE NITRIC OXIDE AFTERGLOW

A thesis
submitted for
the degree of
MASTER OF SCIENCE
in the
UNIVERSITY OF LONDON

by

Bryan Edward Smith, B.Sc. (Wales).

Northern Polytechnic,
London, N.7.

January
1962

CONTENTS

ABSTRACT

The nitric oxide afterglow of a low pressure pulsed, R.F., glow discharge in nitrogen with small admixtures of oxygen has been investigated. An oxygen inlet system was devised, and added to the discharge tube vacuum system used by Mr. J. Sutherland. A technique was developed for obtaining a uniform mixture of nitrogen with $\sim$ 0.1% of oxygen.

Individual bands of the afterglow spectrum were studied, and it was found that all the observed bands decayed exponentially with time. The decay constant of the nitrogen afterglow was greater than that of the nitric oxide $v^1 = 0$, γ bands; and the $v^1 = 0$, γ band decay constant was 15% larger than that of the $v^1 = 0$ β bands. The relative intensity of $v^1 = 0$, β and γ bands was unchanged when up to 0.15% of oxygen was added to the nitrogen.

The variation of the intensity and decay rate of the afterglow bands with oxygen added was consistent with the source of the nitric oxide afterglow being,

$$N + O + M \rightarrow NO^* + M$$

$$NO^* \rightarrow NO + h\nu \text{ (nitric oxide } \beta \text{ or } \gamma \text{ band photon)}$$

where M is an inactive particle. The rate constant for the combination of nitrogen and oxygen atoms was estimated to be $(1.3 \pm 0.5) \times 10^{-32}$ $cc^2\ mol^{-2}\ sec^{-1}$. The rate constant for $N + O_2 \rightarrow NO + O$ was $(1.4 \pm 0.3) \times 10^{-15}$ $cc\ mol^{-1} sec^{-1}$ in the glow discharge, and was $\sim 2 \times 10^{-16}$ $cc\ mol^{-1} sec^{-1}$ in the afterglow. The average intensity

of nitrogen afterglow bands corresponded to about 0.2% nitrogen atoms in the glow discharge. This was consistent with the other measurements. There was evidence that the rate of attachment of oxygen atoms to the walls of the system was proportional to the amount of oxygen added in the range of oxygen concentrations studied.

ACKNOWLEDGEMENTS

I wish to thank the Governing Body of the Northern Polytechnic for a Research Assistantship which enabled me to carry out this work.

For the encouragement, and thoughtful advice given by my supervisor Dr. M.E. Pillow at all stages of the research, I am most grateful. I would also like to thank Mr. J. Sutherland for his interest in this work.

To the departmental technicians, and to Mr. K. Pike of the glass shop, my gratitude is due for much invaluable assistance.

I wish to thank Miss A.E. Ramster for help with the proof reading.

A.E.R.E. Harwell were especially helpful in allowing me leave of absence, and financial assistance with the later stages of this work.

SUMMARY

The aim of the work was to study the decay with time, and the intensity of individual emission bands of the afterglow spectrum of nitrogen with small admixtures of oxygen. Most of the work was concentrated on the bands of the nitric oxide afterglow. Active nitrogen was produced by pulses of R.F. current through nitrogen at about 1 mm Hg pressure, drawn from a reservoir of B.O.C. 'spec-pure' nitrogen. The R.F. discharge tube, which was evacuable to 10^{-5} mm Hg base pressure, had external electrodes and a quartz window. The afterglow was yellow in appearance, when no oxygen had been added; and its spectrum contained the 1st positive bands of the nitrogen afterglow, and the nitric oxide afterglow β and δ bands. Individual bands of the afterglow spectrum were selected using a monochromator; and the decay of their intensity with time was recorded using a photomultiplier, and a Brown Recorder. It was found that the strongest afterglows were visible for about 20 seconds in a dark room.

A shutter shielded the monochromator entrance slit from the light of the R.F. glow discharge, but opened at the end of each R.F. glow discharge pulse. The measured afterglow intensities correspond to the intensity recorded a short time, Δt, after the shutter opened. In practise the afterglow intensity varied from pulse to pulse in a random manner; and it was necessary to run the discharge cycle for more than half an hour to reduce this random variation to a minimum before making any measurements.

Two procedures were used to obtain a uniform mixture of a small percentage of oxygen with nitrogen in the discharge tube vacuum system.

In the first method oxygen was admitted to the evacuated system to a pressure of the order of 10^{-4} mm Hg, and nitrogen was then admitted to about 1 mm Hg pressure. Using this procedure, the afterglow bands of part of the 1st positive system of nitrogen, and some nitric oxide β and γ bands were recorded. The decay with time of the afterglow intensity of the observed nitrogen 1st positive, and nitric oxide β and γ bands was exponential down to the lowest observable intensities. For example :-

$$R_{NO} = \frac{-\,d \log It2363}{dt} \neq \text{function of time,}$$

$$\text{similarly } R_{N_2} = \frac{-\,d \log It5755}{dt} \neq \text{function of time;}$$

where It2363 is the afterglow intensity of the γ (0,1) nitric oxide band at time t seconds after the shutter opened, and It5755 is the corresponding integrated intensity of the (10,6), (11,7) and (12,8) bands of the nitrogen 1st positive system. In general R_{N_2} and R_{NO} were of the order of unity, and R_{N_2} was larger than R_{NO}. It was deduced from the form of the decay with time of the observed afterglow bands that the active particles in the afterglow were removed mainly by attachment to the walls of the system. The values of R_{NO} for different $v^1 = 0$, β and γ bands of nitric oxide differed by 5% to 20% but in one particular run R_{NO} for the β bands

was 35% less and in another run 36% more than R_{NO} for the γ bands. This was probably due to adsorption or desorption of oxygen by the walls of the discharge tube during these runs.

In the alternative procedure, which was more satisfactory a specially devised pressure reducer was used to admit doses of 0.025% of oxygen to the nitrogen in the discharge tube vacuum system. Only the nitric oxide afterglow was studied using this procedure, and it was found that as in the previous method R_{NO} = constant independent of time. On average R_{NO} was 15% greater for the nitric oxide afterglow γ bands than for the nitric oxide afterglow β bands for all oxygen concentrations studied. However, this difference may have been due to some cyclic variation in the concentration of oxygen adsorbed on the walls of the system.

There was a slight increase in R_{NO} with added oxygen e.g. for the $\gamma(0,3)$ nitric oxide band $\frac{dR_{NO}}{dn_3} = 3.8 \times 10^{-16}$ mol^{-1}cc sec^{-1}, where n_3 is the number of oxygen molecules per cc of nitrogen.

It was found that there was no change in the relative intensity of the $v^1 = 0$, β and γ nitric oxide afterglow bands with added oxygen up to 0.15%, the largest amount added. Bands from higher levels were in general much weaker, and were not studied. For the $v^1 = 0$, β and γ bands it was found that the mean variation of (afterglow intensity)$^{-\frac{1}{2}}$ was given by $Ip^{-\frac{1}{2}} = E + Fn_3$ where E and F are constants. In fact there was a small oscillation about this mean variation. For the observed $v^1 = 0$ β and γ bands,

$I_{op}^{\frac{1}{2}} \cdot \frac{dI_p^{-\frac{1}{2}}}{dn_3}$ was about 4×10^{-14} mol^{-1}, the values lying within $\pm$ 5%. I_{op} is the afterglow intensity of an individual band, when no oxygen was added i.e. $n_3 = 0$.

Using the monochromator and photomultiplier system, the intensities of the R.F. glow discharge bands, as well as the afterglows, were recorded for some nitric oxide bands. It was found that the intensity of each band decayed very rapidly for the first 0.1 seconds, 0.2 seconds after the end of the R.F. pulse, and then decayed exponentially at a slower rate. The maximum glow intensity was about 10% greater than the initial intensity of the slow afterglow; and the initial intensity of the slow afterglow was about 10% greater than the afterglow intensity, measured using a shutter.

Using a tungsten lamp, the optical and recording system was calibrated in photons sec^{-1} generated per cc of discharge tube. It was found that

$$K5000 = \frac{\left(\begin{array}{l}\text{Intensity in photons } cc^{-1}sec^{-1} \text{ in discharge tube} \\ \text{corresponding to wavelength range 4925 Å to 5075 Å.}\end{array}\right)}{\left(\begin{array}{l}\text{Corresponding deflection of Brown Recorder in chart} \\ \text{divisions } (R_2), \text{ (Monochromator entrance slit 0.005 cm,} \\ \text{exit slit 0.06 cm.)}\end{array}\right)}$$

$$= (6.7 \pm 5) \times 10^{11} = (7 \pm 5) \times 10^{11} \text{ photons } cc^{-1}sec^{-1}div^{-1}.$$

Using published data it was estimated that $I_{N_2} = 1.2$ K5000. I5755. By measurement it was found that $I_{NO} = 0.1$ K5000 I2363. From the value of K5000 it was calculated that about 0.1% of nitrogen molecules were dissociated into atoms in the glow discharge.

According to the accepted theories the energy of the nitrogen

afterglow is derived from the three body recombination of nitrogen atoms; and the source of the nitric oxide afterglow is the combination of nitrogen and oxygen atoms in collision with a third inactive particle,

$$N + O + M \rightarrow NO^{*} + M$$

$$NO^{*} \rightarrow NO + h\nu \ (\beta, \gamma \text{ nitric oxide band photons}).$$

On the basis of these reactions and others, expressions have been derived in the present work for the initial intensity of the nitrogen, and nitric oxide afterglows. These expressions are consistent with the result, and used in conjunction with them indicate that the rate constant for the combination of nitrogen and oxygen atoms in collision with a third body is $(1.3 \pm 0.5) \times 10^{-32}$ cc^2 mol^{-2} sec^{-1}.

This is in fair agreement with the value 5×10^{-33} cc^{2}mol^{-2}sec^{-1} obtained by P. Harteck et al ('Progress in Reaction Kinetics', Pergamon Press, 1961).

It is assumed in the discussion of the results, that the nitrogen and nitric oxide afterglow intensity is reduced by the addition of oxygen, due to the reactions $N + O_2 \rightarrow NO + O$ and $N + NO \rightarrow N_2 + O$. The rate constant for the first reaction is estimated to be $(1.4 \pm 0.3) \times 10^{-15}$ cc.mol^{-1}sec^{-1} in the glow discharge and to be $\sim 2 \times 10^{-16}$ cc mol^{-1}sec^{-1} in the afterglow. According to the formula given by Kistiakowsky (1957) the value of this rate constant is about 2×10^{-16} cc mol^{-1}sec^{-1} at room temperature. The values of the calculated rate constants, and the values of R_{NO} and R_{N_2} were reasonably consistent with the 0.2% nitrogen atom concentration calculated from the value of K5000.

There was some evidence for the rate of attachment of oxygen atoms to the walls of the system being proportional to the amount of oxygen added to the system.

INTRODUCTION

1.1 Note on Atomic and Molecular Spectra.

1.1.1 Atomic Spectra.

If an electric current is passed through an atomic gas, and the light emitted is resolved into a range of wavelengths, i.e. a spectrum of wavelengths, by a prism, a pattern of lines is observed. The wavelength of the lines depends only on the nature of the substance, though the intensity of different lines may depend on the conditions. Such a pattern of lines is known as an atomic spectrum. According to the quantum theory the atomic line spectrum is due to transition of the outer electrons of an atom from one specified energy level to another specified energy level. Only some transitions are allowed. Thus only certain wavelengths, defining certain energies, appear in the atomic spectrum.

According to the quantum theory explanation of atomic spectra, each electron can be described by the following quantum numbers.

1. PRINCIPAL QUANTUM NUMBER n determines the magnitude or scale of the electron orbit.
2. AZIMUTHAL QUANTUM NUMBER l determines the orbital angular momentum. l is allowed values n-1, n-2 down to 0. Electrons corresponding to l = 0,1,2,3, etc. are called s,p,d,f electrons.
3. MAGNETIC QUANTUM NUMBER M_l determines the component

of angular momentum along a magnetic field.

$M_l = l, l-1, \quad -2 \text{ --------}, \quad -l$. Thus $2l + 1$ states correspond to a given value of l, i.e. the multiplicity $= 2l + 1$.

4. SPIN QUANTUM NUMBER M_s. $M_s = \pm \frac{1}{2}$. M_s determines the angular momentum of the electron due to its spinning motion. Normally the quantum numbers of individual electrons combine to give a resultant L. Similarly the spins combine to give a resultant S. States corresponding to L = 0, 1, 2, 3 etc. are known as S, P, D, F states. The multiplicity = 2 S + 1 if $L \geq S$ and = 2 L + 1 if $L < S$, because L and S combine to form a resultant J which takes values L + S, L + S - 1, ---- L - S. To describe an atomic state the following symbol is used. $(2S + 1)L_J$ e.g. a $^4D_{\frac{5}{2}}$ state has multiplicity 4, thus $S = 1\frac{1}{2}$, also L = 2 and $J = \frac{5}{2}$.

1.1.2 Molecular Spectra (Diatomic Molecules).

In the case of molecules the spectrum is not a series of lines but is usually a series of broad bands. If an individual band is examined by an instrument of high resolving power, it can be seen that each band is made up of fine lines. According to theory a molecule possesses energy of rotation and vibration in addition to that possessed by an atom. Changes in rotational energy alone are ~ 100 cm^{-1} while vibrational energy changes are ~ 1000 cm^{-1}.

The region of the spectrum in which a band system occurs is determined by the electronic transition; the distribution of bands in the system depends on vibrational energy changes, and the fine line structure depends on changes in rotational energy. The transitions are governed by specified changes in the molecular quantum numbers.

The energy of a molecule can be expressed as follows

$$E = E_e + E_v + E_r$$

= Electronic Energy	+ Vibrational Energy of Nuclei about equilibrium position.	+ Rotational Energy about centre of gravity of system.

The energy states of a diatomic molecule are determined by the following quantum numbers.

1. Λ determines the component of orbital angular momentum along the internuclear axis. States corresponding to Λ = 0,1,2,3 are known as $\Sigma, \Pi, \Delta, \phi$ states.
2. SPIN QUANTUM NUMBER, Σ, determines the component of spin momentum S along the internuclear axis. The multiplicity is 2S + 1.
3. $\Omega = \Lambda + \Sigma$ = resultant momentum vector along the internuclear axis.

   The symbol describing molecular states is $^{(2S+1)}\Lambda_\Omega$

   e.g. $^3\Pi_2$ has triplet multiplicity (S = 1), Λ = 1, Σ = 1.

   Transitions from one vibrational level to another are

normally described as (v^1, v^{11}) transitions, e.g. (0,2) where the vibrational level of the upper state was the zero one, and the lower vibrational level was the 2nd one of the lower state.

If the electronic eigenfunction of a homonuclear molecule is unaltered by reflection at the origin it is a gerade (g) state; if it is altered it is an ungerade (u) state.

For a transition to have a high probability, the following selection rules must be obeyed, where Δ denotes the change in a quantum number.

$$\Delta\Omega = 0, \pm 1$$
$$\Delta\Lambda = 0, \pm 1$$
$$\Delta S = 0, \text{ Weak } \Delta S = \pm 1$$

There are other selection rules connected with the symmetry of molecular states which will not be dealt with in this short account.

1.1.3 Interaction of Unlike Atoms and Corresponding Molecular States.

When two atoms 1 and 2 approach each other there is a strong field along the internuclear axis which splits L_1 into components

$|ML_1| = L_1, L_1 - 1, \ldots 0;$ and L_2 into components

$|ML_2| = L_2, L_2 - 1, \ldots 0.$

For the resulting molecule $\Lambda = |ML_1 + ML_2|$

and $S = S_1 + S_2, S_1 + S_2 - 1, \text{---} S_1 - S_2$

the multiplicity is 2S + 1.

Atomic States	Corresponding Molecular States
S + S	Σ
S + P	Σ , Π
S + D	Σ , Π , Δ

1.1.4 Selection Rules for Predissociation.

It is possible for a molecule in a stable electronic state of greater energy than the dissociation energy to radiate or to undergo a radiationless transition to an unstable state having the same energy, if such a state exists. If the molecule should undergo a radiationless transition to the unstable state and then dissociate, it is said to have undergone predissociation.

The selection rules are

$\Delta S = 0$ (strong), $\pm$ (weak)

$\Delta \Lambda = 0, \pm 1$

$\Delta J = 0, \Delta K = 0$ in restricted cases.

$\Delta \Omega = 0, \pm 1$ in restricted cases.

As in the case of transitions accompanied by radiation there are other selection rules connected with the symmetry of molecular states.

1.2 The Nitrogen Afterglow.

1.2.1 Introduction.

When an electrical current is passed through nitrogen at a low pressure, a pink glow is emitted from the nitrogen.

When the current is switched off an afterglow may be seen, its duration and appearance depending on the gas purity and the condition of the walls of the discharge tube.

In 1865 Morren studied an afterglow in a nitrogen discharge tube. Using a condensed discharge in pure nitrogen the spectrum of the afterglow was found to be banded. When considerable traces of oxygen were present, the spectrum was observed to be continuous.

In 1900 Lewis found that a golden yellow afterglow remained for several seconds when a nitrogen discharge was switched off. Strutt discovered that the nitrogen associated with the afterglow had enhanced chemical activity and it came to be known as 'active nitrogen'. Strutt (1911) suggested that active nitrogen was atomic nitrogen. He observed that the deep yellow nitrogen afterglow was destroyed by oxygen and that a bluish white luminosity remained (1912) which he thought at the time to be due to the formation of nitric oxide, since adding a trace of nitric oxide gave the same effect.

The yellow afterglow in nominally pure nitrogen came to be known as the 'Lewis-Rayleigh' afterglow. This consists of bands of the 1st positive system of the nitrogen molecule, which corresponds to $B^3\Pi_g \rightarrow A^3\Sigma_u^+$ transitions. Usually the β and γ and sometimes δ ultra-violet bands of nitric oxide accompany the Lewis-Rayleigh afterglow owing to small traces of oxygen being present in the nitrogen. These bands constitute the 'nitric oxide afterglow'.

Since 1900 the properties of the Lewis-Rayleigh afterglow have been determined with increasing precision. Various theories explained some of the phenomena, though in some cases the observations on which they were based were invalid. In the last ten years much evidence has been obtained to show that the energy of active nitrogen is almost entirely due to the presence of ground state (^4S) nitrogen atoms. Also there is much experimental evidence to support the currently accepted mechanism of the nitric oxide afterglow.

1.2.2 The Intensity and Decay of the Nitrogen Afterglow.

The intensity of the nitrogen afterglow is proportional to the square of the concentration of active nitrogen, Bonhoeffer and Kaminsky (1926); and is also proportional to the total gas pressure, Rayleigh (1940). The decay rate of the nitrogen afterglow has its minimum value, when the containing walls are coated with metaphosphoric acid; and the form of the intensity decay indicates that it is due to a chemical reaction of the form $A + B \rightarrow AB$, Rayleigh (1935). Kneser (1928) concluded from the decay rate of the afterglow, that the energy of the afterglow was derived from triple collisions of two nitrogen atoms, and an inactive particle.

Easson and Armour (1927 - 1928) observed that active nitrogen excited the 1850 Å line of iodine vapour. The energy required to dissociate the iodine molecule and excite this line is 8.4 volts. Taking 8.4 volts as being just less

than the dissociation energy of the nitrogen molecule the observation of the 1850 Å line suggested that active nitrogen is atomic nitrogen. However the dissociation energy of the nitrogen molecule was not known to be 9.76 e.v., and values ranging from 7 e.v. to 11 e.v. were postulated by different workers.

1.2.3 The Carlo-Kaplan Theory.

The afterglow intensity distribution of the 1st positive bands of nitrogen differs from the normal glow discharge intensity distribution e.g. bands from the $v^1 = 12$ and $v^1 = 6$ levels of the $B^3\Pi_g$ state are especially prominent in the afterglow, and no bands are observed with v^1 greater than 12.

Kaplan (1929) had observed bands of nitrogen of excitation energy greater than the accepted value of the dissociation energy of the nitrogen molecule. This was taken as evidence for the presence of 8 e.v. metastable molecules in active nitrogen.

Carlo and Kaplan (1929) thus accounted for the enhanced intensity of the $v^1 = 12$ and $v^1 = 6$ bands of the nitrogen afterglow as follows. Active nitrogen contains metastable $A^3\Sigma_u^+$ molecules in the lowest vibrational level. These are excited to the $v^1 = 12$ and $v^1 = 6$ levels of the $B^3\Pi_g$ state by ^2P and ^2D nitrogen atoms respectively. The energy of the $v^1 = 12$ level is 9.76 e.v. above ground state and that of the $v^1 = 6$ level is 8.37 e.v.

$$N\,(^2P) + N_2\,(A^3\Sigma_u^+) \rightarrow N_2\,(B^3\Pi_g) + N\,(^4S)$$

$$3.56\ e.v. + 6.2\ e.v. \rightarrow 9.76\ e.v.$$

$$N\,(^2D) + N_2\,(A^3\Sigma_u^+) \rightarrow N_2\,(B^3\Pi_g) + N\,(^4S)$$

$$2.37\ e.v. + 6.2\ e.v. \rightarrow 8.37\ e.v.$$

$$N_2\,(B^3\Pi_g) \rightarrow N_2\,(A^3\Sigma_u^+) + h\nu$$

Herbert, Herzberg and Mills (1937) found no absorption at 1492 Å and 1742 Å by the ^2D and ^2P atomic states of nitrogen, and concluded that their concentration was at least 18 times less than the Carlo-Kaplan theory predicted.

1.2.4. Mitra's Theory.

In 1945 Mitra proposed that active nitrogen was positive ions of the nitrogen molecule in the N_2^+ (X^1) state). The following reactions were postulated to produce the afterglow.

$$N_2^+\,(X^1) + e + N_2 \rightarrow N_2\,(B^3\Pi_g) + N_2\,(A^3\Sigma_u^+)$$

$$N_2\,(B^3\Pi_g) \rightarrow N_2\,(A^3\Sigma_u^+) + h\nu$$

The first step accounted for the long life of the afterglow, and also for the ionisation associated with active nitrogen. The energy required for the 1st step in Mitra's mechanism is 15.85 e.v., since the energies of the $B^3\Pi_g$ and $A^3\Sigma_u$ states are 9.75 e.v. and 6.1 e.v. respectively. This was supported by Kenty and Turner's observation that 16.3 e.v. electrons were required for the production of active nitrogen.

Kaplan (1948) pointed out that Mitra's theory did not account for the spectrum of the auroral afterglow in which N_2 ions in the (X^1) state were known to be present.

Strong evidence against Mitra's Theory was obtained by Worley (1948) who failed to detect absorption by ground state nitrogen molecular ions in a column of glowing gas 15 metres long.

Also Benson (1952) found that the heat released by active nitrogen was sufficient to excite one molecule in 350 to 9.6 e.v., but microwave measurements gave only one free electron per 2.3×10^8 molecules.

1.2.5. The Dissociation Energy of the Nitrogen Molecule.

Van der Zeil (1937) observed weak predissociation (1.1.4) of the 1st positive system of nitrogen for bands with $v^1 > 11$. i.e. with excitation energies > 9.76 e.v. If the resulting nitrogen atoms were ground state atoms, i.e. 4_g atoms, then the dissociation energy of the nitrogen molecule would be 9.76 e.v. However, the predissociation was of a type known to be associated with $\Delta\Lambda = \pm 1$, Gaydon (1953), also both Λ doubling components were weakened. Van der Zeil concluded that a $^3\Delta$ state was predissociating the $B^3\Pi_g$ state.

Gaydon (1944) pointed out that a $^5\Sigma_g^+$ state could equally well predissociate the $B^3\Pi_g$ state, and the change in multiplicity corresponding to $S = 1$ would account for the weakness of the predissociation.

The 3 lowest states of the nitrogen atom are ^4S, with ^2D 2.382 e.v. higher, and ^2P 3.575 e.v. still higher. According to the correlation rules between atomic and molecular states (1.13) two ^4S nitrogen atoms can give rise to a $^5\Sigma_g^+$ state; and a ^4S

and a ^2D atom to a $^3\Delta$ state. According to Van der Zeil's explanation of the predissociation of the $B^3\Pi_g$ state the dissociation energy of nitrogen is 9.76 e.v. minus the excitation energy of the ^2D state, i.e. D (N_2) = 7.38 e.v. According to Gaydon the dissociation energy is 9.76 e.v.

1.2.6 Recent Evidence that Active Nitrogen is Mainly Ground State Nitrogen Atoms.

Carlo and Reineke (1949) showed that by assuming that two normal nitrogen atoms collide on a slightly stable $^5\Sigma_g^+$ potential curve, crossing the $B^3\Pi_g$, the selective enhancement of some bands in the nitrogen afterglow was explained. However, they could not account for the complete intensity distribution of bands in the nitrogen afterglow.

Jackson and Schiff (1955) investigated the products of a nitrogen discharge using a mass spectrometer. They found a 1% increase in the $\frac{M14}{M28}$ ratio with the discharge running, where M14 and M28 are the magnitudes of the mass 14 and mass 28 peaks respectively. Measurements were made of the current between two electrodes in the nitrogen for different potential differences between the electrodes i.e. the ionisation efficiency of the gas was measured. For argon, and for $\frac{M}{E}$ = 28, where M = mass of particle and where E is the ionic charge, the ionisation efficiency remained the same whether the discharge was on or not. However, the ionisation efficiency for $\frac{M}{E}$ = 14.

increased, when the discharge was actuated, and the appearance potential deduced from these observations corresponded to ionisation of ^4S atoms. Berkowitz, Chupka and Kistiakowsky (1956) examined the Lewis-Rayleigh afterglow with a mass spectrometer and a photomultiplier simultaneously. They found that the magnitude of the mass 14 peak increased by a factor of a 1000 when the discharge was actuated, and that the appearance potential for mass 14 was 14.8 e.v. in good agreement with the value for ^4S nitrogen atoms. ^2P and ^2D atoms were not detected and the upper limit of the concentration of metastable $A^3\Sigma_u^+$ and $a'\Pi g$ molecules was very small. They found that the afterglow intensity was proportional to $(M_{14})^2$ for all wavelength ranges investigated, where M_{14} is the magnitude of the mass 14 peak. Berkowitz, Chupka and Kistiakowsky proposed that the following reactions explain the nitrogen afterglow,

$$N + N + M \rightarrow N_2^{**} + M$$
$$N_2^{**} + M \rightarrow N + N + M$$
$$N_2^{**} + M \rightarrow N_2^{*} + M$$
$$N_2^{*} \rightarrow N_2^{1} + h\nu$$

Where the nitrogen atoms are ground state (^4S) nitrogen atoms; N_2^{**} is a $^5\Sigma_g^+$ nitrogen molecule, N_2^{*} is a $B^3\Pi g$ nitrogen molecule; N_2^1 is an $A^3\Sigma_u^+$ nitrogen molecule, and M is an inactive particle.

Assuming that the $^5\Sigma_g^+$ potential curve crossed the $B^3\Pi g$ level near $v' = 12$, then the enhancement of the intensity of

the 12th vibrational level is explained by collision induced transitions from $^5\Sigma_g^+$ to $B^3\Pi g$. Also, if the reaction $N_2^{**} + M \rightarrow N + N + M$ is faster than $N_2^{**} + M \rightarrow N_2 + M$, it would be competitive with the production of nitrogen afterglow photons. The energy for the reaction $N_2^{**} + M \rightarrow N + N + M$ is derived from the thermal energy of the nitrogen molecules involved, and since the dissociation energy of the $^5\Sigma_g^+$ state is small the rate of this reaction would increase appreciably with temperature. Thus assuming $N_2^{**} + M \rightarrow N + N + M$ is competitive with the afterglow, the decrease of afterglow intensity with increase in temperature is explained.

Bayes and Kistiakowsky (1960) measured the relative intensities of $B^3\Pi g \rightarrow A^3\Sigma_u^+$, and $Y \rightarrow B^3\Pi g$ nitrogen afterglow bands from 5000 Å to 11000 Å. They noted changes in the relative intensities of bands when the temperature was altered or foreign gases were added, and deduced 5 different kinetic origins for the different groups of bands. At low temperatures the highest populated levels of $B^3\Pi g$ and Y states tended to a limit about 850 cm^{-1} below the dissociation energy of the nitrogen molecule and they suggested that this was the dissociation energy of the $^5\Sigma_g^+$ state.

1.3 The Effect of Oxygen on the Intensity and Decay of the Nitrogen Afterglow.

1.3.1 Introduction.

The presence of small percentages of oxygen in a nitrogen

discharge has several effects depending on the actual concentration of O_2.

In very small amounts it causes an increase in the intensity of the nitrogen afterglow. As the oxygen concentration is increased the visible afterglow disappears and, when the percentage of oxygen is increased still further, a whitish continuum afterglow is observed known as the airglow.

1.3.2 Low Oxygen Content.

Tiede and Domke (1913) and (1914) purified nitrogen by passing it over hot copper and could not obtain an afterglow.

Strutt (1915) after some controversy with Tiede and Domke conceded that trace concentrations of many foreign gases increase the yield of active nitrogen. Rayleigh (1942) observed the effect of adding a small percentage of oxygen to a stream of active nitrogen flowing from a gas discharge tube. He noted that in some cases the intensity of the nitrogen afterglow rose 32 times and observed a time lag between the change in intensity of the gas and the change of gas composition. Because of the time lag he concluded that the action of oxygen was on the walls of the system.

Berkowitz, Chupka and Kistiakowsky (1956) observed that the afterglow intensity increased when the oxygen concentration was increased from 0.003% to 0.03%. They attributed this to deactivation of the walls by oxygen so reducing atomic recombination. However,

Kaufman and Kelso (1960) from studies of increased dissociation of oxygen by addition of nitrogen concluded that such catalytic effects were due to homogeneous gas phase reactions. The main discharge product was found to be nitric oxide in 90% yeild. They suggested that such reactions as $N + O_2^+ \rightarrow NO^+ + O$ and $NO^+ + e \rightarrow N + O$ were occurring.

Berkowitz et al (1956) also observed using their flow system, that, when the oxygen added to the stream of nitrogen was increased from 1.8% to 7%, the intensity of the afterglow decreased by a factor of about 5; and that plots of log I and log M_{14} vs oxygen added were straight lines with slopes in the ratio 1 to 2. I was the observed afterglow intensity and M_{14} was the magnitude of the mass 14 peak.

Kurzweg, Bass and Broida (1957) added oxygen to a stream of nitrogen flowing through a discharge tube. They found that the intensity of the nitrogen 1st positive system decreased by a factor of 10 when 5% of oxygen was added to the nitrogen, the total pressure being 1 mm Hg. The intensity of the nitric oxide β bands increased, when 1% of oxygen was added; but decreased to a value about 8 times less than the initial intensity, when up to 5% of oxygen was added to the nitrogen. It can be seen that there is quite good agreement between the results of Berkowitz et al and Kurzweg et al, both using flow systems.

Anderson, Kavadas, and McKay (1957) observed the decay of the afterglow intensity I with time over a period of about 50 seconds. They found that plots of $I^{-\frac{1}{2}}$ vs time were linear for about 20 seconds, and plots of log I vs time were linear after about 10 seconds. The slopes of the $I^{-\frac{1}{2}}$ vs time plots did not vary much with added oxygen until 0.3% of oxygen had been added. But the slope increased rapidly by a factor of about 15 between 0.3 and 0.4% of oxygen. They concluded that initially the oxygen added was depositing on the walls of the discharge tube and that chemical effects set in at 0.3% when oxygen started going into the volume.

Anderson, Kavadas and McKay in contrast to Berkowitz et al and Kurzweg et al did not use a flow system for their experiments. They made their observations using nitrogen added to the system from a reservoir at the start of each experiment. Although they were primarily interested in the decay of the nitrogen afterglow some information regarding the effect of oxygen on the initial intensity of the afterglow can be deduced from fig.7 of the above reference. This is summarised in the table below.

$I^{-\frac{1}{2}}$	I	Percentage Oxygen Added
0.01	100	0.01
0.03	33	0.03
0.06	16.7	0.05
0.08	12.5	0.12
0.11	9.1	0.2
0.16	6.3	0.30

I is the observed initial afterglow intensity just after the discharge was cut off. It can be seen that using the static system the amount of oxygen required to lower the afterglow intensity by a factor of 10 is almost 2 orders of magnitude less than that required in the experiments of Berkowitz et al and Broida et al using flow systems.

It will be seen that in the present work, where a static system was used, the results are much closer to those of Anderson et al than to those of Berkowitz et al or Broida et al.

1.4 The Nitric Oxide Afterglow.

1.4.1 The Intensity of the Nitric Oxide Afterglow.

The origin of the nitric oxide β and γ bands which usually accompany the Lewis-Rayleigh afterglow is bound up with the nature of active nitrogen itself. In the last two decades,

since it has been established that active nitrogen is [48] nitrogen atoms, much evidence has been accumulated for the currently accepted mechanism of the nitric oxide afterglow.

Strutt (1917) investigated the so called β and γ bands of nitrogen emitted when oxygen containing gases were added to active nitrogen. He could detect no oxidation of the nitrogen and thought the bands did not originate from the nitric oxide molecule.

H.P. Knauss (1928) observed that the maximum excitation energy of the β and γ bands was about 3.4 e.v. less than the dissociation energy of the nitrogen molecule. He concluded that nitrogen atoms recombined emitted the nitrogen 1st positive bands and then excited nitric oxide spectra.

Willey (1937) investigated the chemical reactions occurring in a discharge in nitrogen and oxygen. He found that the only oxide of nitrogen formed in appreciable concentration was nitric oxide, and that in nitrogen rich mixtures some of the nitric oxide was removed by active nitrogen. Willey suggested that the reaction $O_2\ (A^1\Sigma) + N_2 \rightarrow 2NO$ was occurring; $A^1\Sigma$ oxygen molecules being formed by collision of unexcited oxygen and energetic nitrogen molecules. The energetic nitrogen molecules would be formed by recombination of N_2^+ ions and electrons.

In 1944 Gaydon made a study of the β, γ and δ bands of nitric oxide emitted in the presence of active nitrogen. He observed nitric oxide bands up to the following vibrational levels :

β, $v^1 = 6$; γ, $v^1 = 3$; δ, $v^1 = 0$ (β corresponds to $B^2\pi \rightarrow X\,^2\pi$, γ to $A^2\Sigma^+ \rightarrow X\,^2\pi$; and δ to $C^2\Sigma \rightarrow X\,^2\pi$ transitions). The observed vibrational levels correspond to an excitation energy around 52,000 cm^{-1}. Other workers also failed to obtain nitric oxide bands from vibrational levels higher than those observed by Gaydon. Thus it appeared that predissociation of some of the excited states of nitric oxide was occurring at about 6.49 e.v. ($\equiv$ 52500 cm^{-1}). This view was supported by Gaydon's evidence (1944) for the dissociation energy of the nitrogen molecule being 9.76 e.v. (1.2.5). From thermochemical experiments 2 NO = N_2 + O_2 + 1.87 e.v., also D (O_2) = 5.084 e.v., Eichowsky and Rossini. If D (N_2) = 9.76 e.v. it follows that D (NO) = 6.49 e.v. agreeing with the predissociation limit observed by Gaydon and others.

Tanaka (1954) made similar observations to Gaydon on the emission bands of a nitric oxide afterglow, and on the spectrum of a transformer discharge through nitric oxide. He noted that the afterglow spectrum was cut off at 1915 A (6.47 e.v.), but that nitric oxide bands of shorter wavelength were emitted from the transformer discharge. The intensity distribution was also different.

Tanaka proposed the following mechanism for the nitric oxide afterglow :

$$N(^4S) + O(^3P) + NO(X^2\Pi) \rightarrow NO^* + NO(X^2\Pi)$$

$$NO^* \rightarrow NO\ X^2\Pi + h\nu\ (\beta, \gamma)$$

Kaufman and Kelso (1957) used N^{14} and N^{15} isotopes of nitrogen. They added $N^{15}O$ to $N_2{}^{14}$ containing active nitrogen, i.e. N^{14} atoms. The resulting nitric oxide bands were emitted by $N^{14}O$ only supporting the reactions

$$N^{14} + N^{15}O \rightarrow N_2{}^{14,15} + O$$

$$N^{14} + O + M \rightarrow N^{14}O^* + M$$

$$N^{14}O^* \rightarrow NO + h\nu\ (\beta, \gamma)$$

i.e. the nitric oxide bands are due to the combination of ground state nitrogen and oxygen atoms in collision with an inactive particle.

Tanaka (1959) made observations on the afterglows of nitrogen and oxygen mixtures. By adding sufficient oxygen to the nitrogen he obtained the nitric oxide afterglow. The absorption spectra of oxygen and nitrogen atoms were present in this stage but nitric oxide was not observed to be present in absorption.

Barth, Schade, Kaplan (1959) observed that when helium was added to a nitrogen, oxygen mixture the vibrational intensity distribution of the β and γ bands was different from that in a mixture containing no rare gas. They stated that this was strong evidence of an intermediate state being formed, as in the nitrogen afterglow. The helium cannot affect the intensity distribution of the $A^2\Sigma$ and $B^2\Pi$ states once they are formed

since these states have lifetimes $\sim 10^{-3}$ secs., but the time between collisions is $\sim 10^{-7}$ secs. at the pressures used. They proposed that the mechanism is

$$N\,(^4S) + O\,(^3P) + He \rightarrow NO\ (\text{int.}) + He$$
$$\rightarrow NO\ (A^2\Sigma, B^2\Pi) + He$$

Vanderslice, Mason and Maisch (1959) were able to calculate potential curves for the $^4\Pi$, $^2\Sigma$ etc. states of nitric oxide derived from combination of a ground state nitrogen and oxygen atom, using some spectroscopic data. They concluded that the $^4\Pi$ state was a weakly bound state crossing the $A^2\Sigma$ and $C^2\Pi$ levels.

Such curve crossings, if collision induced, would explain the effect of foreign gases on the vibrational intensity distribution of nitric oxide bands.

The work of Kaufman and Kelso, and Barth et al suggests that the origin of the nitric oxide afterglow is the combination of a ground state oxygen and nitrogen atom in collision with a third inactive particle rather than excitation of a nitric oxide molecule, in the manner described by Tanaka.

1.4.2 Decay of the Nitric Oxide Afterglow.

Brömer (1960) observed the decay of the nitrogen and nitric oxide afterglow intensity over 4 orders of magnitude. He observed a very fast initial decay from the glow intensity which he attributed to the removal of electronic excitation. The

afterglow lasted for about 40 seconds. The decay of the nitric oxide and nitrogen 1st positive bands was not exponential. A plot of $I^{-\frac{1}{2}}$ vs. t was straight for about 21 seconds where I is the intensity of the 1st positive bands and t is time. This implies, since $I = K^1 n^2$ that $-\frac{dn}{dt} = Kn^2$ where n is the concentration of nitrogen atoms and K^1, K are constants. After 20 seconds the rate of decay increased, implying that another process was removing nitrogen atoms. Bromer concluded that the rate of this process which became comparable with the recombination rate of nitrogen atoms after 20 seconds was due to

$$N + O + M \rightarrow NO^* + M$$

$$NO^* \rightarrow NO + h\nu \ (\beta, \gamma)$$

By using a closed system and cleaning up the oxygen present the $B^2\Sigma u^+ \rightarrow X^2\Sigma_g^+$ bands of N_2^+ were produced.

Under these conditions the decay of N_2 1st positive and nitric oxide bands was almost exponential. Bromer considered that this was not due to destruction of atoms at the walls. He stated that in a 5 litre vessel at 3 mm.Hg. pressure, wall decay would be too slow to account for the rapid decay of the afterglow, and so the three body recombination of nitrogen atoms must be hindered in some way.

APPARATUS AND PRELIMINARY EXPERIMENTS

2.1 Apparatus.

The aim of the work was to study the decay with time, and the intensity of individual emission bands of the afterglow spectrum of nitrogen, oxygen mixtures. Most of the work was concentrated on the nitric oxide afterglow spectrum in which only the β and γ bands of nitric oxide were observed. The afterglow studied was the afterglow of a low pressure, pulsed, high frequency (R.F.) glow discharge.

The R.F. discharge tube which had a quartz window, and was 50 cm. long and 5 cm. in internal diameter formed part of the vacuum system shown in Fig 1. The power from the pulsed R.F. source was fed onto two copper rings on the outside of the discharge tube; the rings being $\frac{1}{2}$ cm. wide, and separated by about 20 cms. In the experiments described later, the period of each R.F. pulse was 0.5 seconds and the pulse repetition time was 6 seconds.

The afterglow following each pulse was analysed by a Hilger quartz monochromator, and detected by an E.M.I. 13 stage 6256B photomultiplier. The decaying afterglow intensity was recorded on a Brown Recorder. The walls of the discharge tube were coated with metaphosphoric acid to inhibit recombination of atoms at the walls.

The vacuum system shown in fig.1 was designed by Mr. J. Sutherland and the glassblowing was done by Mr. K. Pike. An oxygen inlet system (fig.11) was added to the system as shown.

The electrical and optical system fig.2 was assembled by Mr. Sutherland who designed the pulse generator. The pulse generator operated the relay which controlled the shutter between the discharge tube and the monochromator entrance slit. It also operated the switch for pulsing the R.F. voltage supplied to the discharge tube. A delay box was included to synchronise the end of the R.F. pulse and the opening of the shutter. The shutter was arranged to isolate the discharge tube from the monochromator during the R.F. pulse and to be open during the afterglow for about 6 seconds.

The purpose of the shutter was to avoid overloading the sensitive photomultiplier; though it was later discovered that it was not essential when the pulsed R.F. voltage was used, as the glow intensity of a band was of about the same order of magnitude as the afterglow intensity recorded just after the shutter opened. The use of the shutter was in fact disadvantageous as far as measurements of afterglow intensities were concerned.

The electron current from the photomultiplier was allowed to flow to earth through a resistance box. The voltage developed across this resistance was the input voltage of the cathode follower. The time constant of the photomultiplier and the resistance box was less than that of the decaying afterglow intensity, even when the resistance box was set at maximum resistance. By varying the resistance of the box in steps of ten, the sensitivity of the detection system could be varied in steps of ten.

In practise only the two most sensitive ranges (R_1) corresponding to maximum sensitivity, and (R_2) corresponding to $\frac{1}{10}$ x maximum

Fig.1 Vacuum System.

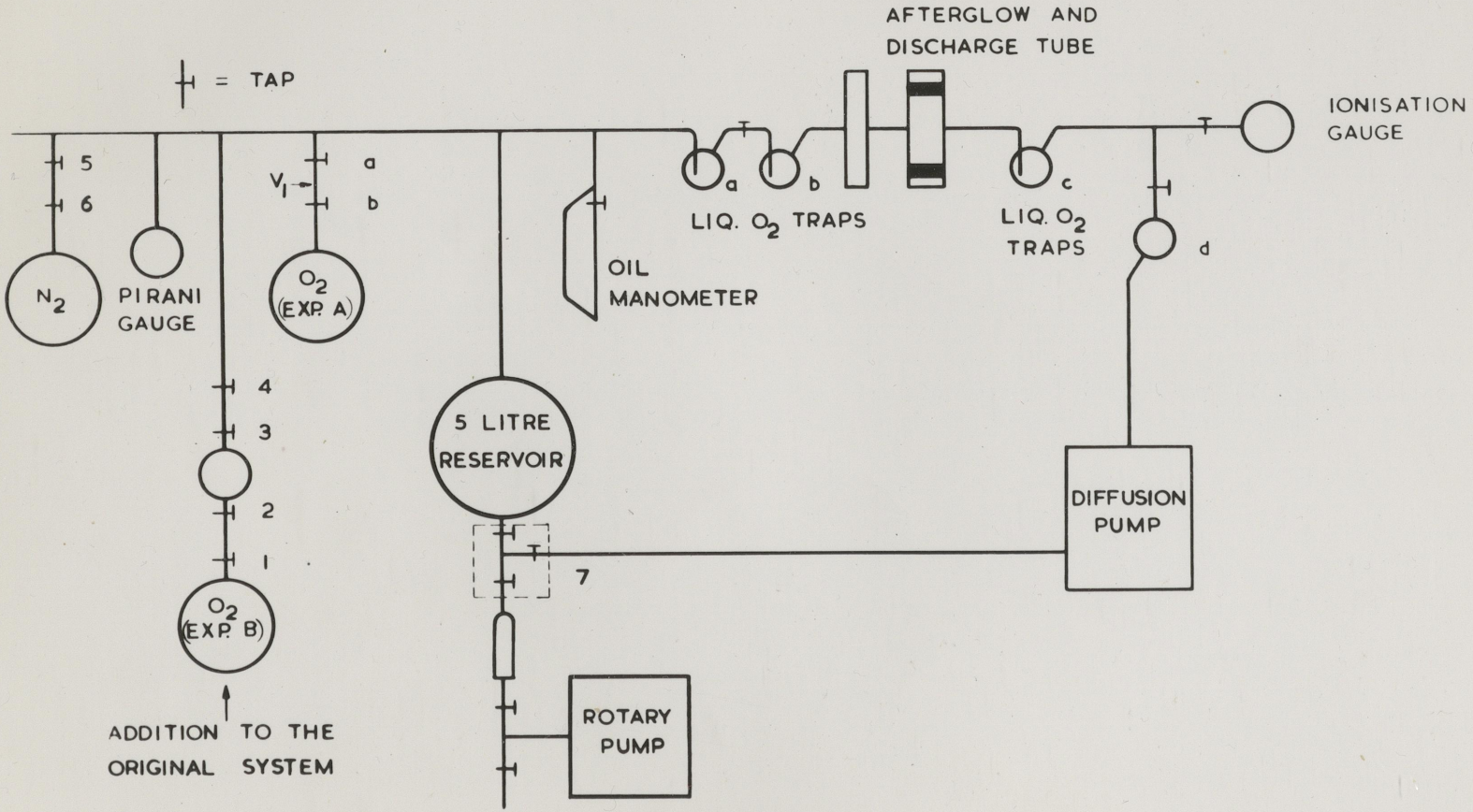
AFTERGLOW AND
DISCHARGE TUBE
= TAP
IONISATION
GAUGE
5
6
V_1
a
b
a
b
c
d
N_2
PIRANI
GAUGE
O_2
(EXP. A)
LIQ. O_2 TRAPS
LIQ. O_2
TRAPS
OIL
MANOMETER
4
3
2
1
5 LITRE
RESERVOIR
DIFFUSION
PUMP
7
O_2
(EXP. B)
ADDITION TO THE
ORIGINAL SYSTEM
ROTARY
PUMP

FIG. 1

Fig.2 Optical System and Power Supply.

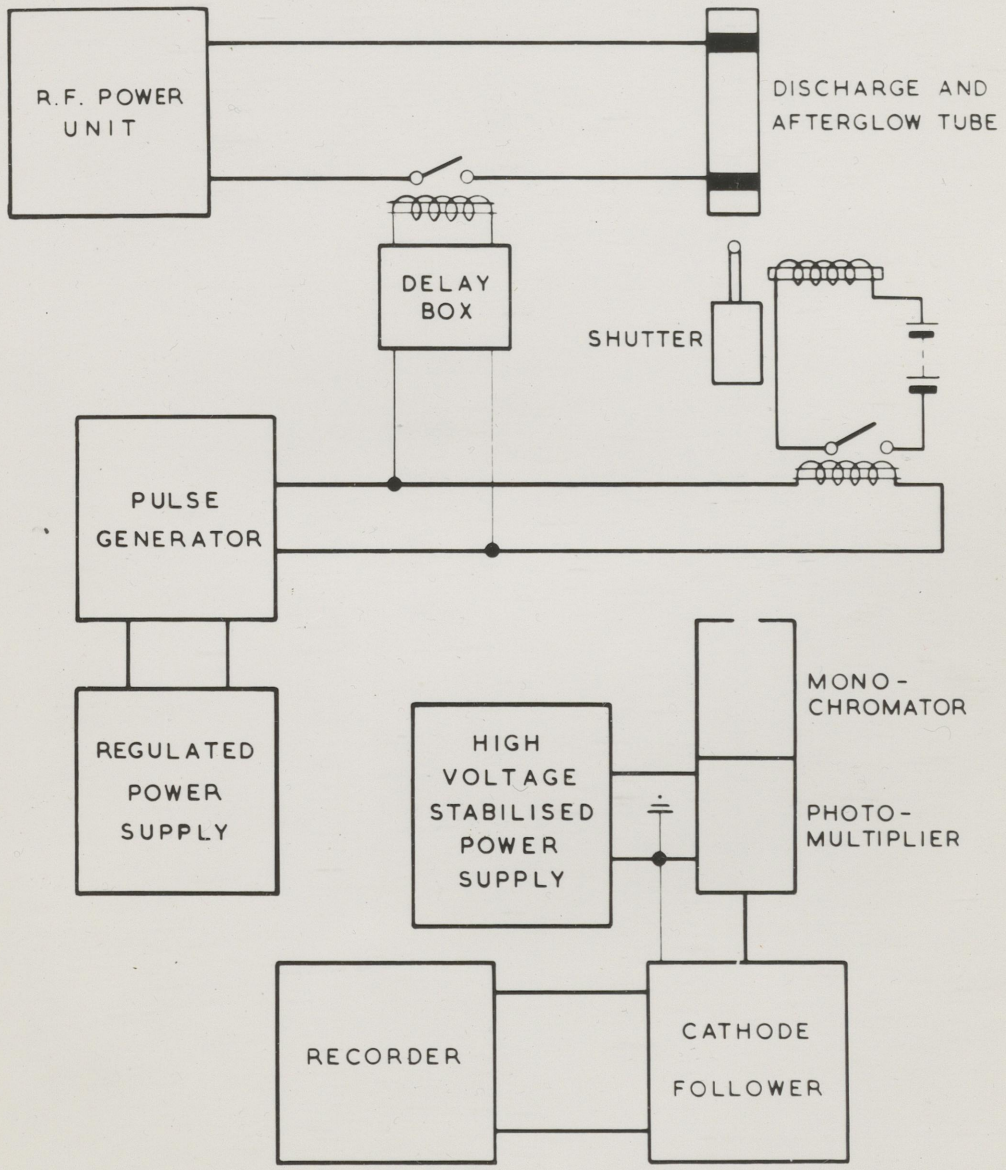
R.F. POWER UNIT
DISCHARGE AND AFTERGLOW TUBE
DELAY BOX
SHUTTER
PULSE GENERATOR
REGULATED POWER SUPPLY
HIGH VOLTAGE STABILISED POWER SUPPLY
MONO-CHROMATOR
PHOTO-MULTIPLIER
RECORDER
CATHODE FOLLOWER

FIG. 2

sensitivity were used.

The nitrogen used in the experiments was drawn from a reservoir of B.O.C. 'spec. pure' nitrogen (maximum impurity concentration 0.01% of oxygen), and the oxygen used was B.O.C. 'spec. pure' oxygen. These gases were supplied at about atmospheric pressure. The total gas pressure in the system was measured by a manometer containing apiezon B oil of density 0.86 gms.cc^{-1}. Lower gas pressures were measured using an Edwards Pirani gauge, and an IG2 ionisation gauge.

2.2 Preliminary Experiments and Investigations of the Afterglow of an R.F. Discharge in Nitrogen.

At first some time was spent in investigating the characteristics of the discharge tube vacuum system. After evacuating the discharge tube system, and admitting nitrogen to a pressure of about 1 mm Hg., the R.F. voltage was applied to the tube and an orange discharge observed with blue portions near the electrodes. No afterglow was observed when the discharge was switched off, the room being completely dark. The system was evacuated and the procedure repeated several times. This helped to remove impurities from the tube, and a yellow afterglow was then observed in the discharge tube when the R.F. discharge was cut off. The afterglow intensity appeared uniform throughout the tube, and it remained visible for about 10 - 15 seconds. It was found that the brightest afterglow was obtained when the total gas pressure was about 1mm Hg. The impurities residing in the system after evacuation to about 10^{-4} mm Hg were identified from the spectrum of a low pressure R.F. glow discharge.

Such impurities as CO, CO_2, OH, H_2 were present. It was sometimes found that the afterglow of the discharge in nitrogen became weaker and weaker after each succeeding R.F. pulse and also greyish in appearance. This was thought to be due to the desorption of impurities from the walls of the discharge tube by the glow discharge. Often no afterglow could be obtained. Eventually it was found that, when no afterglow was present, the β and γ bands of nitric oxide were very strong in the glow discharge spectrum. It was known that oxygen destroys the nitrogen afterglow, Tanaka, (1959), and that nitric oxide would be formed because of the presence of oxygen. It appeared that atmospheric oxygen was leaking in at the junction of the nitrogen gas cylinder to the system. Eventually the gas cylinder was replaced by a bulb of B.O.C. 'spec. pure' nitrogen black waxed onto the system using a cone and socket joint. The afterglow was then more yellow in appearance and the afterglow pulses succeeding each R.F. glow discharge pulse remained reproducible over the longest period in which observations were made.

It was found that, even when using 'spec. pure' oxygen, the afterglow intensity varied randomly from pulse to pulse. By running the cycle of R.F. pulses for up to 2 hours, the magnitude of this variation could be reduced. This is demonstrated in table 1 below. The intensity values are afterglow intensities recorded at a fixed time, Δ t seconds, after the shutter opened. Two values are shown, the maximum value and the minimum value of sets of 12

consecutive pulses, recorded within $\pm \frac{1}{2}$ minute of the times shown. The intensities were measured using the monochromator and photomultiplier and are equal to deflections of the Brown recorder on range (R_2).

TABLE 1. RANDOM INTENSITY VARIATION OF AFTERGLOW PULSES.

Monochromator Setting 2471 Å ; Entrance Slit Width 1 mm.								
Maximum Afterglow Intensity Chart Divs.(R_2)	18	18	18.5	18	18	17.5	17.5	17.5
Minimum Afterglow Intensity Chart Divs.(R_2)	15.5	14.5	16.9	15.5	16.5	15.5	16	17
Time hrs. mins.	2.50	3	3.9	3.20	3.30	3.38	3.45	4.20

In view of these results the cycle of R.F. glow discharge pulses was usually continued for a $\frac{1}{2}$ hour before measurements were made of afterglow band intensities or decay rates.

A typical afterglow trace is shown in fig.3.

2.3 Linearity of the Recording System.

Two checks were made on the recording system. The linearity of the photomultiplier and cathode follower was tested as follows. The entrance slit of the monochromator was set at various widths, and the Brown recorder reading noted with and without a half silvered plate between the white light source and the monochromator.

Fig.3. Brown Recorder traces, showing decay with time of 2595 Å - 2587 Å δ (0,3) Nitric Oxide Afterglow Band

(a) 0% oxygen added

(b) 0.1% oxygen added.

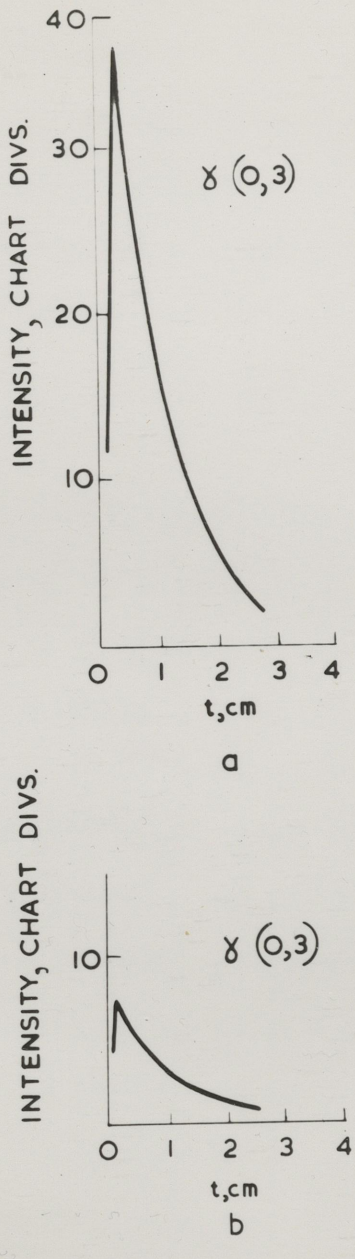
40
30
20
10
INTENSITY, CHART DIVS.
γ (0,3)
0 1 2 3 4
t,cm
a
10
INTENSITY, CHART DIVS.
γ (0,3)
0 1 2 3 4
t,cm
b

FIG. 3

As shown, a plot of Brown recorder deflection without filter versus the corresponding deflection with filter (fig.4) is a straight line passing through the origin, showing that the ratio of deflections remained constant throughout the intensity range observed. Since the experimental work was completed, it has been pointed out that the straight line plot (fig.3) indicates only that the following law is obeyed.

$$I^1 = kI^n$$

where I^1 = Brown Recorder deflection.

k = constant.

I = intensity of light emitted from the discharge tube.

n = constant.

However, if I^1 is a function of a single power of I then on empirical grounds it is most likely that $n = 1$, and therefore that the response of the system is a linear function of the intensity being studied.

In the second case a constant intensity source was used, and the Brown Recorder deflection plotted against nominal slit width reading (fig.5). It can be seen that this curve is not linear. Thus it cannot be assumed that intensity is proportional to the entrance slit width used. Where intensities measured using different entrance slit widths have been compared, this curve has been used to obtain the scaling factors.

Fig.4. Brown Recorder Deflection I_1 without filter
vs. Brown Recorder Deflection I_2 with neutral filter.

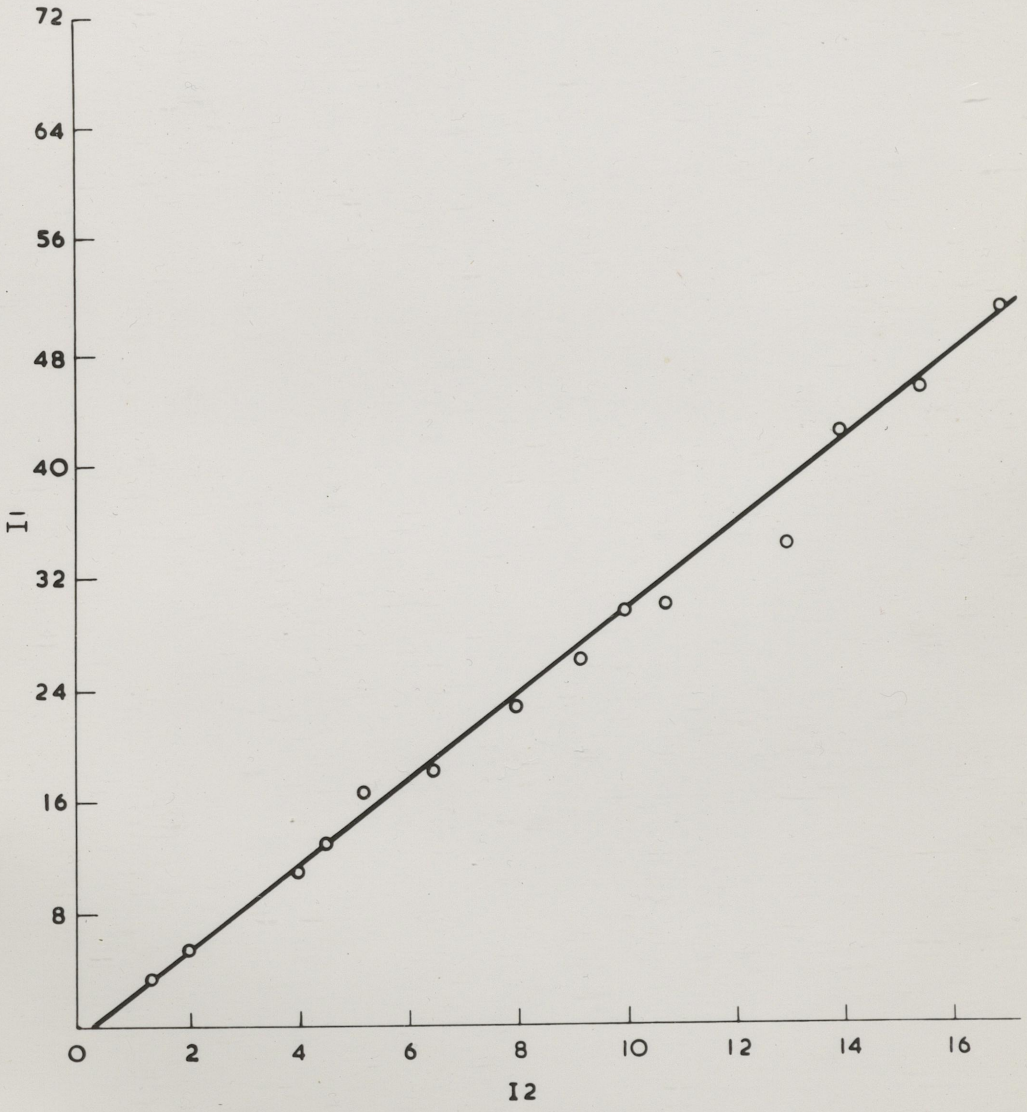

FIG. 4

Fig.5 Brown Recorder Deflection vs Monochromator Entrance Slit Width.

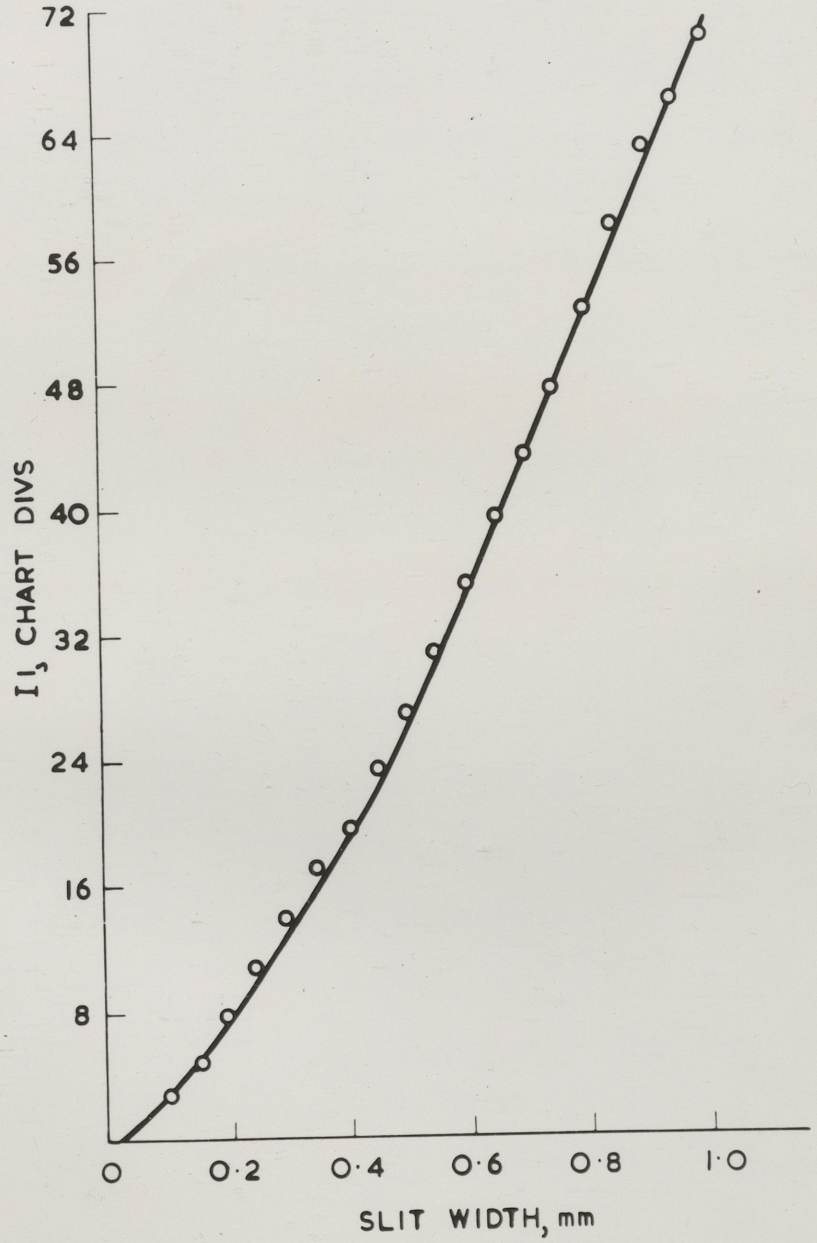
72
64
56
48
40
32
24
16
8
I_1, CHART DIVS
0
0·2
0·4
0·6
0·8
1·0
SLIT WIDTH, mm

FIG. 5

2.4 The Nitric Oxide Spectrum of the R.F. discharge and the Afterglow.

Spectra of the R.F. glow discharge (fig.6) and the afterglow (fig.6a) were photographed using a Hilger small quartz spectrograph, and Ilford H.P.S. plates. The shutter was used to shut off the light of the R.F. glow discharge, when photographing the afterglow spectrum. The wavelength scale was checked against an iron arc spectrum and found to be reliable to within a few angstroms in the range 2300Å to 2500 Å. For higher wavelengths the scale was more difficult to read, and the accuracy decreased. Precision intensity measurements were not made; but the densities of the bands recorded on the photographic plates were measured using a Jarrel-Ash densitometer, and a planimeter to determine the area of the peaks on the densitometer chart. The measured photographic densities of the bands are shown in tables 2 and 3. The density distribution of nitric oxide bands for the glow and the afterglow was in fair agreement with the estimated intensities published in ~~Pierce~~ Pearse and Gaydon's 'The Identification of Molecular Spectra' (I.M.S.). Thus no striking abnormalities were evident in the intensity distribution of the nitric oxide β and δ bands in the glow or afterglow.

From the table 2 it can be seen that the sum of the observed glow band densities is 109.7, and that of the bands from (I.M.S.) is 134. In order to compare the two sets of intensity parameters, the observed glow band densities were each multiplied by $\frac{100}{109.7}$, and the bands from (I.M.S.) were multiplied by $\frac{100}{134}$. It can be seen that the agreement between the two sets of parameters is fair.

Fig. 6 R.F. Glow Discharge Spectrum.

Fig. 6a Afterglow Spectrum.

Fig. 6

Fig. 6a

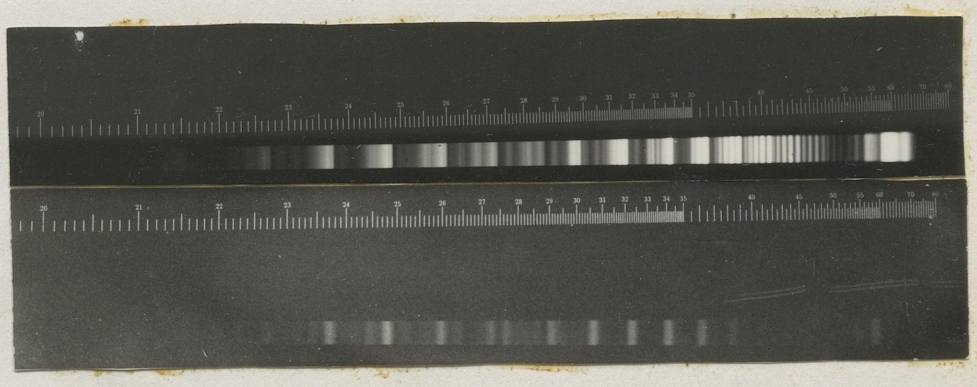

The procedure of comparing the present measurements with published values, in this way, is open to the objection that it is rather fortuitous that the relative intensities of bands originating from different vibrational levels should be the same in two independent measurements. However, as stated above, the agreement between the two sets of intensity parameters is fair. The exceptions to this are the $\gamma(1,0)$ and $\gamma(2,2)$ bands, for which the agreement is poor; possibly due to the sensitivity of the photographic emulsion falling off at lower wavelengths. The agreement is also poor for the $\beta(1,4)$, $\beta(4,4)$, $\beta(5,6)$ and $\gamma(1,5)$ bands, which were partly overlapped by neighbouring bands on the photographic plate.

The same procedure was applied to the measured densities of the afterglow bands in order to compare them with the intensities from (I.M.S.). In this case the observed bands were well spaced on the photographic plate, and it can be seen that the agreement between the two sets of intensity parameters is quite good.

TABLE 2. COMPARISON OF MEASUREMENTS OF THE R.F. GLOW DISCHARGE NITRIC OXIDE SPECTRUM WITH PREVIOUS MEASUREMENTS.

R.F. Glow Discharge Nitric Oxide Band Densities						Nitric Oxide, Band Intensities, Pierce and Gaydon 'The Identification of Molecular Spectra'.	
Band Wave Length Å	(v^1, v^{11})	Band Area inches^2	Band Width inches	Observed Glow Band Density = Area / Width	Observed Glow Band Density $\times \frac{100}{109.7}$	Estimated Intensity	Estimated Intensity $\times \frac{100}{134}$
2154 2149	γ (1,0)	3.35	3.2	1.0	0.91	7	5.2
2222 2216	γ (2,2)	3.25	2.1	1.6	1.5	3	2.2
2254 2239	γ (1,1)	15.55	2.5	6.2	5.7	3	8.2
2269 2262	γ (0,0)					8	
2289 2284	γ (3,4)	3.05	2.4	1.3	1.2	2	1.5
2316 2309	γ (2,3)	4.3	2.2	2	1.8	2	1.5
2331 2326	β (3,3)	13.7	3	4.6	4.2	3	4.2
2370 2363	γ (0,1)	15.05	2	7.5	6.8	10	7.5

Table 2. (Cont'd.)

R.F. Glow Discharge Nitric Oxide Band Densities						Nitric Oxide Band Intensities, Pierce and Gaydon 'The Identification of Molecular Spectra'.	
Band Wave Length Å	(v^1, v^{11})	Band Area inches^2	Band Width inches	Observed Glow Band Density = Area / Width	Observed Glow Band Density x 100/109.7	Estimated Intensity	Estimated Intensity x 100/134
2376 2372	β (4,4)	6	2.5	2.4	2.2	1	0.75
2433 2428	β (3,4)	18.7	3.7	5.0	4.6	7	5.2
2471 2478	γ (0,2)	21.5	2.6	8.3	7.6	10	7.5
2493 2487	β (2,4)	4.4	1.4	3.2	2.9	7	5.2
2528 2523	β (5,6)	7	1.5	4.7	4.3	1	0.75
2557 2551	β (1,4)	17.1	2.3	7.4	6.7	5	3.7
2595 2587	γ (0,3)	20.6	2.5	8.2	7.5	9	6.7
2608 2602	β (2,5)	3.1	0.9	3.4	3.1	6	4.5
2626 2620	β (0,4)	9.5	1.9	5	4.6	6	4.5

Table 2. (Cont'd)

R.F. Glow Discharge Nitric Oxide Band Densities						Nitric Oxide Band Intensities, Pierce and Gaydon 'The Identification of Molecular Spectra'	
Band Wave Length Å	(v^1, v^{11})	Band Area inches^2	Band inches	Observed Glow Band Density = Area / Width	Observed Glow Band Density x 100/109.7	Estimated Intensity	Estimated Intensity x 100/134
2680 2671	γ (1,5)	16.6	2.4	6.9	6.3	5	3.7
2722 2713	γ (0,4)	18.8	2.5	7.5	6.8	8	6
2754 2747	β (0,5)	10.3	2.2	4.7	4.3	9	6.7
2810 2800	γ (1,6)	19.5	2.9	6.7	6.1	4	6.7
2809 2802	β (1,6)					5	
2859 2849	γ (0,5)	13.2	1.9	7	6.4	7	5.2
2885 2892	β (0,6)	10.2	2	5.1	4.6	10	7.5
				Σ Density = 109.7		Σ Intensities = 134	

TABLE 3. COMPARISON OF MEASUREMENTS OF THE AFTERGLOW NITRIC OXIDE SPECTRUM WITH PREVIOUS MEASUREMENTS

Afterglow Nitric Oxide Band Densities						Nitric Oxide Band Intensities Pierce and Gaydon 'The Identification of Molecular Spectra'.	
Band Wave-Length Å	(v^1, v^{11})	Band Area inches^2	Band Width inches	Observed Afterglow Band Density = Area / Width	Observed Afterglow Band Density x 10/17.6	Estimated Intensity	Estimated Intensity x 10/116
2316 2309	$\gamma(2,3)$	0.9	2.2	0.4	0.23	2	0.17
2331 2326	$\beta(3,3)$	1.15	1.9	0.6	0.34	3	0.26
2370 2363	$\gamma(0,1)$	7.4	4.9	1.5	0.85	10	0.86
2433 2427	$\beta(3,4)$	2.2	2.5	0.9	0.51	7	0.6
2478 2471	$\gamma(0,2)$	5.2	2.4	2.2	1.25	10	0.86
2595 2587	$\gamma(0,3)$	3.5	2.5	1.4	0.8	9	0.77
2626 2620	$\beta(0,4)$	1.7	2.4	0.8	0.45	6	0.52

TABLE 3. (Cont'd.)

Afterglow Nitric Oxide Band Densities						Nitric Oxide Band Intensities Pierce and Gaydon 'The Identification of Molecular Spectra'.	
Band Wave-Length Å	(v^1, v^{11})	Band Area inches^2	Band Width inches	Observed Afterglow Band Density = Area / Width	Observed Afterglow Band Density $\times \frac{10}{17.6}$	Estimated Intensity	Estimated Intensity $\times \frac{10}{116}$
2754 2748	β (0,5)	2.2	2	1.1	0.62	9	0.77
2892 2885	β (0,6)	4.5	3.4	1.3	0.74	10	0.86
3043 3034	β (0,7)	3.7	2.3	1.6	0.91	10	0.86
3206 3198	β (0,8)	4.1	2.2	1.9	1.1	10	0.86
3386 3376	β (0,9)	3.9	2.3	1.7	0.97	10	0.86
3583 3572	β (0,10)	3.3	2.3	1.4	0.79	10	0.86
3868 3800	β (0,11)	1.9	2.4	0.8	0.45	10	0.86
				Σ Densities = 17.6			Σ Intensities = 116

THE EFFECT OF OXYGEN ON THE NITRIC OXIDE AND NITROGEN AFTERGLOWS.

3.1 Procedure A.

The aim of the experiments was to study the effect of oxygen on the individual bands of the afterglow of nitrogen, oxygen mixtures; rather than on the integrated intensity as Anderson, Kavadas, and McKay (1957) had done. In fact the integrated intensity of some bands of the nitrogen 1st positive system was recorded, and the ultra-violet bands of the nitric oxide β and δ systems were recorded individually.

The practical problem in the experiments on nitrogen, oxygen mixtures was to add known small amounts of oxygen (less than 0.1% of the nitrogen added) to the discharge tube vacuum system. Eventually two procedures A, and B were used. When considering such experiments, the following aims were decided on.

(i) Removal of the maximum possible amount of oxygen from the system.

(ii) To keep measurements comparable the same amount of oxygen should be removed from the system each time, by, for example, evacuating and outgassing the system until the intensity of a nitric oxide band in the R.F. glow discharge spectrum had decreased to a given value. This procedure was not used as the time required to reach a given base pressure was much greater after discharges in nitrogen with $\sim$ 0.05% oxygen, than after discharges with no oxygen added.

(iii) To admit to the system a known amount of oxygen, the minimum concentration being about 0.01% of the nitrogen concentration. The last aim was adopted because Anderson, Kavadas, and McKay (1957) had admitted oxygen in steps $\sim$ 0.01% to a nitrogen discharge, and had observed marked changes in the rate of decay of the nitrogen afterglow.

The following procedure was used to evacuate the discharge tube system. The system was pumped down to about 10^{-3} mm Hg using the backing pump. Trap d was then filled with liquid oxygen; and using the diffusion pump the system was evacuated to 10^{-4} mm Hg, when all traps a, b and c were filled. When a pressure of $\sim 2 \times 10^{-5}$ mm Hg was reached, outgassing of the discharge tube was carried out by running the pulsed R.F. discharge in the tube using the maximum R.F. voltage, and a pulse repetition time of about 6 seconds. The outgassing did not lower the base pressure much lower than 10^{-5} mm Hg, but was done to remove impurities which would have evaporated off the walls during subsequent running of the discharge. The most effective way of cleaning the system, however, was to admit nitrogen to a pressure of the order of 1 mm Hg and to run the R.F. discharge cycle for about 1 hour. It was then found possible to pump down the system to base pressure in a much shorter time than in the preceding evacuation. If however about 0.05% of oxygen was present in the nitrogen when the R.F. discharge was run, the time required subsequently to evacuate the system to base pressure was longer. The following

procedure for admitting known amounts of nitrogen and oxygen to the system was the one found to be practicable. The system was evacuated and outgassed to a base pressure of about 2×10^{-5} mm Hg. Using the double tap device above the oxygen bottle (fig.1) oxygen was admitted to V1 by opening Tap b. Tap b was then closed and Tap a opened. The oxygen pressure in the system rose to about 0.1 mm Hg with the backing pump and diffusion pump running. The system was then evacuated to a pressure of 5×10^{-4} mm Hg and isolated from the pumps. The oxygen pressure was noted, and nitrogen admitted to a pressure of about 1 mm Hg. The large initial rise in oxygen pressure to 0.1 mm Hg was unavoidable using the double tap system for admitting oxygen to the system. The procedure was advantageous, however, because it helped to saturate the walls of the liquid nitrogen traps on which oxygen would have been adsorbed more readily than on the other parts of the system.

After admitting the nitrogen to the system, the pulsed R.F. discharge was run for about 30 minutes to obtain reproducible afterglow pulses. The monochromator was then set at the wavelengths shown in table 4, and the decaying afterglows of the corresponding afterglow bands recorded using the photomultiplier and Brown recorder. About 12 afterglow pulses were recorded for each wavelength setting. The widths of the monochromator entrance, and exit slits are also shown in table 4. The shutter described above (2.1) was used to shield the monochromator entrance slit from the glow discharge light.

TABLE 4. AFTERGLOW BANDS RECORDED IN EXPERIMENT A.

Band Wavelengths Å	(v^1, v^{11})	Setting of Monochromator Wavelength Drum Å	Entrance Slit Width mms	Exit Slit Width mms	Symbol for Band Afterglow Intensity at time t secs. after opening of shutter. Chart Divs. (R_2)	Symbol for Band Afterglow Intensity at time t secs. after opening of shutter. Chart Divs. (R_2)
2370-2363	NO γ (0,1)	2363	1	1.6	Ip2363	It2363
2478-2471	NO γ (0,2)	2471	1	1.3		
2892-2885	NO β (0,6)	2890	1	1.3	Ip2890	It2890
3043-3034	NO β (0,7)	3034	0.5	0.6		
3206-3198	NO β (0,8)	3200	0.5	0.6	Ip3200	It3200
5854	N_2 1st +ve (10,6)					
5804	N_2 1st +ve (11,7)	5755	0.5	0.6	Ip5755	It5755
5755	N_2 1st +ve (12,8)					

3.2 Results A.

3.2.1 Afterglow Intensity Measurements.

The results obtained using the procedure A are shown in tables 5 to 11. It should be noted that in runs 7 and 8 no oxygen was actually added. The amounts stated correspond to the oxygen content given by B.O.C. Ltd. A random selection of afterglow pulses was chosen from the sequence of pulses corresponding to each wavelength setting of the monochromator, and the afterglow intensity of each selected band was measured. The afterglow intensity of a band is, in this context, equal to the Brown recorder deflection on range (R_2) at time Δt after the shutter opened; where Δt is constant and $\sim$0.5 secs. The results of measurements of the integrated afterglow intensity Ip5755 of the (10,6), (11,7) and (12,8) nitrogen 1st positive bands are shown in table 5, and afterglow intensity values Ip2363 of the γ(0,1) nitric oxide band are shown in table 6. Afterglow intensities Ip2890 and Ip3200 of the β(0,6) and β(0,8) bands are included in table 7.

The first two intensities in table 5 were measured using an entrance slit width of 0.3 mm and an exit slit width of 0.2 mm. They were multiplied by a factor of 6 so as to be comparable with the other measurements.

From Fig.5 when the entrance slit width is increased from 0.3 to 0.5 mm the Brown Recorder deflection increases by a factor

TABLE 5. INTEGRATED AFTERGLOW INTENSITY Ip5755 OF THE 5854 Å (10,6), 5804 Å (11,7), 5755 Å (12,8) NITROGEN 1st POSITIVE BANDS VS. OXYGEN ADDED.

Run	Ip5755 Chart Divs. (R_2)	Mean Ip5755 Chart Divs. (R_2)	Number of Oxygen Molecules Added cc^{-1}
7	10.8 8.4 9.6 8.4	9.3	3.7×10^{12}
8	10.4 9.5 8.7	9.5	3.7×10^{12}
5	19 18.5 20 18.5 19.5 19.8	19.2	7×10^{12}
6	18.5 18.1 17.4 18.3 18.7 18.5	18.3	3.6×10^{13}
3	11.5 12.5 12 10.6 12	11.7	3.7×10^{13}

TABLE 6. AFTERGLOW INTENSITY Ip2363 OF THE 2370 Å - 2363 Å δ(0.1). NITRIC OXIDE BAND VS. OXYGEN ADDED.

Run	Ip 2363 Chart Divs. (R_2)	Mean Ip 2363 Chart Divs. (R_2)	Number of Oxygen Molecules Added cc^{-1}
7	29 26.5	27.8	3.7×10^{12}
8	27.5 32.5 29.5	29.8	3.7×10^{12}
5	29 28.8 23.9 27	26.7	7×10^{12}
6	44.5 43.5 45 45.5 45.5	44.8	3.6×10^{13}
3	28.7 30.7 27.7 29.2	29.1	3.7×10^{13}

TABLE 7. AFTERGLOW INTENSITIES Ip2890 AND Ip3200 OF THE 2892 Å - 2885 Å β(0.6) AND 3206 Å - 3198 Å β(0.8) NITRIC OXIDE BANDS VS. OXYGEN ADDED.

Run	Mean Ip2890 Chart Divs.(R_2)	Mean Ip3200 Chart Divs.(R_2)	Number of Oxygen Molecules Added cc^{-1}
7	21.3	-	3.7×10^{12}
8	14	8.1	3.7×10^{12}
5	26.5	15.5	7×10^{12}
6	37.5	22.5	3.6×10^{10}
3	32.9	18.5	3.7×10^{13}

of $\frac{26}{13}$. A photograph of the glow or afterglow spectrum has the nitrogen 1st positive system recorded as a continuous band because of the low dispersion of quartz in the visible region. Thus the effect of decreasing the exit slit width by a factor of 3 should be to reduce the intensity by a factor of 3. The correction factor is therefore $\frac{26}{13} \times 3 = 6$.

3.2.2 Afterglow Decay Rate Measurements.

The most important source of error in determining the form of the decay of the afterglow bands with time was measurement of the background intensity. As the intensity of the afterglow decreased towards zero, it became comparable with , or smaller than the background intensity. A 10% error in background could, in some cases, introduce a 50% error into the measured intensity. The error was reduced by taking the mean of several intensity measurements and also by not attempting to measure intensities smaller than 2 or 3 chart divisions (R_2). Within the accuracy obtainable the decay of the intensity of the nitrogen and nitric oxide bands was exponential. For example :-

$$R_{NO} = \frac{-\,d \log It2363}{dt} \neq \text{function of time,}$$

$$\text{and } R_{N_2} = \frac{-\,d \log It5755}{dt} \neq \text{function of time}$$

It2363 is the afterglow intensity of the $\gamma(0,1)$ nitric oxide band at time t seconds after the shutter opened and It5755

is the corresponding integrated intensity of the (10,6), (11,7) and (12,8) bands of the nitrogen 1st positive system. Log It5755 is plotted versus time in figs. 7 and 8, the gradient of this plot being - R_{N_2}. Plots of log It2363 versus time are shown in figs.9 and 10. Values of R_{N_2} are shown in table 8 for various amounts of oxygen added to the system. Similarly values of R_{NO} for the γ (0,1), β (0,6) and β (0,8) bands are included in tables 9, 10 and 11.

The afterglow decay constants R_{N_2} and R_{NO} in tables 8 to 11 do not vary regularly with the oxygen added to the system. They probably depend on the previous treatment of the tube as well as the amount of oxygen added; e.g. R_{NO} and R_{N_2} in run 6 are smaller in magnitude than R_{NO} and R_{N_2} respectively in run 3 though the amount of oxygen added was about the same in each case. This difference appears to be due to the fact that in run 2, (not recorded here), the discharge was run in nitrogen containing an amount of oxygen comparable with that present in run 3, whereas in run 5 the oxygen used was comparably pure.

In the case of run 7 the values of R_{NO} for the β (0,6) and β (0,8) nitric oxide bands are 35% greater than the value of R_{NO} for the γ (0,1) nitric oxide band. In run 6 the values of R_{NO} for the β (0,6) and β (0,8) bands are respectively 31% and 40% less than the value of R_{NO} for the γ (0,1) band. In other runs the differences in the values of R_{NO} for these 3 bands vary from 5% to 20%.

Figs. 7 and 8. Decay with time of the Integrated Afterglow Intensity I_{t5755} of the 5854 Å (10,6), 5804 Å (11,7), 5755 Å (12,8) Nitrogen 1st positive bands.

Fig.7. 3.7×10^{12} oxygen molecules cc^{-1} present.

Fig.8. 3.6×10^{13} oxygen molecules cc^{-1} added.

0.88%.

(1 cm of chart ≡ 2.36 seconds)

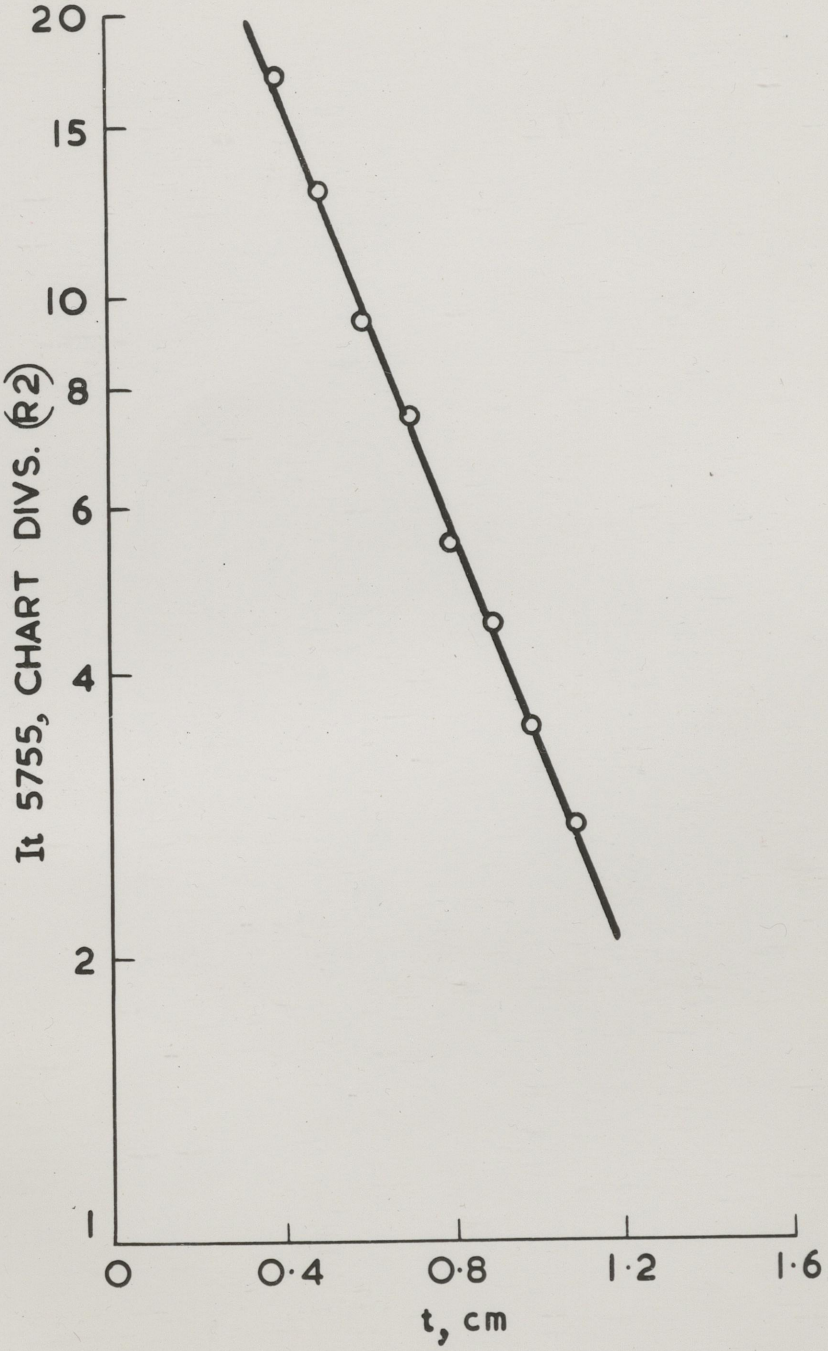

FIG. 7

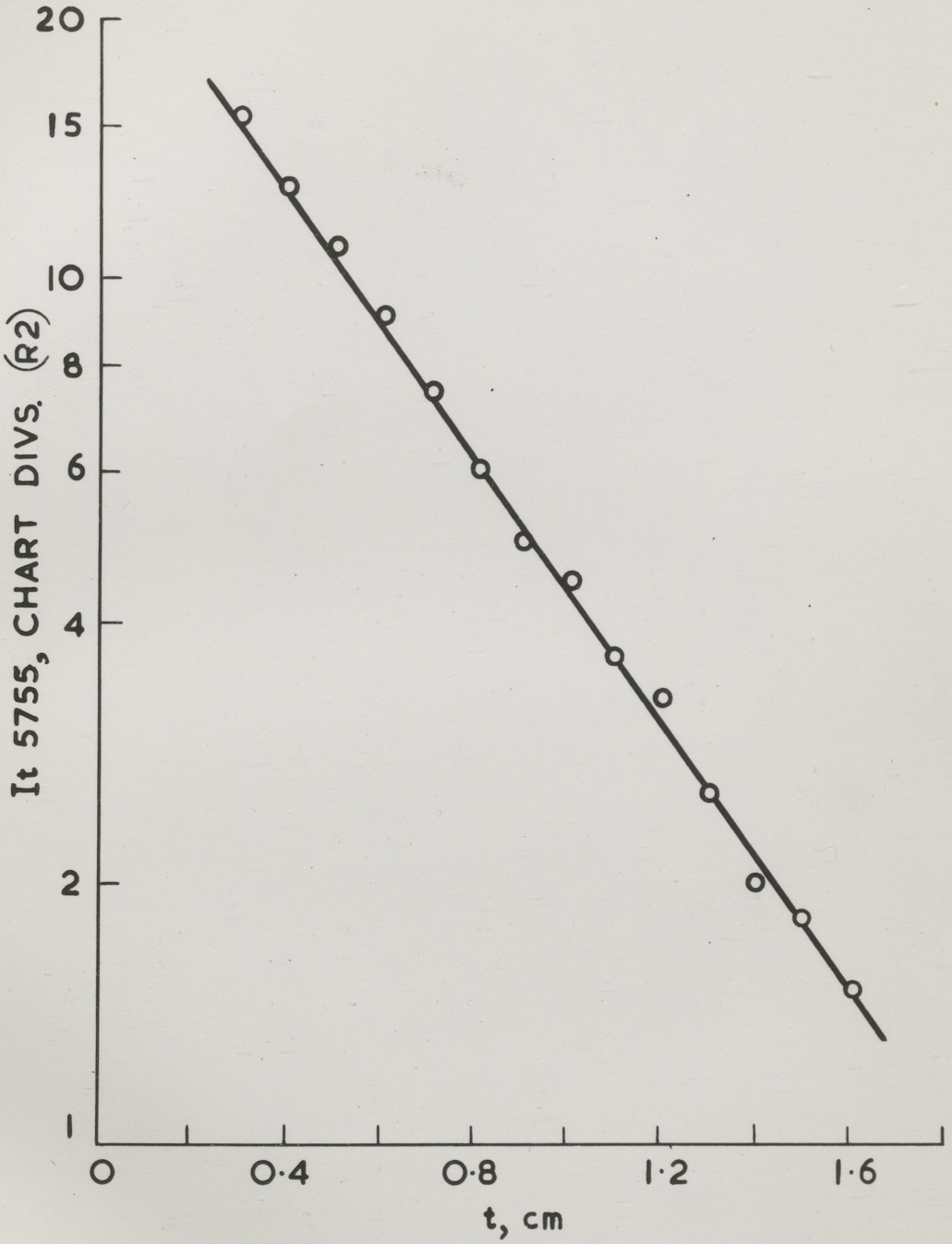

FIG. 8

Figs. 9 and 10. Decay with time of the Afterglow Intensity I_{t2363} of the 2370 A - 2363 A γ (0,1) Nitric Oxide Band.

Fig. 9. 3.7×10^{12} oxygen molecules cc^{-1} present.

Fig.10. 3.6×10^{13} oxygen molecules cc^{-1} added.

(1 cm of chart $\equiv$ 2.36 seconds)

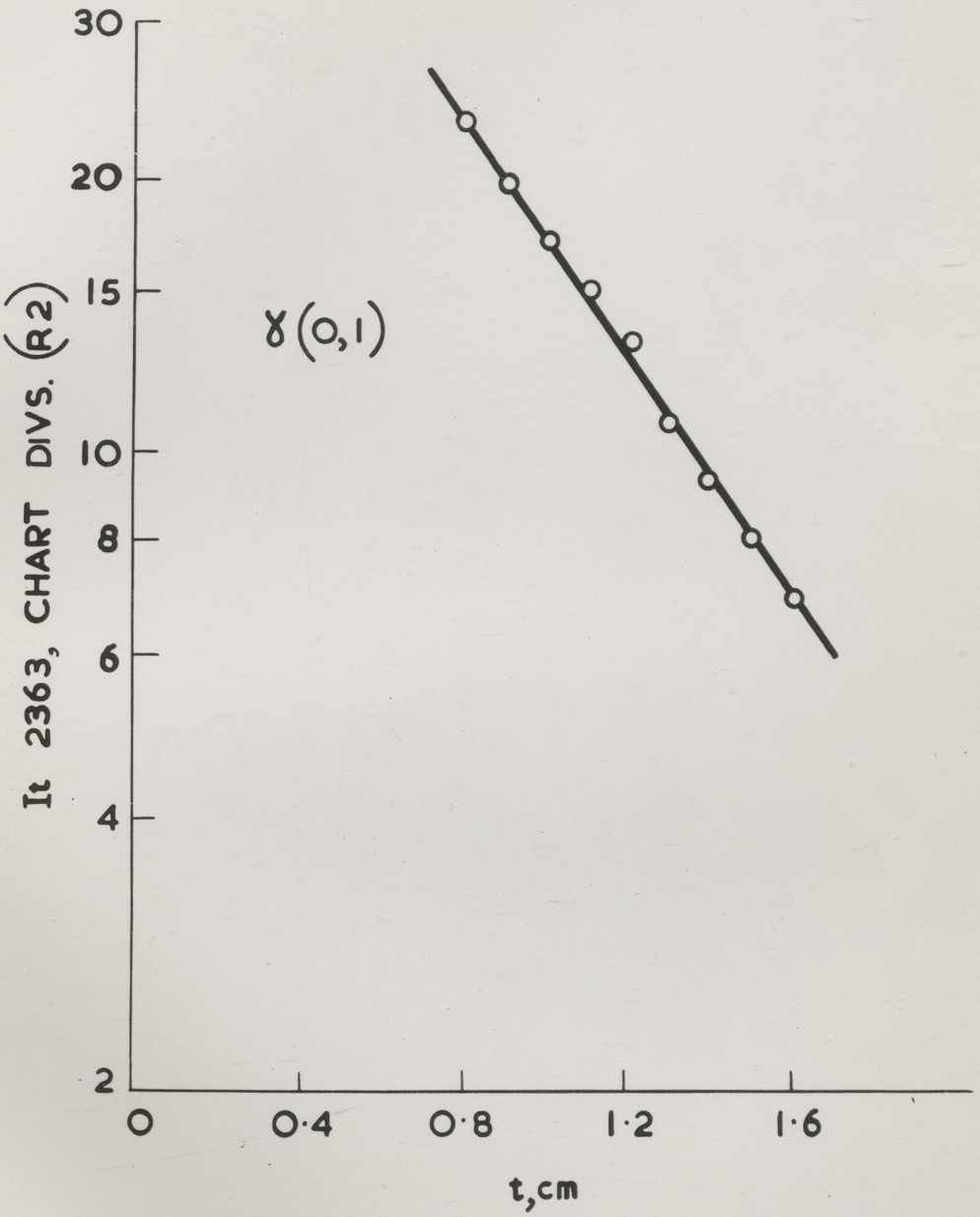

FIG. 9

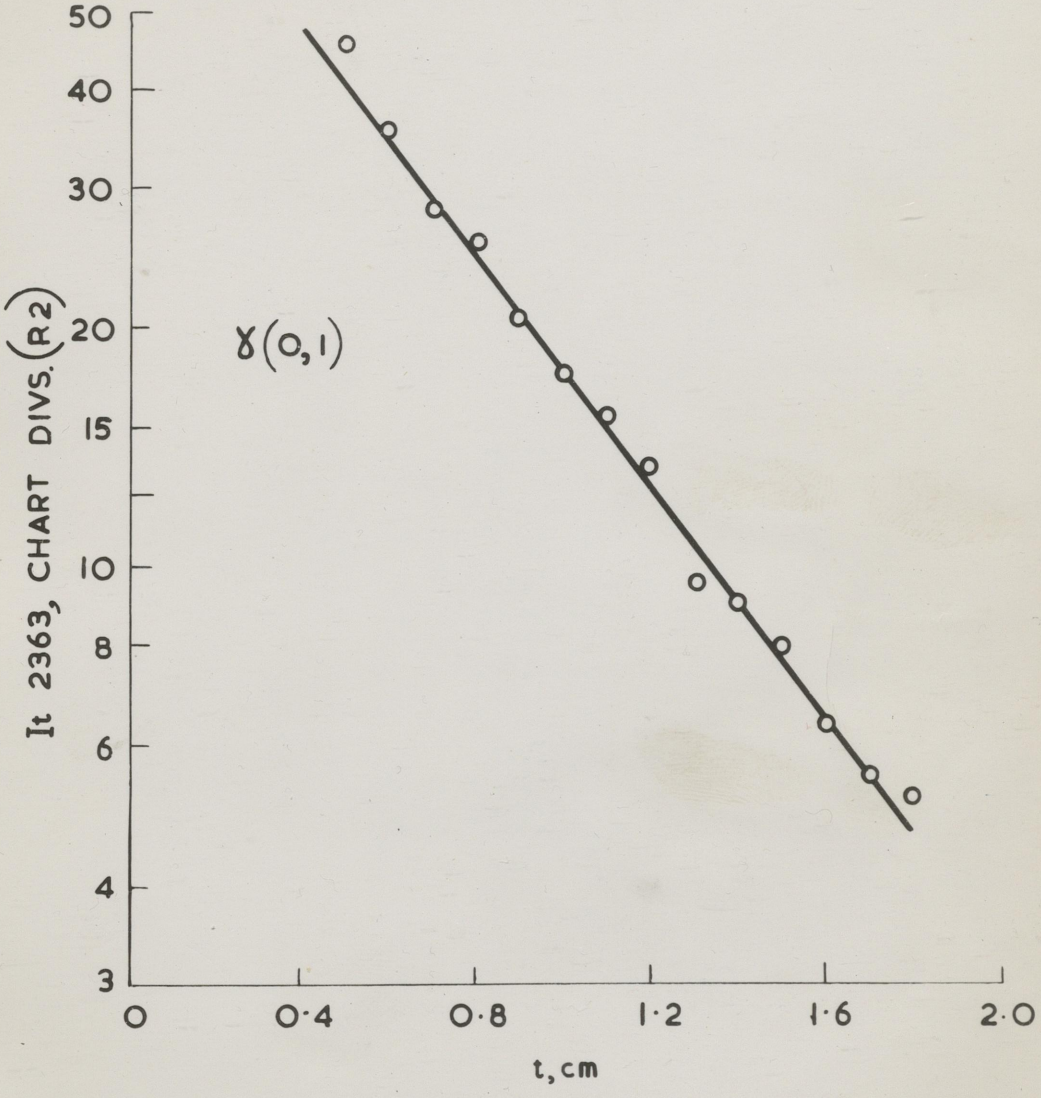
50
40
30
20
15
10
8
6
4
3
It 2363, CHART DIVS. (R2)
γ(0,1)
0
0·4
0·8
1·2
1·6
2·0
t, cm

FIG. 10

TABLE 8. AFTERGLOW DECAY CONSTANT R_{N_2} OF THE 5854 Å (10,6), 5804 Å (11,7), 5755 Å (12,8) NITROGEN 1ST POSITIVE BANDS VS. OXYGEN ADDED.

Run	R_{N_2} sec^{-1} $= \frac{-d \log It5755}{dt}$	Mean R_{N_2} sec^{-1}	Number of Oxygen Molecules cc added cc^{-1}
7	1.21 1.26 1.32	1.26	3.7×10^{12}
8	1.14 1.04 1.04	1.07	3.7×10^{12}
5	0.585 0.583	0.58	7×10^{12}
6	0.758 0.78 0.78	0.77	3.6×10^{13}
3	1.15 1.185	1.17	3.7×10^{13}

TABLE 9. AFTERGLOW DECAY CONSTANT R_{NO} OF THE 2370 Å - 2363 Å γ (0.1) NITRIC OXIDE BAND VS. OXYGEN ADDED.

Run	R_{NO} sec^{-1} $= \frac{-d \log It2363}{dt}$	Mean R_{NO} sec^{-1}	Number of Oxygen Molecules added cc^{-1}
7	0.663 0.663	0.66	3.7×10^{12}
8	0.65 0.655 0.608	0.63	3.7×10^{12}
5	0.382 0.317 0.34	0.35	7×10^{12}
6	0.72 0.66 0.76	0.75	3.6×10^{13}
3	0.976 0.94 0.976	0.96	3.7×10^{13}

TABLE 10. AFTERGLOW DECAY CONSTANT R_{NO} OF THE 2892 Å - 2885 Å $\beta(0,6)$ NITRIC OXIDE BAND VS. OXYGEN ADDED.

Run	R_{NO} sec^{-1} $= \frac{-d \log I_{t2890}}{dt}$	Mean R_{NO} sec^{-1}	Number of Oxygen Molecules added cc^{-1}
7	0.9	0.9	3.7×10^{12}
8	0.6 0.57 0.55	0.51	3.7×10^{12}
5	0.324	0.32	7×10^{12}
6	0.513 0.53 0.51	0.52	3.6×10^{13}
3	0.92 1.18 1.18	1.1	3.7×10^{13}

TABLE 11. AFTERGLOW DECAY CONSTANT R_{NO} OF THE 3206 Å - 3198 Å β (0.8) NITRIC OXIDE BAND VS. OXYGEN ADDED.

Run	R_{NO} sec^{-1} $= \frac{-d \log It3200}{dt}$	Mean R_{NO} sec^{-1}	Number of Oxygen Molecules added cc^{-1}
7	0.9	0.9	3.7×10^{12}
8	0.605 0.605	0.61	3.7×10^{12}
5	0.324 0.324	0.32	7×10^{12}
6	0.446 0.446 0.446	0.45	3.6×10^{13}
3	0.95 0.88	0.91	3.7×10^{13}

About an hour was needed to record all the afterglow bands during a run, and it seems likely that some change was taking place in the discharge tube vacuum system during this time, e.g. either adsorption or desorption of oxygen by the walls of the vacuum system. It will be seen that in experiment B, where more precautions were taken R_{NO} for the $v^1 = 0, \gamma$ bands is $(15 \pm 5)\%$ greater than R_{NO} for the $v^1 = 0$ β bands, (3.6.3).

3.3 Procedure B. The Oxygen Inlet Device.

In order to obtain results which could be more easily interpreted, it was decided to devise a method of adding small, known amounts of oxygen to the nitrogen already in the system. It was impossible to measure the amount added by the corresponding rise in pressure in the system as this was undetectable when $\sim 0.01\%$ of oxygen was added to the nitrogen. Using the procedure described below, oxygen was added to the nitrogen in amounts corresponding to a partial pressure $\sim 3 \times 10^{-4}$ mm Hg, and it was found that the intensities and decay constants of the afterglow bands varied in a regular manner with the oxygen added. Also it was found possible to record the afterglow decay curves for up to 7 different percentages of oxygen without pumping the nitrogen from the system.

The oxygen inlet device is shown in fig.11. Using it a small amount of oxygen from the oxygen reservoir could be expanded into the upper bulb and then admitted to the system. The device was set up for an experiment in the following way. The whole system was evacuated to a pressure of about 10^{-5} mm Hg, and outgassed

Fig.11. Oxygen Inlet Device.

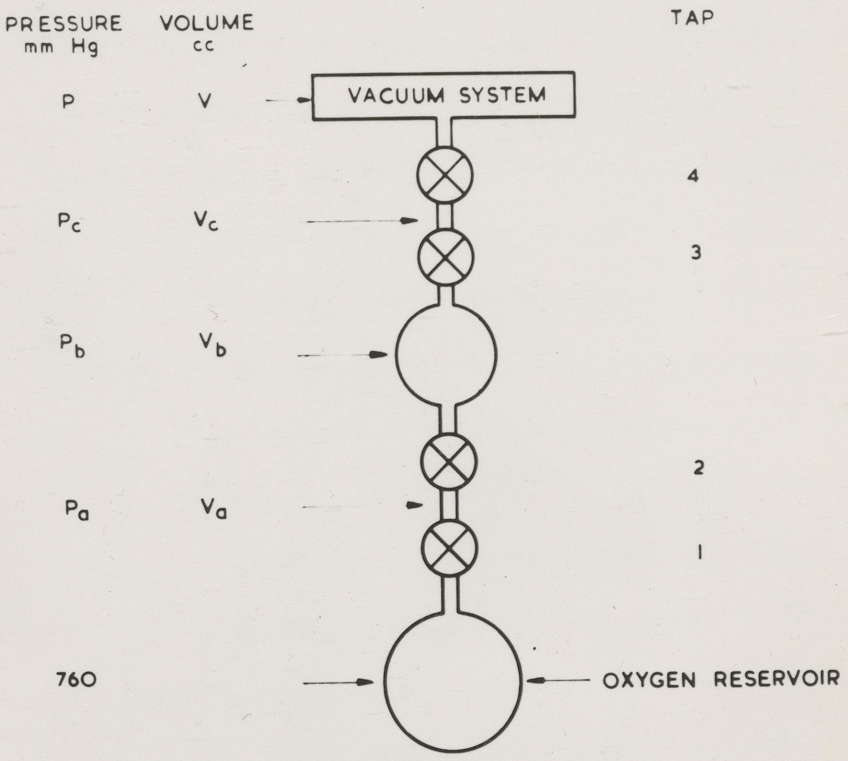
PRESSURE
mm Hg
VOLUME
cc
TAP
P
V
VACUUM SYSTEM
4
Pc
Vc
3
Pb
Vb
2
Pa
Va
1
760
OXYGEN RESERVOIR

a

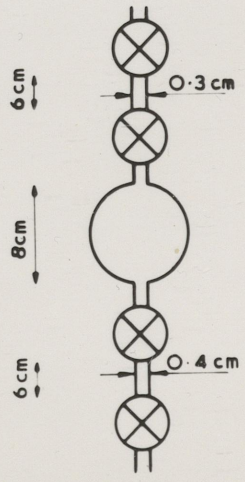
6cm
0·3 cm
8cm
6cm
0·4 cm

b

FIG. 11

using the R.F. power supply and flexible copper electrodes which could be secured to different parts of the system using crocodile clips. The system was then pumped down to base pressure and this pressure maintained using the diffusion pump and the backing pump. All taps 1, 2, 3, 4 of the oxygen inlet device were closed. The seal on the oxygen reservoir bottle was broken, and tap 1 opened for 1 minute to admit oxygen at about atmospheric pressure to the volume V_A. Tap 1 was then closed, and tap 2 opened for 1 minute to expand the oxygen into the bulb of volume V_B; tap 2 was then closed. The backing pump was then isolated from the system by closing tap 7. Nitrogen was admitted to the system to a pressure of about 1 mm Hg using the double tap system above the nitrogen bottle. Tap 4 of the oxygen inlet device was then opened for about a minute to admit nitrogen to the volume V_C. This step was not essential but in any case nitrogen would enter the volume V_C every time tap 4 was opened to admit oxygen to the system. The entry of nitrogen to V_C and V_B would not introduce any serious error into the method as explained below (3.4.2). Tap 3 was then opened, and oxygen and nitrogen allowed to mix in the volume V_B plus V_C.

In procedure B the diffusion pump was used as a circulating pump to ensure that the oxygen introduced at a relatively high pressure at one point of the system would be uniformly mixed with the nitrogen. Thus after setting up the oxygen inlet device

as described above, the procedure for the rest of the experiment was as follows. Tap 7 was adjusted so that the discharge tube vacuum system became a complete circuit; and, with the R.F. pulsed discharge running in the discharge tube with a pulse period of 0.5 seconds and a repetition time of 6 seconds, the diffusion pump was used to circulate the B.O.C. nitrogen in the system for about 15 minutes. This was done so that the procedure would be unchanged even when no oxygen had been added. The diffusion pump was then switched off and allowed to cool, and after a further 15 minutes the afterglow pulses succeeding each pulse of R.F. glow discharge became more reproducible. The monochromator was then set at the wavelengths shown in table 12; and the decaying afterglows of the corresponding nitric oxide bands recorded, using the photomultiplier and Brown recorder. About 12 afterglow pulses were recorded for each wavelength setting. The sequence of R.F. discharge pulses was not interrupted between the recording of the afterglows of different bands. This was the case for all recordings of afterglow bands in procedure B. After all the afterglow bands had been recorded; tap 3 of the oxygen inlet device was closed, the discharge cycle stopped, and the diffusion pump switched on. After about 5 minutes it was confirmed that the gas in the system was circulating by running the discharge for a moment and observing the afterglow streaming out of the discharge tube. Tap 4 of the oxygen inlet device was then opened and about

5 minutes later the cycle of R.F. glow discharge pulses was started. After about 15 minutes the diffusion pump was switched off; tap 4 of the oxygen inlet device was closed, and tap 3 opened to allow oxygen and nitrogen to mix in the volume V_B plus V_C. After a further 15 minutes the afterglow pulses following each R.F. glow discharge pulse had become reasonably reproducible, and bands of the afterglow spectrum were then recorded as described above. When all the afterglow bands had been recorded, tap 3 of the oxygen inlet device was closed and a further dose of oxygen was added to the nitrogen in the system. The afterglow bands emitted from this nitrogen, oxygen mixture were then recorded. This procedure was repeated several times; and in the results described in (3.6) seven sets of afterglow bands are recorded, corresponding to seven different oxygen concentrations.

3.4 Calibration of the Oxygen Inlet Device.

3.4.1 Measurement.

The device was calibrated as follows. The discharge tube vacuum system was evacuated and oxygen was admitted to the system in steps after expansion in the inlet device as described in (3.3). The gas pressure in the system after each amount of oxygen had been added was estimated using the ion gauge. However, after each dose of oxygen had been added the pressure in the system decreased rapidly after the initial rise, presumably because of adsorption of gas on the walls of the system. In order to prevent

this pressure variation occuring $\sim$0.1 mm Hg of oxygen (measured on the Pirani gauge) was admitted to the system and pumped out without outgassing the system. This procedure saturated the walls of the vacuum system with oxygen. As before oxygen was admitted to the system in steps using the inlet device; and the gas pressure then remained almost perfectly steady after each addition of oxygen. The gas pressure in the system was noted just before and after each addition of oxygen using the ion gauge; the difference of the two readings being a measure of the oxygen dose added to the system in one complete cycle of the oxygen inlet device. The mean oxygen dose measured on the ion gauge and corrected for the sensitivity of the gauge to oxygen was 3.1×10^{-4} mm Hg.

3.4.2 Calculation.

Measurements were made of the approximate dimensions of the oxygen inlet system shown in fig.11 b. The internal diameter of the bulb was about 8 cm and so its volume was 268 cc. The internal diameters of the lengths of tubing corresponding to V_A and V_C were 0.4 cm and 0.3 cm respectively. The pressure P_A of the oxygen in the reservoir was approximately 760 mm.

From the measured dimensions

$$V_A = 6 \times \pi \times 0.04 \text{ cc} = 0.75 \text{ cc}$$

$$V_B = \frac{4}{3} \pi \times 4^3 = 286 \text{ cc}$$

$V_C = 6 \times \pi \times 0.0225$ cc $= 0.42$ cc

$P_A = 760$ mm Hg

$P_A V_A = 760 \times 0.75 = 570$ mm Hg.cc. When the oxygen from V_A was expanded into the bulb V_B, its pressure fell to P_B.

According to Boyle's Law

$$P_A V_A = P_B V_B$$

Thus $P_B = \frac{570}{286} = 2.0$ mm Hg.

When the oxygen was expanded from the bulb V_B into the volume there would be only about a 0.2% decrease in pressure.

Thus $P_C = P_B = 2.0$ mm Hg.

Thus $P_C V_C = 2.0 \times 0.42 = 0.84$ mm Hg.cc.

The volume of the system V which contained a 5 litre reservoir was estimated as 7.5×10^3 cc. Thus when the oxygen from V_C was expanded into the system the resulting pressure would be given by

$$P = \frac{0.84}{7.5 \times 10^3} = 1.1 \times 10^{-4} \text{ mm Hg.}$$

The discrepancy with the measured value was probably due to inaccuracies in the measurement of the internal diameter of the volumes V_A and V_C, and the measured value of 3.1×10^{-4} mm Hg was taken as the correct value. There would be a slight decrease in the reservoir pressure after a few experiments. This would be quite small and in fact all experiments were done with an almost full reservoir; also there would be a

0.2% decrease in the pressure of oxygen in the 286 cc bulb each time oxygen was expanded into $V_C \simeq 0.4$ cc. Each time tap 3 was opened the nitrogen percentage in bulb V_B increased by about 0.1%, as the nitrogen pressure in V_C was ~ 1 mm Hg since this volume was directly connected to the system at various times during the experiments. All these errors were small or could be allowed for.

3.5 Monochromator Slit Width Settings.

Table 12 shows the nitric oxide β and γ bands recorded in experiment B and the corresponding settings of the monochromator wavelength drum, entrance slit and exit slit. The slit widths used in experiment B were determined by the conflicting requirements to allow the maximum amount of light from the afterglow to enter the photomultiplier and to look at only one band at a time.

The magnification of the monochromator prism for a beam of light was unity, since the light leaving the exit slit always passed through the prism parallel to one of its edges in the position of minimum deviation.

Thus the width, Δ Å of each band at the exit slit was equal to the width of the entrance slit $\Delta 2$ Å plus the extra amount due to the finite width of the band $\Delta 1$ Å. The width of the exit slit $\Delta 3$ Å was usually made just greater or just less than the total width Δ Å of the band being studied. The values of $\Delta 2$ Å and $\Delta 3$ Å were calculated from the dispersion curve for the

TABLE 12. EXPERIMENT B. NITRIC OXIDE BANDS INVESTIGATED AND THE CORRESPONDING MONOCHROMATOR SETTINGS.

Band Wave-length Å	Band Width Δ_1 Å	(v^1, v^{11})	Mono-chromator Wave-length setting. Å	Mono-chromator Entrance Slit Width mm	Mono-chromator Entrance Slit Width Δ_2 Å	Total Band Width Δ Å	Mono-chromator Exit Slit Width mm	Mono-chromator Exit Slit Width Δ_3 Å	Symbol for Band Afterglow Intensity at time Δ t secs. after opening of shutter Chart Divs. (R_2)	Symbol for Band Afterglow Intensity at time t secs. after opening of shutter Chart Divs. (R_2)
2370 2363	7	$\gamma(0,1)$	2365	0.5	12.5	19.5	0.8	20	Ip2363	It2363
2478 2471	7	$\gamma(0,2)$	2475	0.5	17.5	24.5	0.8	27.2	Ip2475	It2475
2595 2587	8	$\gamma(0,3)$	2590	0.5	22.5	30.5	0.6	27	Ip2590	It2590
2892 2885	7	$\beta(0,6)$	2890	0.2	20	27	0.3	25.5	Ip2890	It2890
3043 3034	9	$\beta(0,7)$	3040	0.2	20.5	29.5	0.3	33	Ip3040	It3040
3206 3198	8	$\beta(0,8)$	3200	0.2	22	30	0.3	27.5	Ip3200	It3200

Fig.12a. Widths and Relative Positions of Nitric Oxide Afterglow Bands in Ångstroms. Monochromator entrance slit width 0.5 mm. ($\Delta s = \Delta 3$)

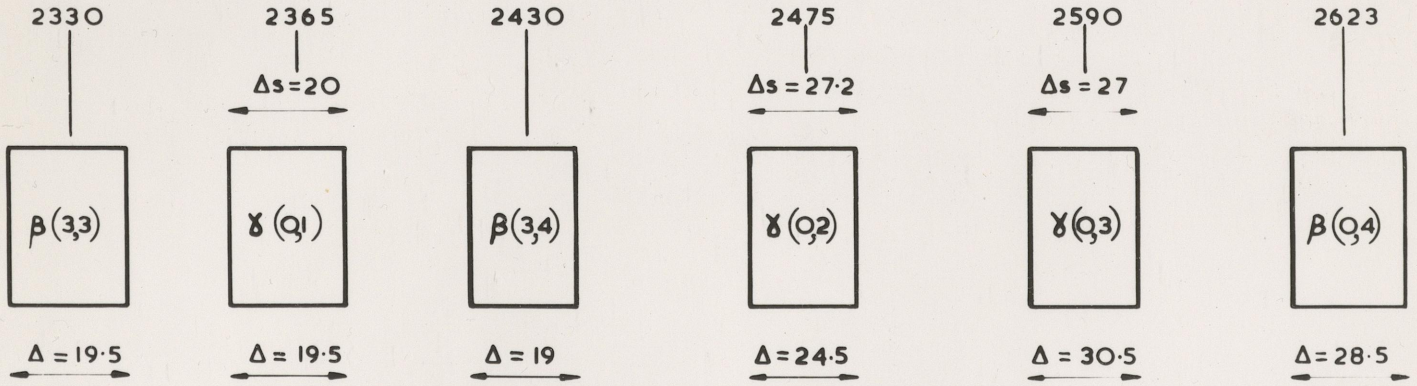
units = Å
2330
2365
2430
2475
2590
2623
Δs = 20
Δs = 27·2
Δs = 27
β (3,3)
γ (0,1)
β (3,4)
γ (0,2)
γ (0,3)
β (0,4)
Δ = 19·5
Δ = 19·5
Δ = 19
Δ = 24·5
Δ = 30·5
Δ = 28·5

FIG. 12a.

monochromator published by Messrs. Hilger. Fig 12a indicates the total width and the relative positions of the nitric oxide bands identified from a photograph of the afterglow spectrum (fig.6a), also the exit slit widths used. It can readily be seen that no overlapping of the nitric oxide bands in the exit slit should occur. The nitrogen dioxide continuum observed with high percentages of oxygen extends from 4000 Å to 7000 Å according to Kurzweg, Bass and Broida (1957), so that even if it were present, it would not overlap the nitric oxide bands studied in experiment B.

3.6 Results B.

3.6.1 Afterglow Intensity Measurements.

Tables 13 to 19 are the results obtained using the procedure described in (3.3). The shutter described in (2.1) was used in the experiment to cover the entrance slit of the monochromator, while the R.F. discharge was running. The afterglow intensities of various nitric oxide bands were measured 0.94 seconds after the opening of the shutter. Measurements of the intensities of the γ (0,3) and γ (0,6) nitric oxide bands versus oxygen added are shown in tables 13 and 14 respectively. Measurements of the intensities of the γ (0,1), γ (0,2) and β (0,7) nitric oxide bands versus oxygen added are included in table 15. In fig.12 log (afterglow intensity) versus oxygen added is plotted for the γ(0,1), γ(0,2), γ (0,3), β(0,6) and β (0,7) bands.

TABLE 13. AFTERGLOW INTENSITY Ip2590 OF THE 2595 Å - 2587 Å

γ (0.3) NITRIC OXIDE BAND VS. OXYGEN ADDED.

Ip2590 Chart Divs. (R_2)	Mean Ip2590 Chart Divs. (R_2)	Number of Oxygen Molecules added cc^{-1}	Percentage of Oxygen added
35 34.5 34	34.5	0	0
15.4 15.4 15.8 14.8 14.9	15.3	10^{13}	0.025
10 8 10 9 9.5	9.3	2×10^{13}	0.05
6 8 6.5 6.5 6.5	6.7	3.1×10^{13}	0.075
4.5 5.5 5.5 5.5 5.5 5.5	5.5	4.1×10^{13}	0.1
3.6 4.1 4.6 4.6 5.6 4.6	4.4	5.1×10^{13}	0.125
3.2 1.8 3.7 2.6 2.85 2.65 3.65 3.1 3.15	3	6.1×10^{13}	0.15

TABLE 14. AFTERGLOW INTENSITY Ip2890 OF THE 2892 Å - 2885 Å β(0,6) NITRIC OXIDE BAND VS. OXYGEN ADDED.

Ip2890 Chart Divs.(R_2)	Mean Ip2890 Chart Divs.(R_2)	Number of Oxygen Molecules added cc^{-1}	Percentage of Oxygen added
7 7 7 7 6 6	6.7	0	0
3 3 3.8 2.9 2.6 3 3	3.04	10^{13}	0.025
2 1.8 1.6 1.6 2 2 2	1.86	2×10^{13}	0.05
1.5 1.2 1.5 1.4 1.4 1.6	1.3	3.1×10^{13}	0.075
0.9 0.9 0.7 1.0 1.1 1.0 1.0	0.94	4.1×10^{13}	0.1
0.9 1.1 0.8 1.0 0.9 1.0 0.9	0.94	5.1×10^{13}	0.125
0.4 0.3 0.4 0.3 0.3 0.4	0.45	6.1×10^{13}	0.15

TABLE 15. AFTERGLOW INTENSITIES Ip2363, Ip2475, Ip3040 OF THE 2370 Å - 2363 Å γ (0,1), 2478 Å - 2471 Å δ (0,2), 3043 Å - 3034 Å β (0,7) NITRIC OXIDE BANDS VS. OXYGEN ADDED.

Mean Ip2363 Chart Divs.(R_2)	Mean Ip2475 Chart Divs.(R_2)	Mean Ip3040 Chart Divs.(R_2)	Number of Oxygen Molecules added cc^{-1}	Percentage of Oxygen added
47	44	8	0	0
	21	3.9	10^{13}	0.025
12.5	12	2.8	2×10^{13}	0.05
7.3	7.7	1.8	3.1×10^{13}	0.075
5.8	6.5	1.4	4.1×10^{13}	0.1
	5.6	1.05	5.1×10^{13}	0.125
	3.8		6.1×10^{13}	0.15

Fig.12. Afterglow Intensity of $v^1 = 0$ Nitric Oxide Bands 0.94 seconds after opening of shutter vs. percentage of Oxygen added.

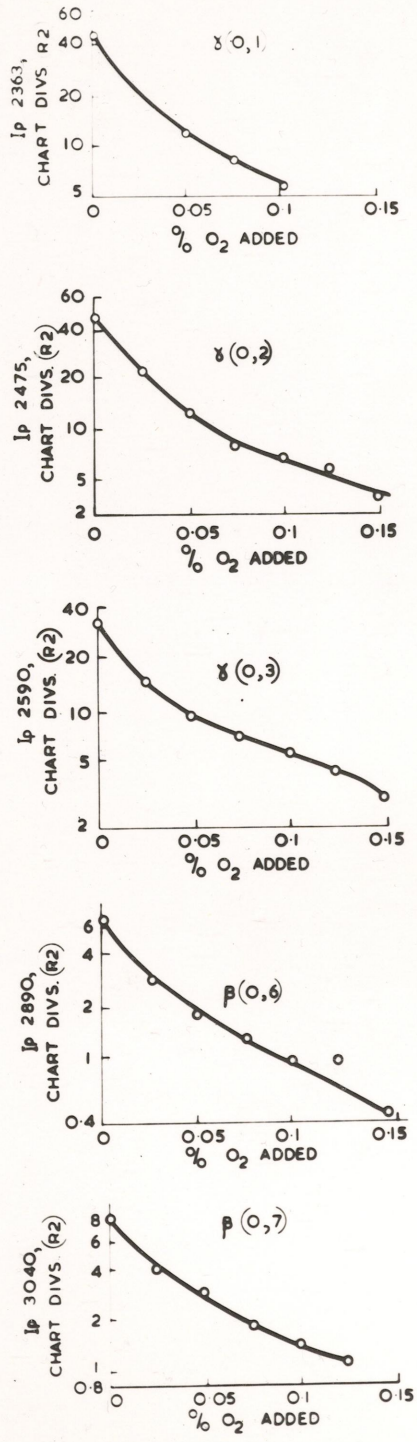
Ip 2363, CHART DIVS R2
60
40
20
10
5
γ (0,1)
0
0·05
0·1
0·15
% O2 ADDED
Ip 2475, CHART DIVS. (R2)
60
40
20
10
5
2
γ (0,2)
0
0·05
0·1
0·15
% O2 ADDED
Ip 2590, CHART DIVS. (R2)
40
20
10
5
2
γ (0,3)
0
0·05
0·1
0·15
% O2 ADDED
Ip 2890, CHART DIVS. (R2)
6
4
2
1
0·4
β (0,6)
0
0·05
0·1
0·15
% O2 ADDED
Ip 3040, CHART DIVS (R2)
8
6
4
2
1
0·8
β (0,7)
0
0·05
0·1
0·15
% O2 ADDED

FIG. 12

No striking change in the relative intensities of the $v^1 = 0$, β and γ nitric oxide afterglow bands is evident. The large scatter of points about the average curve for the β (0,6) band, for percentages of oxygen above 0.1%, is probably due to errors in the estimation of the background intensity. The lower intensities of this band were recorded on range 1 as they were too small to be measured on range 2 of the recording system.

3.6.2 <u>(Afterglow Intensity)$^{-\frac{1}{2}}$</u>

In table 16 (afterglow intensity)$^{-\frac{1}{2}}$ is calculated for the γ (0,1), γ (0,2), γ (0,3), β (0,6) and β (0,7) nitric oxide bands. In figs.13 to 16 (afterglow intensity)$^{-\frac{1}{2}}$ is plotted against oxygen added per cc of the discharge tube vacuum system for the γ (0,2), γ (0,3), β (0,6) and β (0,7) nitric oxide bands. Straight lines have been drawn through the experimental points and the scatter of points about the straight lines is not, in general, large. There is a small but noticeable oscillation about the mean gradient, however, which is reproduced in each curve. In table 17 the gradients of the plots in figs. 13 to 16 are compared. Each gradient is multiplied by (afterglow intensity)$^{\frac{1}{2}}$ of the corresponding nitric oxide band for zero addition of oxygen in order to bring the gradients onto a comparable scale. There is some variation in these values, $\sim$15% of the largest value, but the closeness of the values

TABLE 16. (AFTERGLOW INTENSITY)$^{-\frac{1}{2}}$ VS. OXYGEN ADDED.

γ (0,1) $Ip^{-\frac{1}{2}}$2363 (Chart Divs.$(R_2))^{-\frac{1}{2}}$	γ (0,3) $Ip^{-\frac{1}{2}}$2590 (Chart Divs.$(R_2))^{-\frac{1}{2}}$	γ (0,2) $Ip^{-\frac{1}{2}}$2475 (Chart Divs.$(R_2))^{-\frac{1}{2}}$	β (0,6) $Ip^{-\frac{1}{2}}$2885 (Chart Divs.$(R_2))^{-\frac{1}{2}}$	β (0,7) $Ip^{-\frac{1}{2}}$3040 (Chart Divs.$(R_2))^{-\frac{1}{2}}$	Number of Oxygen Molecules added cc^{-1}	Percentage of Oxygen added
0.15	0.17	0.15	0.39	0.35	0	0
	0.26	0.22	0.57	0.51	10^{13}	0.025
0.28	0.33	0.29	0.73	0.6	2×10^{13}	0.05
0.37	0.39	0.36	0.88	0.75	3.1×10^{13}	0.075
0.415	0.43	0.39	1.0	0.85	4.1×10^{13}	0.1
	0.48	0.42	1.0	0.98	5.1×10^{13}	0.125
	0.58	0.52	1.5		6.1×10^{13}	0.15

Figs. 13, 14, 15 and 16. (Afterglow Intenaity of Nitric Oxide Bands 0.94 seconds after opening of shutter)$^{-\frac{1}{2}}$ vs. Percentage of Oxygen added.

Fig.13. 2478 A - 2471 A γ (0,2) Band

Fig.14. 2595 A - 2587 A γ (0,3) Band

Fig.15. 2892 A - 2885 A β (0,6) Band

Fig.16. 3043 A - 3034 A β (0,7) Band.

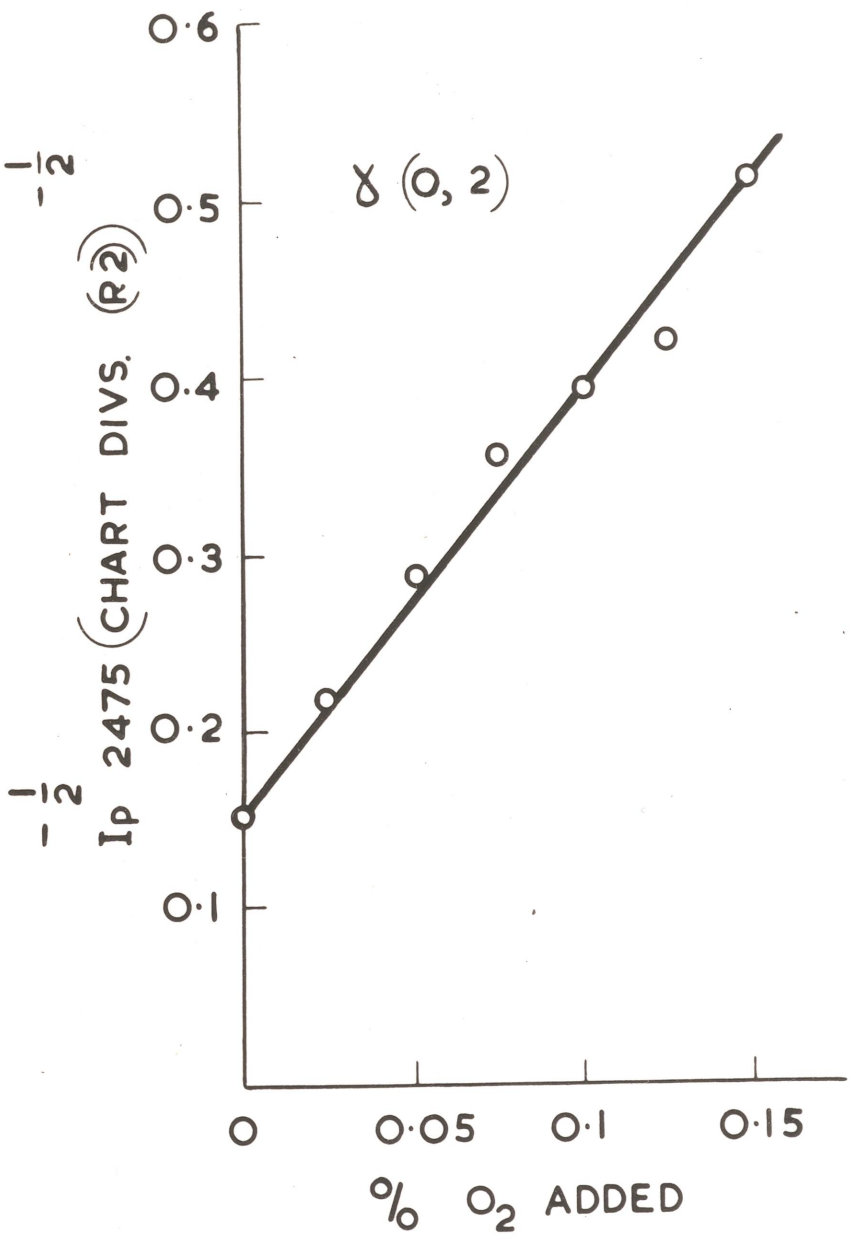
0·6
0·5
0·4
0·3
0·2
0·1
$I_p^{-\frac{1}{2}}$ 2475 (CHART DIVS. (R2))$^{-\frac{1}{2}}$
γ (0, 2)
0
0·05
0·1
0·15
% O_2 ADDED

FIG. 13

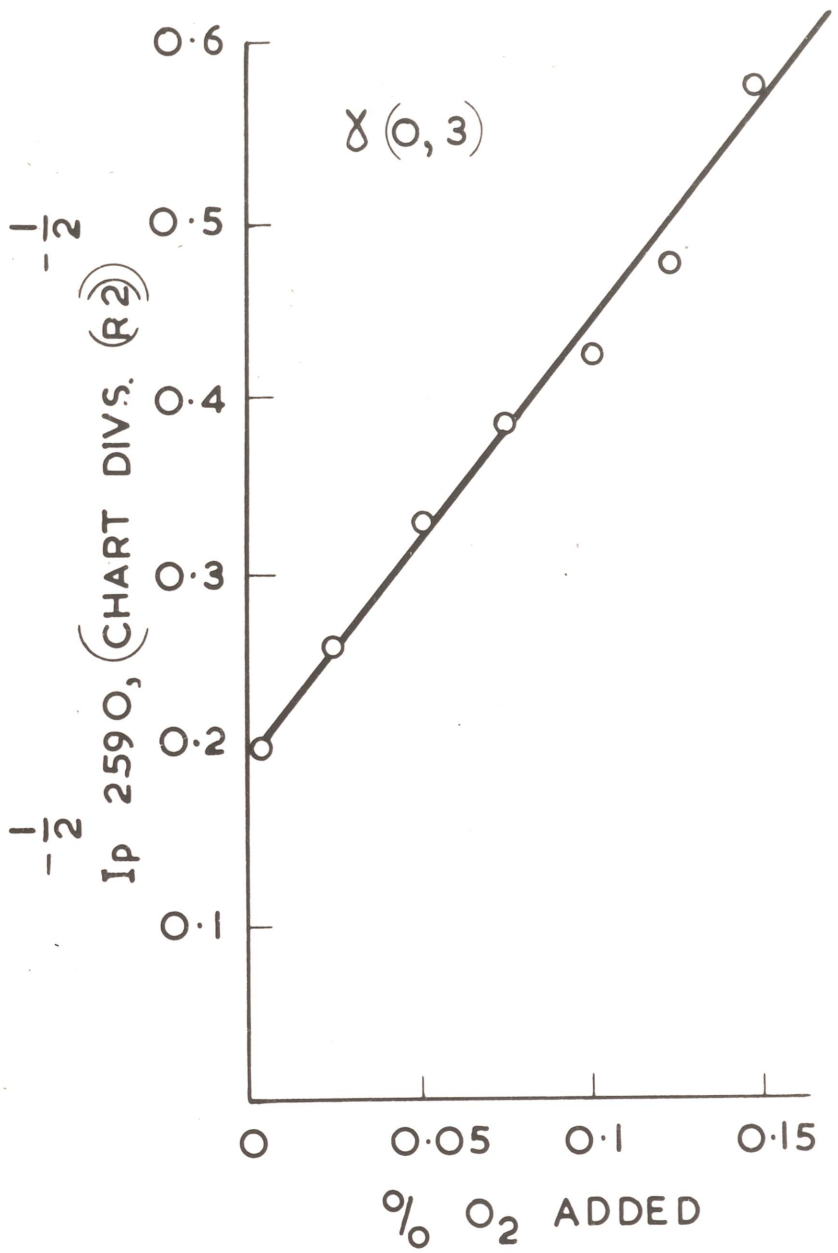
0·6
0·5
0·4
0·3
0·2
0·1
γ (0, 3)
$I_{p}^{-\frac{1}{2}}$ 2590, (CHART DIVS. (R2))$^{-\frac{1}{2}}$
0
0·05
0·1
0·15
% O_2 ADDED

FIG. 14

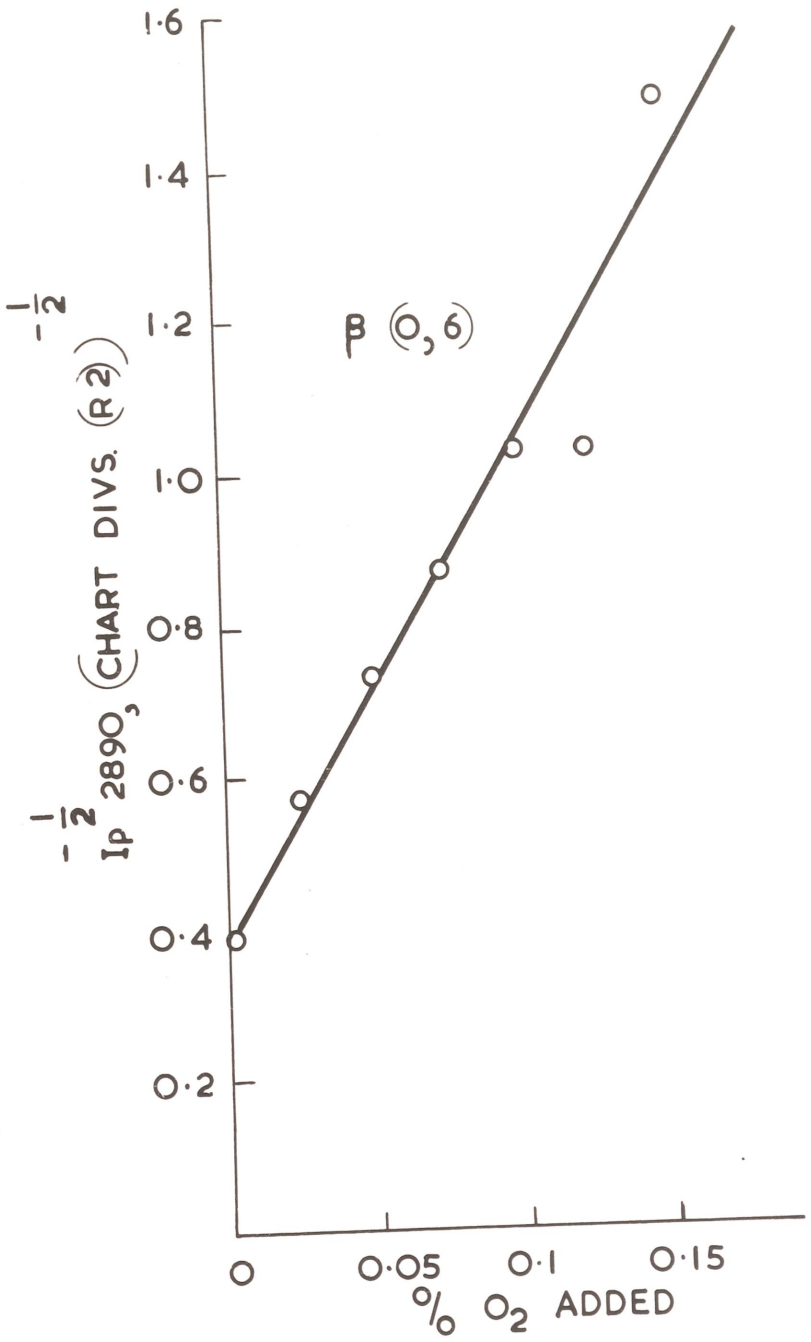
1·6
1·4
1·2
1·0
0·8
0·6
0·4
0·2
$I_p^{-\frac{1}{2}}$ 2890, (CHART DIVS. (R2))$^{-\frac{1}{2}}$
B (0, 6)
0
0·05
0·1
0·15
% O_2 ADDED

FIG. 15

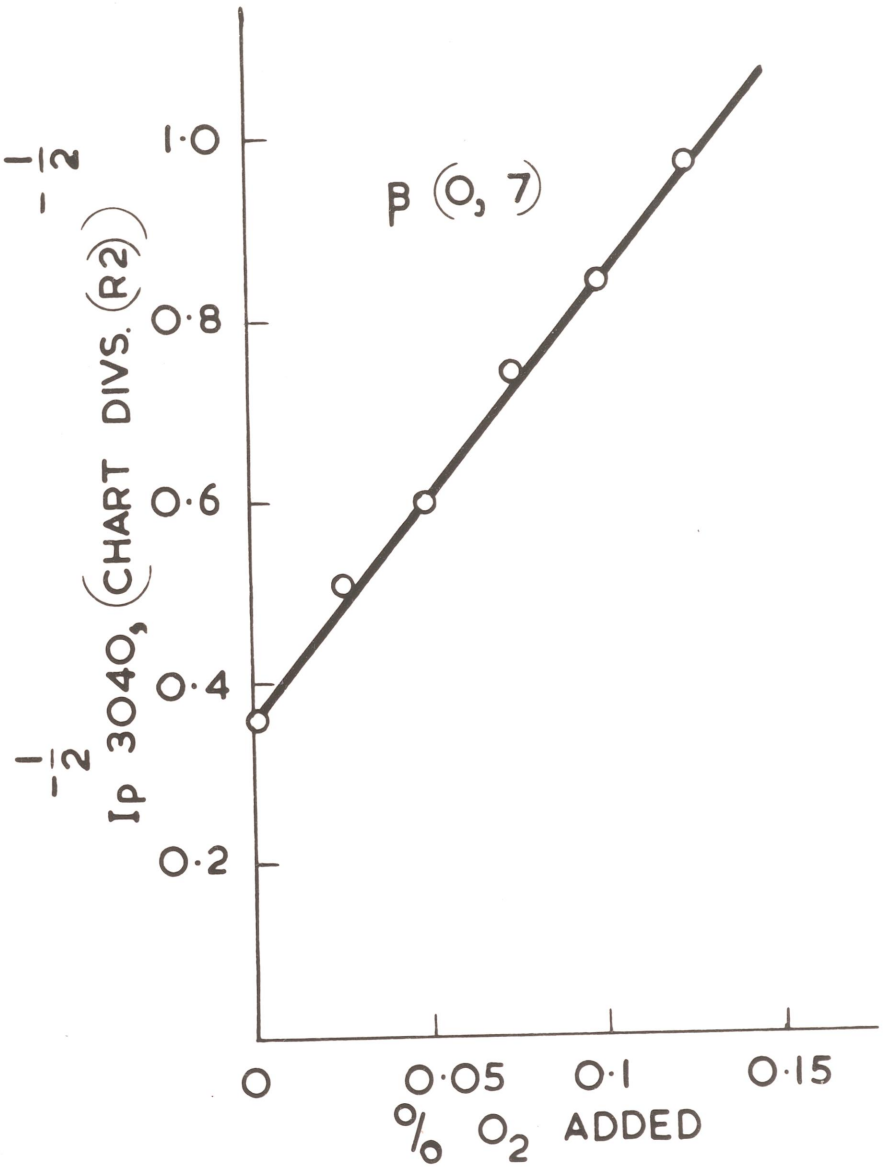
I_p 3040, (CHART DIVS. (R2))$^{-\frac{1}{2}}$
I_p 3040, (CHART DIVS. (R2))$^{-\frac{1}{2}}$
1·0
0·8
0·6
0·4
0·2
β (0, 7)
0
0·05
0·1
0·15
% O_2 ADDED

FIG. 16

TABLE 17. COMPARISON OF GRADIENTS OF AFTERGLOW INTENSITY AND OXYGEN ADDED FOR VARIOUS NITRIC OXIDE BANDS.

γ (0,2) $I_{op}^{\frac{1}{2}}2475 \times \frac{dI_p^{-\frac{1}{2}}2475}{dn_3}$ mol.$^{-1}$	γ (0,3) $I_{op}^{\frac{1}{2}}2590 \times \frac{dI_p^{-\frac{1}{2}}2590}{dn_3}$ mol.$^{-1}$	β (0,6) $I_{op}^{\frac{1}{2}}2890 \times \frac{dI_p^{-\frac{1}{2}}2890}{dn_3}$ mol.$^{-1}$	β (0,7) $I_{op}^{\frac{1}{2}}3040 \times \frac{dI_p^{-\frac{1}{2}}3040}{dn_3}$ mol.$^{-1}$
4.1×10^{-14}	3.7×10^{-14}	4.3×10^{-14}	3.9×10^{-14}

Note : n_3 mol.cc^{-1} = number of oxygen molecules added per cc of the discharge tube vacuum system.

of the quantities in table 17 and the linearity of the plots in figs. 13 to 16 appear to be significant. They show that (afterglow intensity)$^{-\frac{1}{2}}$ = E + F. (oxygen added cc^{-1}), where E and F are independent of oxygen added to the system. Since as mentioned above there is a small oscillation about the straight lines drawn in figs. 11 to 14 the above equation represents the mean variation of (afterglow intensity)$^{-\frac{1}{2}}$ with added oxygen.

3.6.3 Afterglow Decay Rate Measurements.

As observed in experiment A the decay of the afterglow intensity was exponential with respect to time, i.e.

$$\frac{d \log It}{d t} = - R_{NO} \text{ sec}^{-1}, \quad \text{where}$$

R_{NO} is a constant, t is time and It is the intensity of an individual afterglow band at time t seconds after the opening of the shutter. Plots of log It versus time are shown in figs. 17 and 18 for the 2595 A - 2587 Å γ (0,3) nitric oxide band for 0% and 0.1% of oxygen added to the nitrogen. The gradients of these graphs are equal to - R_{NO}. In table 18 values of R_{NO} are shown for the γ (0,3) and β (0,6) nitric oxide bands and percentages of oxygen up to 0.15%. R_{NO} for the γ(0,3) band is (15 $\pm$ 5)% greater than R_{NO} for the β (0,6) band from table 18.

In fig.19 R_{NO} is plotted versus oxygen added for the γ (0,3) and β (0,6) bands. Straight lines have been drawn

Fig. 17 and 18. Decay with time of the Afterglow Intensity It2590 of the 2595 Å - 2587 Å γ (0,3) Nitric Oxide Band. Fig.17. 0% oxygen added. Fig.18. 0.1% oxygen added.

(1 cm of chart ≡ 2.36 seconds)

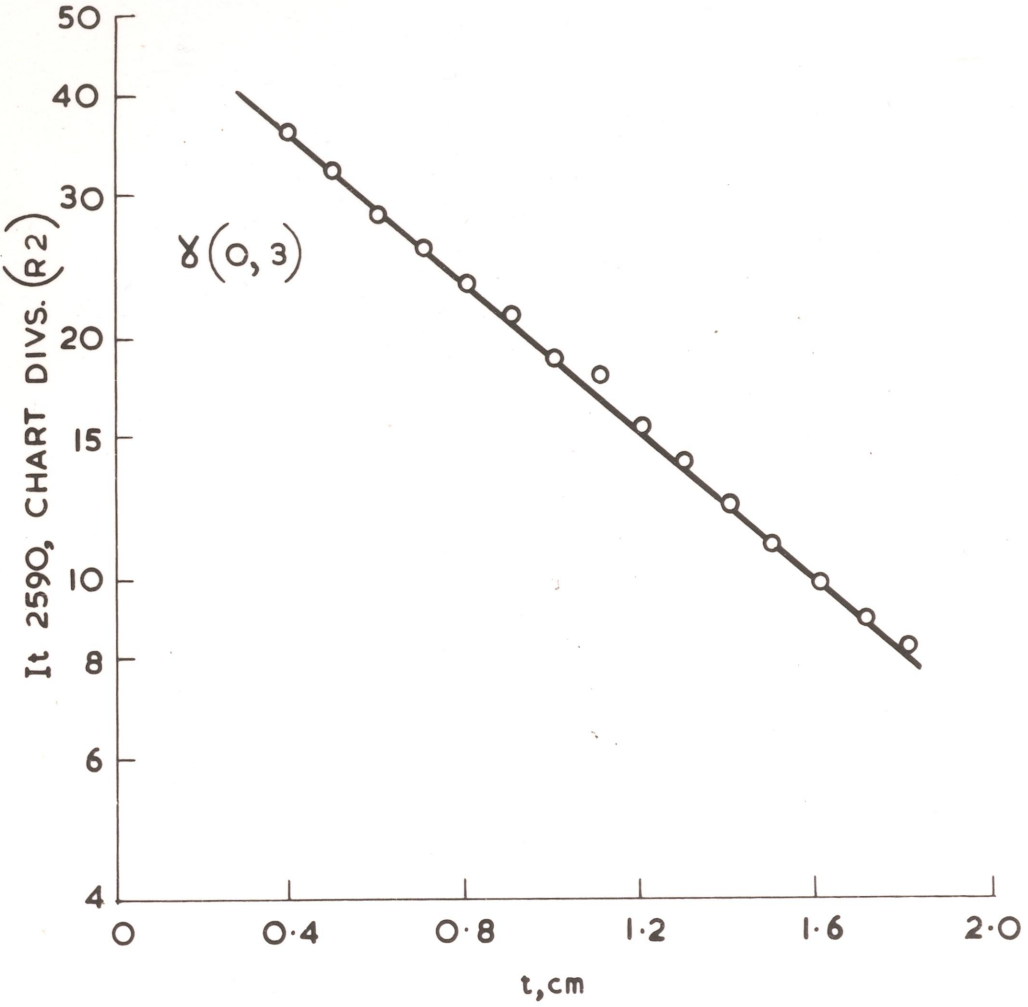

FIG. 17

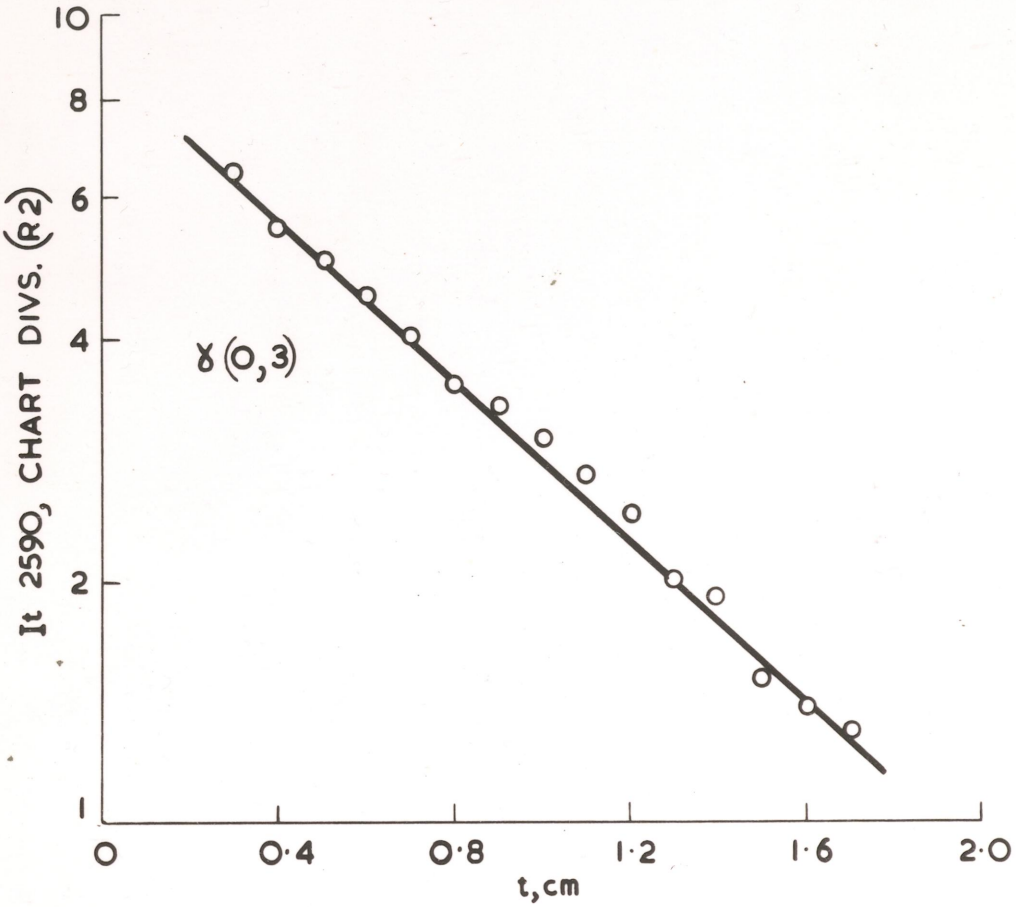

FIG. 18

TABLE 18. AFTERGLOW DECAY CONSTANT R_{NO} OF THE 2595 Å - 2587 Å γ (0,3), AND THE 2892 Å - 2885 Å β (0,6) NITRIC OXIDE BANDS VS. OXYGEN ADDED.

R_{NO} sec^{-1} $= \frac{- d \log It2590}{dt}$	γ (0,3) Mean R_{NO} sec^{-1}	R_{NO} sec^{-1} $= \frac{- d \log It2890}{dt}$	β (0,6) Mean R_{NO} sec^{-1}	Number of Oxygen Molecules added cc^{-1}	Percentage of Oxygen added
0.427 0.46 0.436	0.44	0.384 0.41	0.39	0	0
0.453 0.444	0.45	0.414 0.388	0.4	10^{13}	0.025
0.463 0.476	0.47	0.406 0.406	0.41	2×10^{13}	0.05
0.545 0.486 0.513	0.52	0.39 0.382	0.39	3.1×10^{13}	0.075
0.49 0.52 0.523	0.51	0.37	0.37	4.1×10^{13}	0.1
0.535 0.525	0.53	0.384 0.406	0.4	5.1×10^{13}	0.125
0.52 0.358 0.42 0.42	0.47	0.434 0.434	0.43	6.1×10^{13}	0.15

Fig.19. Afterglow Decay Constants $R_{NO} = \frac{-d \log It2590}{dt}$ sec^{-1} and $R_{NO} = \frac{-d \log It2890}{dt}$ sec^{-1} vs. percentage Oxygen added.

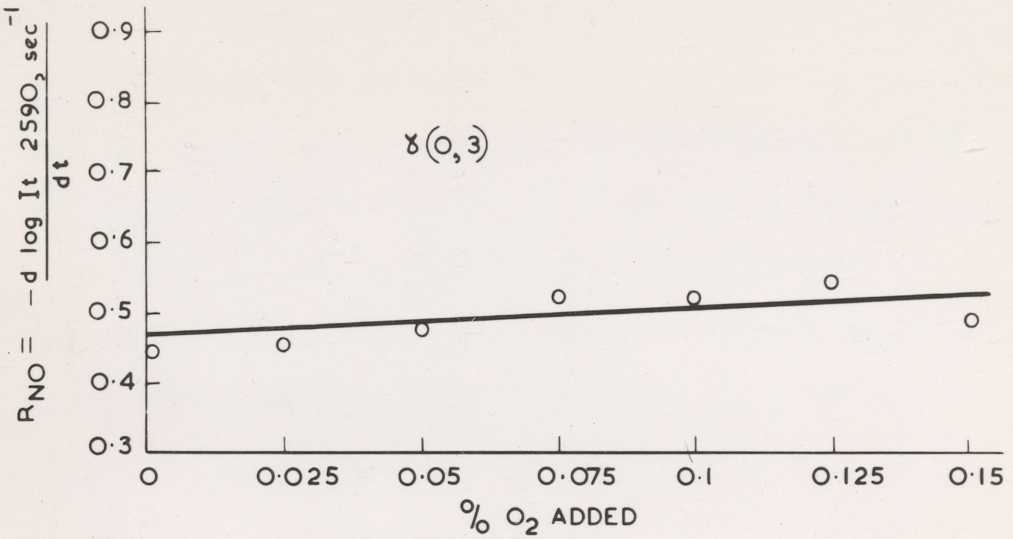
$R_{NO} = -\frac{d \log It\ 2590_3\ sec^{-1}}{dt}$
0·9
0·8
0·7
0·6
0·5
0·4
0·3
γ (0, 3)
0
0·025
0·05
0·075
0·1
0·125
0·15
% O_2 ADDED

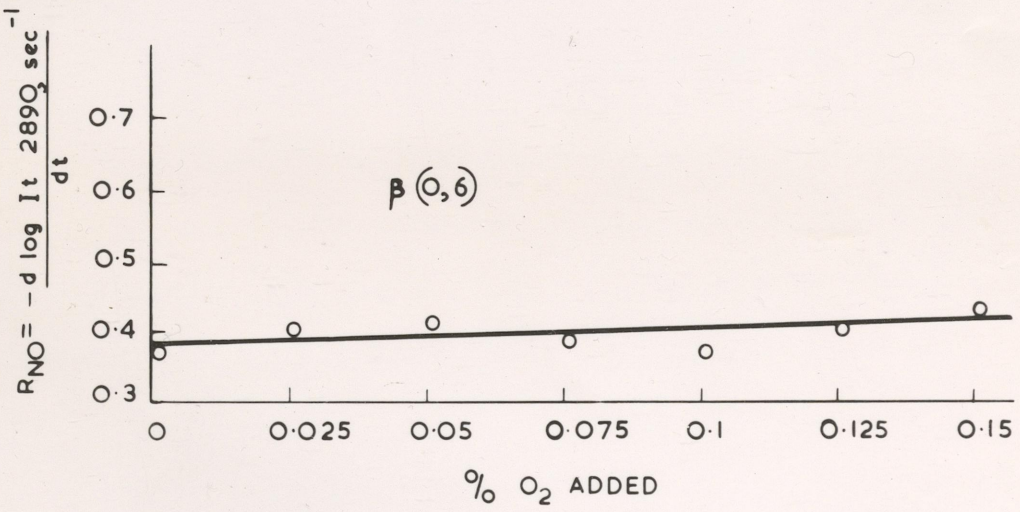
$R_{NO} = -\frac{d \log It\ 2890_3\ sec^{-1}}{dt}$
0·7
0·6
0·5
0·4
0·3
β (0, 6)
0
0·025
0·05
0·075
0·1
0·125
0·15
% O_2 ADDED

FIG. 19

through the experimental points in fig.19 for both the γ (0,3) and β(0,6) bands. Due to the scatter of points, there is some uncertainty in the slope of these lines. The lines drawn have the maximum slope which it is reasonable to associate with the plots. Lines with slope = 0 could also be drawn through these points. The gradients of the lines drawn are 7.5×10^{-16} cc sec^{-1} $molecule^{-1}$ for the γ (0,3) band and 6.3×10^{-16} cc sec^{-1} $molecule^{-1}$ for the β (0,6) band. Thus taking into account the errors involved

$$\frac{d R_{NO}}{dn_3} = (3.8 \pm 3.8) \times 10^{-16} \text{ cc } sec^{-1} molecule^{-1}$$

for the (0,3) band and

$$\frac{d R_{NO}}{dn_3} = (3.2 \pm 3.2) \times 10^{-16} \text{ cc } sec^{-1} molecule^{-1}$$

for the β (0,6) band, where n_3 is the number of oxygen molecules added per cc of the discharge tube vacuum system.

In table 19, values of R_{NO} are shown for the 2370 Å - 2363 Å γ (0,1), 2595 Å - 2587 Å γ (0,3), 2892 Å - 2885 Å β(0,6) and 3206 Å - 3198 Å β(0,8) nitric oxide bands. These values show that the mean decay constant of the $v^1 = 0$, γ nitric oxide bands is greater than that of the $v^1 = 0$, β bands by 15%.

TABLE 19. AFTERGLOW DECAY CONSTANT R_{NO} VS. NITRIC OXIDE BAND WAVELENGTH.

γ (0,1) R_{NO} sec^{-1} $= \frac{-d \log It2363}{dt}$	γ (0,3) R_{NO} sec^{-1} $= \frac{-d \log It2590}{dt}$	β (0,6) R_{NO} sec^{-1} $= \frac{-d \log It2890}{dt}$	β (0,8) R_{NO} sec^{-1} $= \frac{-d \log It3200}{dt}$	Number of Oxygen Molecules$_1$ added cc	Percentage of Oxygen added
0.42	0.44	0.39	0.4	0	0
0.47	0.51	0.37	0.43	4.1×10^{13}	0.1

INVESTIGATIONS OF THE AFTERGLOW INTENSITY

4.1 The Afterglow Intensity.

As mentioned in (2.1), the use of the shutter to cover the monochromator entrance slit during an R.F. glow discharge pulse was disadvantageous to measurement of the intensity of the subsequent afterglow. Most interest was centred on decay rate measurements, when experiments A and B were carried out; though later it was found necessary to obtain intensity values from the data of these experiments. Thus it is necessary to consider the inaccuracies in the intensity values in tables 5 to 7 and 13 to 15, introduced as a result of using the shutter. The shutter was designed to open just after the R.F. discharge pulse was cut off. Thus owing to a slight time lag in the opening of the shutter the afterglow intensity would have decreased below its initial value. Also there was probably a small variation in the time interval between the discharge being cut off and the shutter being in the fully open position.

Using the monochromator, photomultiplier and discharge tube as in experiments A and B but not using the shutter, it was found possible to record both a discharge pulse and its accompanying afterglow by using a narrower monochromator entrance slit. This was due to the fact that, when the shutter was used, and the R.F. glow discharge was pulsed, the intensity of the R.F. glow discharge bands was not appreciably greater than the intensity of the corresponding afterglow bands recorded just after the shutter opened.

The relation between the glow and afterglow intensity is

illustrated in fig.20 below. R.F. glow intensities and the corresponding afterglows were recorded (fig.20a), the afterglow intensity being recorded down to the lowest observable intensity. The same band was then recorded with the same monochromator settings but using the shutter (fig.20b).

TABLE 20. SYMBOLS USED FOR INTENSITY PARAMETERS.

E	=	Maximum glow intensity.
I	=	Initial afterglow intensity.
Ip	=	Afterglow intensity measured at time Δt secs., after the opening of the shutter.
It	=	Intensity measured at time t secs., after the opening of the shutter.
Intensity units	=	chart divs. (R_2)

From fig. 20 it can be seen that the percentage difference between E2363 the maximum R.F. glow intensity and Ip2363 the afterglow intensity was for these two pulses $\pm$12%. It is also evident that when the R.F. pulse was initiated the recorded intensity rose rapidly, remained constant for about 0.2 seconds and then rose sharply to a peak before the intensity decayed slowly away during the afterglow.

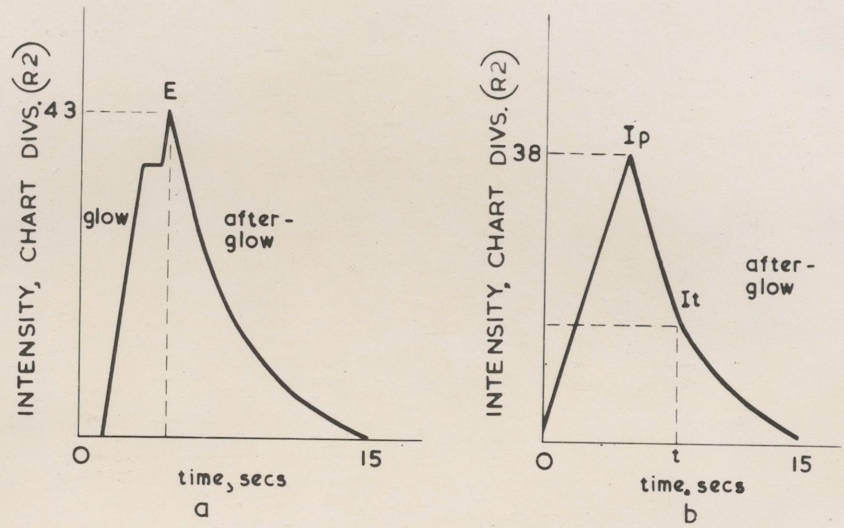

FIG. 20

Fig. 20. Form of (a) glow pulse and its afterglow, (b) afterglow using shutter on recorder chart for the 2370 Å - 2363 Å γ(0,1) nitric oxide band; 0% oxygen added to the system.

The curves shown in figs.21 and 22 were recorded after 0.05% of oxygen had been uniformly mixed with the nitrogen used to obtain curves shown in fig.20. It can be seen from fig.21 that the form of the complete pulse and the afterglow trace was different from that in the more pure nitrogen. When the R.F. pulse was initiated the intensity of the γ (0,1) band rose rapidly, remained constant at the glow intensity E2363 for about 0.5 seconds then fell off rapidly. This initial rate of fall of intensity appeared to be equal to that observed when a constant signal to the Brown Recorder was cut off by breaking an electrical circuit, that is the rate of fall of intensity was greater than the Brown Recorder could measure. This fast decay lasted for about 0.1 seconds. A discontinuity in the afterglow curve occured after the fast afterglow, this was followed by a period of very slow decay. The rate of decay increased in a further period $\sim$0.1 seconds and the intensity then decayed exponentially with time for 10 to 15 seconds down to the lowest intensity recorded. This type of afterglow decay curve was observed by Brömer (1960) for both nitric oxide and nitrogen 1st positive bands. He attributed the initial fast decay of intensity to the decay of electronic excitation of nitric oxide molecules formed in the discharge.

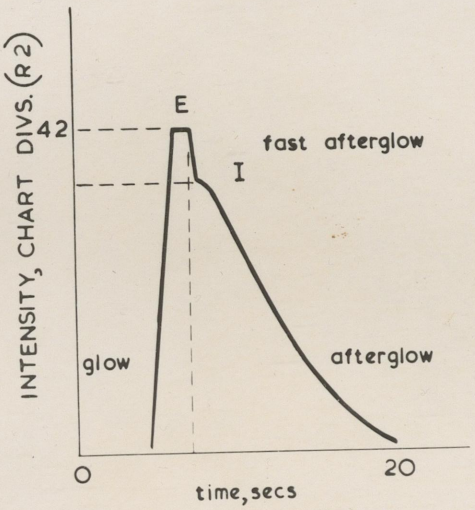

FIG. 21

Fig.21. Form of glow pulse and its afterglow on recorder chart for 2370 Å - 2363 Å γ (0,1) nitric oxide band; 0.05% oxygen added to the system.

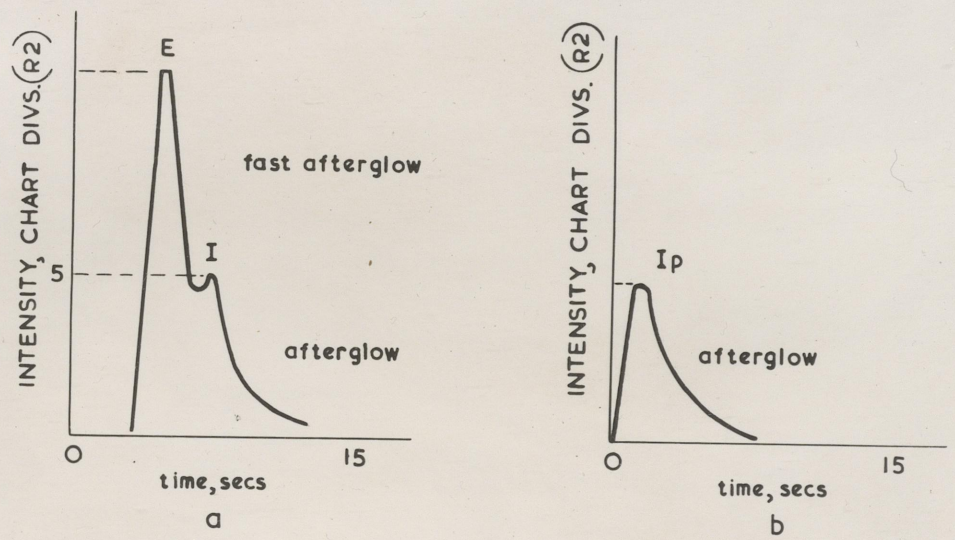

FIG. 22

Fig.22. Form of (a) glow pulse and its afterglow on recorder chart, (b) afterglow using shutter for 2892 Å - 2885 Å β (0,6) nitric oxide band; 0.05% oxygen added to the system.

TABLE 21. INTENSITY VALUES FOR 2892 Å - 2885 Å β(0.6)

NITRIC OXIDE BAND. 0.05% OXYGEN ADDED.

Entrance Slit Width mm	Exit Slit Width mm	Initial Afterglow Intensity I2890 Chart Divs.(R_2)	Afterglow Intensity Ip2890 Chart Divs. (R_2)
0.1	0.3	5	$5 \leqslant Ip \leqslant 7$

The data in table 21 are taken from the curves in fig.22. From table 21 it can be seen that the afterglow intensity Ip2890 was greater than or equal to the initial afterglow intensity for different pulses. This may have been due to the inertia of the Brown Recorder, i.e. in the case where no shutter was used the pen would tend to overshoot downwards after the fast decay. In the case where the shutter was used the pen would have to change direction rapidly and the effect would be to increase the apparent intensity.

The effect of overshooting downwards would be especially marked for the 2892 Å - 2885 Å nitric oxide band as I2890 the maximum glow intensity was about 2 I2890. This was due to bands of the nitrogen 2nd positive system, emitted by the glow discharge-overlapping the 2892 Å - 2885 Å band. The 2nd positive system of nitrogen would decay very rapidly, when the R.F. glow discharge was cut off, as it did not contribute to the slow afterglow. This can be seen from the glow and afterglow spectra in fig.6 and 6a.

The form of the afterglow decay curves in figs.21 and 22 suggests the following hypothesis. When some oxygen was added to the discharge an appreciable equilibrium concentration of stable nitric oxide molecules was built up. These molecules became electronically excited and emitted nitric oxide β and γ bands. When the discharge was switched off, the electronically excited molecules decayed relatively rapidly to the ground state. The slower decay of the nitric oxide β and γ band intensity which followed the fast afterglow indicates that there was a second mechanism of excitation, i.e. the nitric oxide afterglow mechanism. The observed initial intensity due to the second source of excitation was defined to be I. It is assumed in the discussion of the present experiments (6) that the intensity of the nitric oxide β and γ bands generated by the second source of excitation was equal to I in the glow also. The error introduced by assuming this is small, i.e. $\sim$1% considering the initial slowness of the decay of the nitric oxide afterglow. In any case it has been necessary to assume in the discussion (6) that the observed afterglow intensity using the shutter is a good measure of the initial afterglow intensity I. From fig.20 it can be seen that the error introduced would be about 10% for intensities $\sim$ 40 chart divisions (R_2) and $\sim$30% for bands of intensity $\sim$ 5 chart divisions (R_2) which are overlapped by bands excited in the glow discharge only.

4.2. Calibration of the Optical and Recording System.

4.2.1 Experimental.

A tungsten strip filament lamp was set at 12 cm. distance from the monochromator entrance slit as shown in fig.23. The monochromator drum was set at 5000 Å, and the current to the lamp was adjusted until the deflection of the Brown Recorder pen was 30 divisions (R_2). Using a disappearing filament optical pyrometer, the brightness temperature of the tungsten filament, as viewed through the lamp envelope was determined to be 1700°C. The dimensions of the monochromator slits were : entrance slit width = 0.005 cm and length = 1.75 cm, exit slit width = 0.06 cm ≡ 210 Å at 5000 Å. The tungsten filament width = 2 mm.

4.2.2 Outline of Calculation.

The amount of energy entering the monochromator entrance slit in a given wavelength range can be calculated from the filament temperature and the geometry of the system. Hence the number of photons entering the monochromator per second can be calculated. The rate of generation of photons in the discharge tube which gives rise to an identical number of photons entering the system, and to 30 divisions deflection on the Brown Recorder can then be calculated. There is, however, a difference between the number of photons entering the monochromator slit and the number of photons striking the photomultiplier cathode; due to absorption in the monochromator

Fig.23. Apparatus for Calibration of Optical and Recording System.

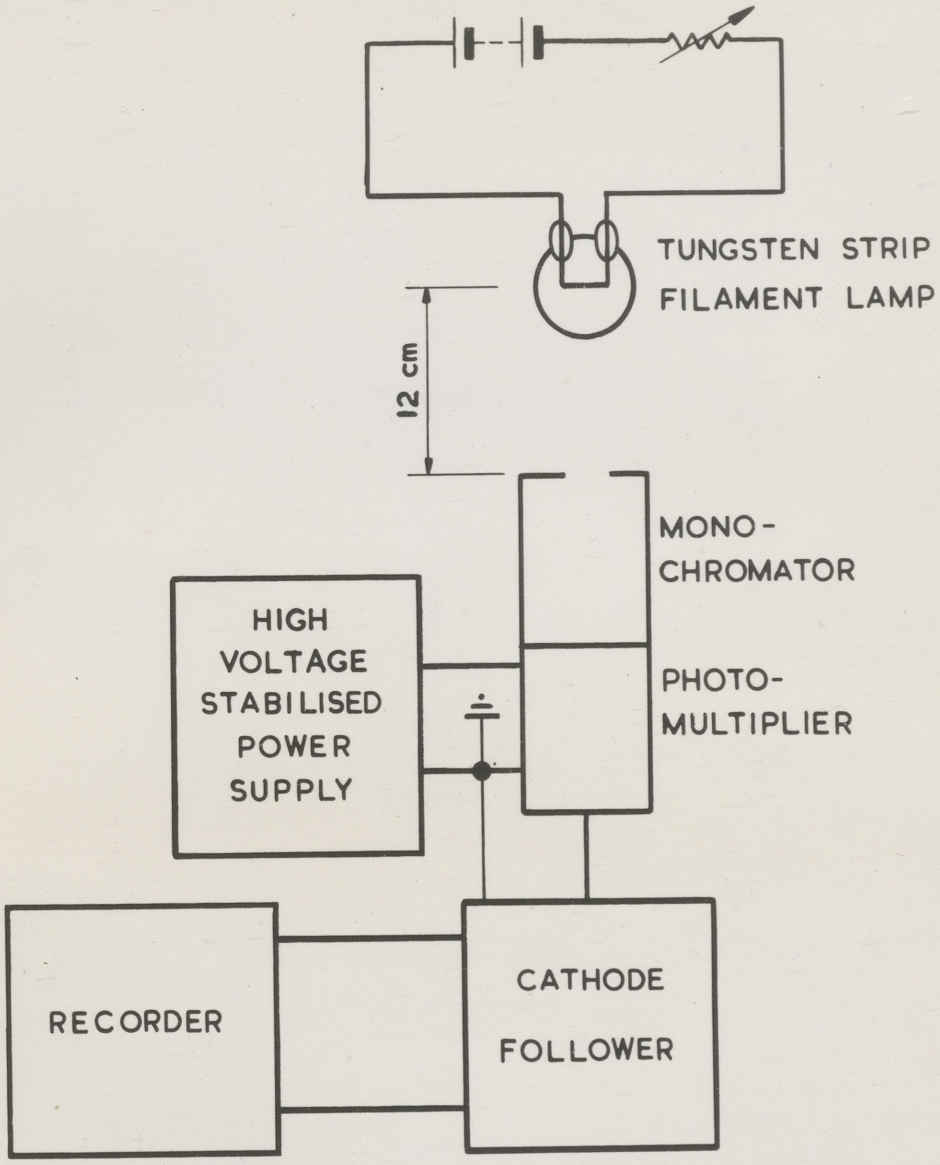
TUNGSTEN STRIP
FILAMENT LAMP
12 cm
MONO-
CHROMATOR
PHOTO-
MULTIPLIER
HIGH
VOLTAGE
STABILISED
POWER
SUPPLY
RECORDER
CATHODE
FOLLOWER

FIG. 23

components, and also due to photons entering the slit at a large angle with the main beam direction. The absorption will attenuate light of equal wavelengths from the filament and the discharge tube equally. There is, however, a difference between the angular distribution of light from the filament and the discharge tube at the monochromator entrance slit. Thus different amounts of light will be lost from the beam in the monochromator, in the case of the filament and the discharge tube. The ratio

$$\frac{\text{Fraction of filament light lost from beam.}}{\text{Fraction of discharge tube light lost from beam.}}$$

is of the order of unity (4.2.7).

4.2.3 The True Temperature of the Tungsten Filament.

The brightness temperature of the tungsten filament = 1700°C ≡ 1973°K. The data in tables 22 and 23 are taken from 'Temperature its Measurement and Control in Science and Industry', American Institute of Physics.

TABLE 22. RELATION BETWEEN TRUE AND BRIGHTNESS TEMPERATURE FOR A TUNGSTEN FILAMENT.

True Temperature °K	Brightness Temperature (0.65 μ) °K
2100	1946
2200	2031

The measured brightness temperature is 1973°K.

Thus the corresponding true temperature lies between 2100°K and 2200°K from table 22. 1973 - 1946 = 27 and 2031 - 1946 = 85. Thus by simple proportion the true temperature corresponding to 1973°K = 2100 + 100 x $\frac{27}{85}$ °K = 2132°K.

4.2.4 The Amount of Energy Radiated by the Tungsten Lamp.

TABLE 23. SPECTRAL EMISSIVITY OF TUNGSTEN

True temperature °K	2000	
Wavelength μ	0.65	0.467
Spectral Emissivity of Tungsten	0.438	0.469

The wavelength setting of the monochromator was λ = 5000 Å. Thus λ T cm deg. = 5 x 10^{-5} x 2132 = 0.1056 cm deg. When λ T = 0.105 cm deg., then for a black body

$$\frac{W^1(\lambda, T)}{W^1 \max (T)} = 2.56 \times 10^{-2} ;$$

where $W^1(\lambda, T)$ = the energy radiated at 5000 Å per micron of wavelength range and per cm^2 of filament, and where $W^1 \max (T) = 1.29 \times 10^{-15} T^5$ watt $cm^{-2} \mu^{-1}$. The equations are taken from the 'American Institute of Physics Handbook (6.6.5)'. When T = 2132°K, $W^1 \max (T)$ = 59.5 watt $cm^{-2} \mu^{-1}$.

Thus $W^1(\lambda, T)$ = 1.52 watt $cm^{-2} \mu^{-1}$ for a black body. For a tungsten filament $W^1(\lambda, T)$ = 0.715 watts $cm^{-2} \mu^{-1}$, since

from table 23 the emissivity of a tungsten filament at 2000°C and 4670 Å is 0.47.

4.2.5 The Amount of Light from the Tungsten Lamp which entered the Monochromator.

The amount of energy entering the slit per second in the wavelength range $\Delta\lambda$ = 210 Å centred on 5000 Å = Fraction of energy from the filament incident on the monochromator slit x area of filament x $W^1(\lambda, T) \times \Delta\lambda$.

We will now consider the fraction of energy from the filament incident per second on the monochromator slit. Fig.24 shows the geometry of the slit-filament system. The lamp filament was longer than the monochromator entrance slit but it is assumed that only the light energy from the length 1.75 cm opposite the slit would reach the detector, the rest being scattered on the inside walls of the monochromator.

Consider an element of area dy. dx. cm^2 on the filament. The amount of energy radiated from this element, which enters a narrow horizontal strip of the monochromator entrance slit of area dA cm^2, is proportional to the solid angle $\frac{dA}{r^2}$; where r is the distance between the elemental areas. dA = r.d η x width of entrance slit = r.dη x 0.005. Thus the solid angle $\frac{dA}{r^2} = \frac{d\eta \times 0.005}{r}$.

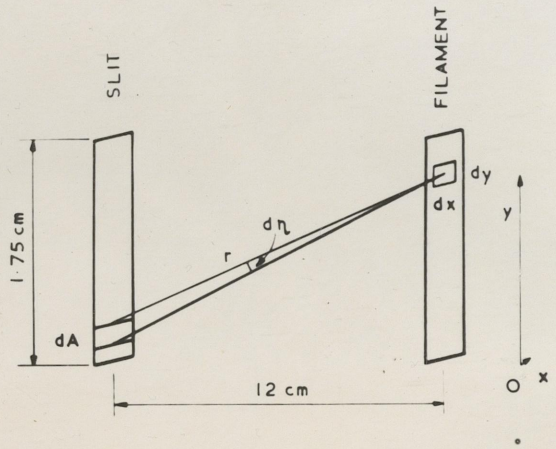

FIG. 24

Fig.24. Monochromator entrance slit and tungsten filament geometry.

r does not vary by more than 10% with position of dA and dy.dx. For if we suppose that dA is at y = 0 and dy.dx at y = 1.75 cm then $r^2 = 12^2 + 1.75^2$, and so r = 12.1 cm : If dA is at y = 0 and dy.dx at y = 0 then r = 12 cm. Thus the total solid angle subtended by the monochromator entrance slit at dy.dx on the tungsten filament

$$= \int \frac{dA}{r^2} = \frac{0.005}{12} \int_{y=0}^{y=1.75} d\eta$$

$$= 4.2 \times 10^{-4} \int_{y=0}^{y=1.75} d\eta$$

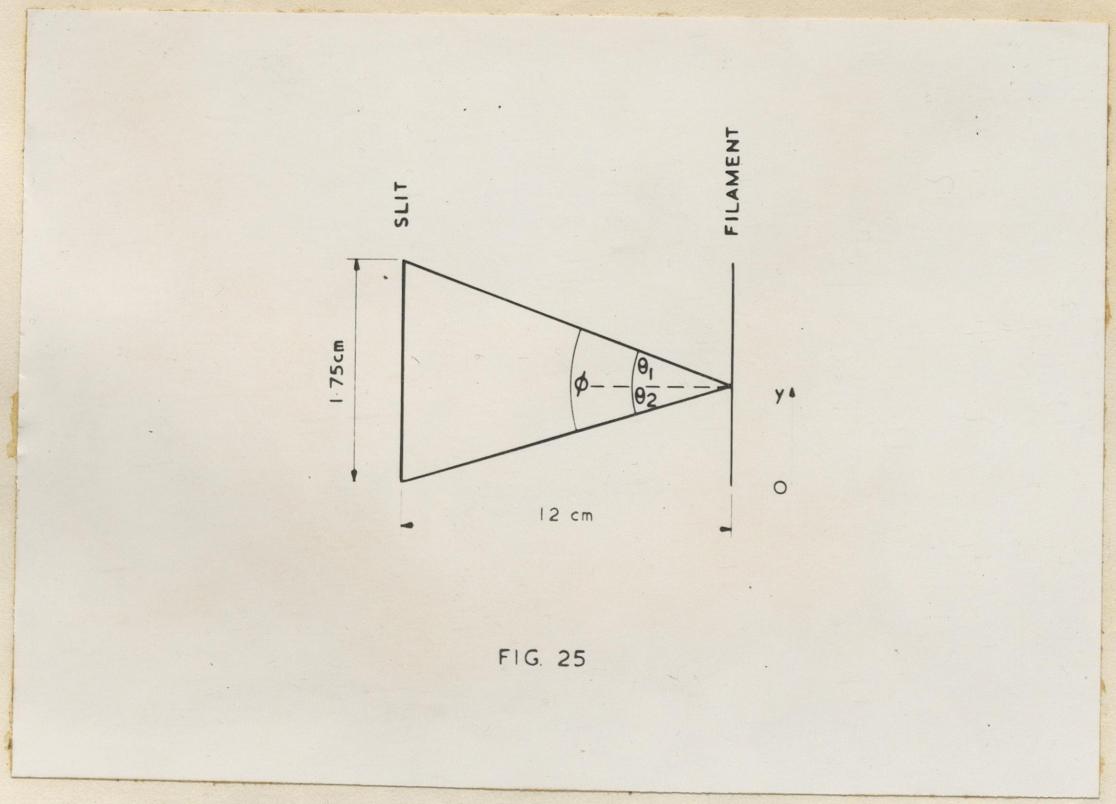

FIG. 25

Fig.25. Vertical section of lamp filament and monochromator entrance slit.

Let $\int_{y=0}^{y=1.75} d\eta = \phi$. The fraction of energy from the element dy.dx of the filament incident on the monochromator slit is proportional to the solid angle 4.2×10^{-4} subtended by the slit at the element dy.dx. The total energy from dy.dx is radiated into a hemisphere, that is into 2 units of solid angle. Thus the fraction of energy incident on the slit $= \frac{4.2 \times 10^{-4} \times \phi}{2\pi}$. This is because for a tungsten filament the energy radiated per unit solid angle is practically equal in all directions. ('Temperature its Measurement and Control in Science and Industry', American Institute of Physics).

Fraction of energy incident on monochromator entrance slit x area of filament =

$$\frac{4.2 \times 10^{-4}}{2\pi} \int_0^{1.75} \phi \, dy \int_0^{0.2} dx = 1.34 \times 10^{-5} \int_0^{1.75} \phi \, dy \text{ cm}^2,$$

since ϕ will not vary much from $x = 0$ to $x = 0.2$ cm. We now consider the integral $\int_0^{1.75} \phi \, dy$. We have from fig.23

$$\phi = \tan^{-1} \tan\theta_1 + \tan^{-1} \tan\theta_2$$
$$= \tan^{-1}\left(\frac{1.75 - y}{12}\right) + \tan^{-1}\frac{y}{12}$$

Let $\int A = \int_0^{1.75} \tan^{-1}\left(\frac{1.75 - y}{12}\right) dy$ and

let $\frac{1.75 - Y}{12} = Z$. Then $-dy = 12\,dz$

and $\int A = -12 \int_{\frac{1.75}{12}}^{0} \tan^{-1} z.\ dz.$

Integrating by parts,

$$\int A = \left[-z \tan^{-1} z + \int \frac{z}{1 + z^2} \cdot dz \right]_{\frac{1.75}{12}}^{0}$$

$$= \left[-z \tan^{-1} z + \frac{1}{2} \log_e (1 + z^2) \right]_{\frac{1.75}{12}}^{0}$$

$$= \left[0 + 0 + 0.146 \times \frac{8.3}{180} \times \pi - \frac{1}{2} \log_e (1.021) \right]$$

$$= 0.011$$

Let $\int B = \int_0^{1.75} \tan^{-1} \frac{Y}{12} \cdot dy$. From fig.23.

it can be seen that by symmetry $\int A = \int B$.

Thus $\int_0^{1.75} \phi \ dy = \int A + \int B = 0.022.$

The amount of energy W radiated from the filament, entering the slit per second in the wavelength range $\Delta\lambda = 210$ Å, centred on 5000 Å = fraction of energy from filament incident on the monochromator slit x area of filament x $W^1 (\lambda, T) * \Delta\lambda$

The first two terms $= 1.34 \times 10^{-5} \int_0^{1.75} \phi \, dy$ cm^2

$= 2.94 \times 10^{-7}$ cm^2

Thus $W = 2.94 \times 10^{-7} \times 0.715 \times 210 \times 10^{-4} \times 10^{7}$ ergs.sec^{-1}

$= 4.42 \times 10^{-2}$ ergs.sec^{-1}.

Let V = the number of photons per second entering the monochromator slit corresponding to W.ergs.sec^{-1}, then $W = Vh\nu$ since the energy of each photon is hν where $h = 6.6 \times 10^{-27}$ ergs.secs. and ν sec^{-1} is the frequency associated with the wavelength $\lambda = 5000$ Å.

$\nu = \frac{3 \times 10^{10}}{5000 \times 10^{-8}}$ sec^{-1} since the velocity of light

$= 3 \times 10^{10}$ $cm^2 sec^{-1}$. Thus $V = \frac{4.42 \times 10^{-2} \times 5000 \times 10^{-8}}{6.6 \times 3 \times 10^{-17}}$

$= 1.11 \times 10^{10}$ photons sec^{-1}.

4.2.6 <u>The Amount of Light from the Discharge Tube which entered the Monochromator Entrance Slit.</u>

Fig.26 shows the relative positions of the discharge tube and the monochromator entrance slit during all the experiments described in this work.

When V photons sec^{-1} from the discharge tube enter the monochromator slit then I photons cc^{-1} sec^{-1} are generated in the discharge tube. According to Berkowitz et al (1956),

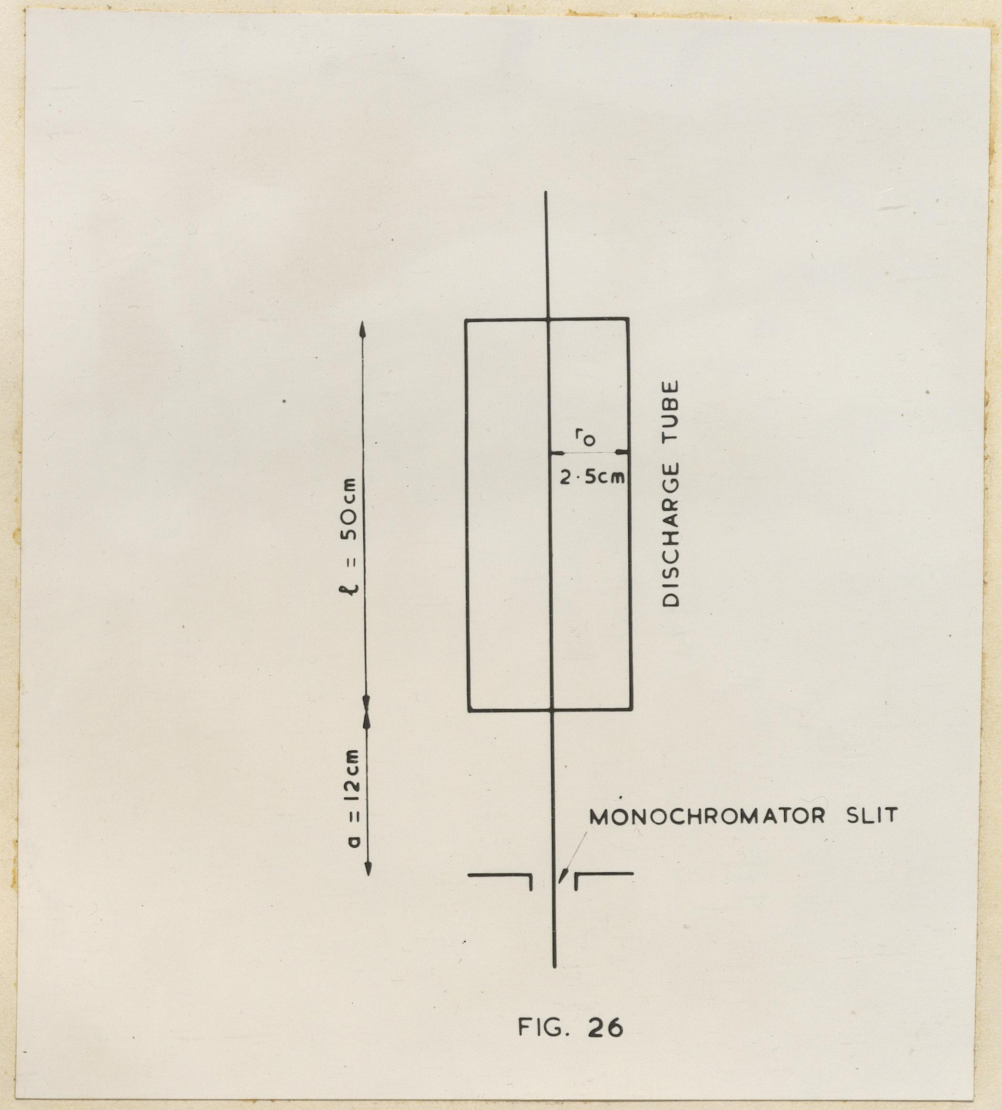

FIG. 26

Fig.26. Horizontal section through discharge tube and monochromator entrance slit.

$$V = \frac{AI}{2} \left[l + (r_o^2 + a^2)^{\frac{1}{2}} - (r_o^2 + (a + l)^2)^{\frac{1}{2}} \right]$$

where A = the area of the slit,

l = the length of the discharge tube,

r_o = radius of the discharge tube,

a = distance from discharge tube to slit.

From (2.1) and (4.2.1) we have l = 50 cm, r = 2.5 cm, a = 12

$$V = \frac{AI}{2} \left[50 + (2.5^2 + 12^2)^{\frac{1}{2}} - (2.5^2 + (12 + 50)^2)^{\frac{1}{2}} \right]$$

$$= \frac{AI}{2} \left[50 + 12.26 - 62.05 \right]$$

$$= \frac{0.21}{2} \times AI \text{ photons sec}^{-1}.$$

$$A = 0.005 \times 1.75 \text{ cm}^2 \qquad (4.2.1)$$

Thus $V = 0.005 \times 1.75 \times I \times 0.105$ photons sec^{-1}

or $I = 1.09 \times 10^3 V$ photons $cc^{-1} sec^{-1}$.

From measurements using the tungsten filament (4.2.1); when the number of photons entering the monochromator slit in the wavelength range selected by the monochromator is $V = 1.11 \times 10^{10}$ photons sec^{-1} (4.2.5), then $I^1 = 30$; where I^1 is the number of chart divisions deflection on the Brown Recorder (R_2). If the 30 divisions deflection had been due to light from the discharge tube as in fig.24 then the rate of generation of photons in the discharge tube would be $I = 1.09 \times 10^3 \times 1.11 \times 10^{10}$ photons $cc^{-1} sec^{-1}$.

$$\text{Let } K5000 = \frac{\left\{\begin{array}{l}\text{(Intensity in photons cc}^{-1}\text{ sec}^{-1}\text{ in discharge tube}\\ \text{(corresponding to the wavelength range 4895 Å to 5105 Å}\end{array}\right\}}{\left\{\begin{array}{l}\text{(Corresponding deflection of Brown Recorder in chart}\\ \text{(divisions (}R_2\text{), (Monochromator entrance slit 0.005 cm,}\\ \text{(exit slit 0.06 cm).}\end{array}\right\}}$$

$$\text{then } K5000 = \frac{I}{I'} = \frac{1.09 \times 10^3 \times 1.11 \times 10^{10}}{30} = 4 \times 10^{11}$$

photons cc $\text{sec}^{-1}\text{div}^{-1}$.

However a correction is applied to K5000 in (4.2.7).

4.2.7 The Fraction of Light lost between the Monochromator Entrance Slit and the Photomultiplier Window.

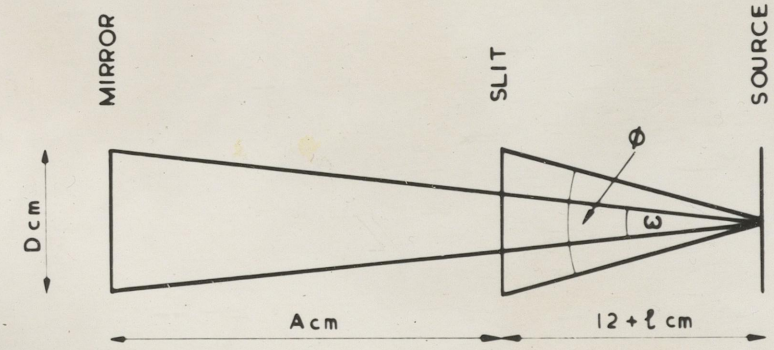

FIG. 27

Fig.27. Vertical section through first Monochromator collimating mirror, and entrance slit; and the light source.

It is assumed that approximately all light striking the first collimating mirror in the monochromator can reach the photomultiplier window, apart from the fraction absorbed. The distance A between the mirror and the slit is approximately 20 cm. The distance of the tungsten filament from slit = 12 cm and distance of a point on the central axis of discharge tube from the slit = 12 + 1 cm.

Light from the tungsten filament will enter the photomultiplier, if at lies within the angle $= \frac{D}{20 + 12} = \frac{D}{32} = \omega$ The variation of ω with vertical position on the filament is ignored in this approximate calculation. Thus the fraction

$$\frac{\text{Light entering Photomultiplier}}{\text{Light incident on slit}} = \frac{D}{32} \times \frac{12}{1.75} = \frac{\omega}{\phi}$$

The angle in which light leaving the discharge tube must lie to enter the photomultiplier depends on l, ignoring the effect of position in the vertical plane, within the tube, on ω.

When $l = 0$ $\quad \frac{\omega}{\phi} = \frac{D}{32} \times \frac{12}{1.75}$ nearest end of tube

$l = 25$ cm, $\quad \frac{\omega}{\phi} = \frac{D}{57} \times \frac{37}{1.75}$ centre of tube

$l = 50$ cm, $\quad \frac{\omega}{\phi} = \frac{D}{82} \times \frac{62}{1.75}$ far end of tube

For the discharge tube the average value of the fraction

$$\frac{\text{Light entering photomultiplier}}{\text{Light incident on slit}} = \frac{\overline{\omega}}{\phi}$$

$$\simeq \frac{1}{3}\frac{D}{1.75}\left(\frac{12}{32} + \frac{37}{57} + \frac{62}{82}\right)$$

$$= \frac{D}{1.75} \times 0.6$$

Thus the ratio

$$f = \frac{\text{fraction of filament light lost from beam}}{\text{fraction of discharge tube light lost from beam}}$$

$$= \frac{0.36}{0.6} = 0.6$$

This means that if V photons sec^{-1} from the filament enter the monochromator slit and produce a deflection I^1 on the Brown Recorder, 1.67 V photons sec^{-1} are required from the discharge tube to produce the same deflection. Thus

$K5000 = 6.7 \times 10^{11}$ photons cc^{-1} sec^{-1} div^{-1}.

4.2.8 The Accuracy of K5000.

According to H.J.J.Braddick, p.21, 'The Physics of Experimental Method', the square of the percentage error of a product is the sum of the squares of the percentage errors of the factors, where the errors are random errors.

Let the percentage error in K5000 = Δ K5000 where

$K5000 = \frac{I}{I^1} \times \frac{1}{f}$, see 4.2.6 and 4.2.7. Thus

$\Delta^2 K5000 = \Delta^2 I + \Delta^2 I^1 + \Delta^2 f$, where the prefix Δ indicates the error in the quantity which follows. We will

consider the errors ΔI, ΔI^1 and Δf.

We have from 4.2.6 that $I = 1.09 \times 10^3 V$ where, from 4.2.5, V = Fraction of energy from filament incident on the monochromator slit x area of filament x $W^1(\lambda, T) \times \Delta\lambda$.

The errors in the individual quantities which determine I are now considered.

$\Delta\ 1.09 \times 10^3$

This factor is calculated in (4.2.6) from the equation

$$V = \frac{AI}{2}\left[1 + (r_o^2 + a^2)^{\frac{1}{2}} - (r_o^2 + (a^2 + 1)^2)^{\frac{1}{2}}\right].$$

The area A is implicit in the expression for V from (4.2.5) given above, so the error in A will be ignored. Any errors in the other quantities on the R.H.S. of

$$V = \frac{AI}{2}\left[1 + (r_o^2 + a^2)^{\frac{1}{2}} - (r_o^2 + (a + 1)^2)^{\frac{1}{2}}\right]$$

are small and cancel out, except for a comparatively small residual error.

Δ Fraction of energy from filament incident on the monochromator slit.

There is a slight error in the calculation of this fraction due to assuming that r is constant (4.2.5). The amount of energy incident on the slit is overestimated by 2% for light entering the monochromator at the most extreme angles from the filament. Thus on average the error is $\pm$ 1% . The error in the dimensions of the monochromator entrance slit cancels as explained under the heading $\Delta 1.09 \times 10^3$.

Δ Area of Filament.

The effective area of the filament was probably 10% less than the nominal value as it was not perfectly flat.

Δ $W^1(\lambda, T)$

The brightness temperature of the tungsten filament determined in 4.2.3 is probably correct to within $\pm$ 20°K. Thus T = 2132 $\pm$ 20 °K.

T °K	λ T cm.deg.
2112	0.1056
2132	0.1066
2152	0.1076

From the American Institute of Physics Handbook (6.6.4) we have the following data.

λ T cm.deg.	$\frac{W^1(\lambda, T)}{W \text{ max } T}$
0.100	1.649×10^{-2}
0.105	2.563×10^{-2}
0.110	3.785×10^{-2}

and

T°K	W max T watt $cm^{-2} \mu^{-1}$
2000	41.27
2100	52.67
2200	66.47

From this data it can be seen that the variation of $\pm$ 20 °K in T corresponds to a variation of about $\pm$ 15% in $W^1(\lambda, T)$.

$\Delta(\Delta\lambda)$

$\Delta\lambda$ depends on the exit slit width. This was correct to $\pm$ 0.002 cm which corresponds to an error of about $\pm$ 3%.

From the discussion of the individual errors it can be seen that $\Delta^2 I = \Delta^2 W^1(\lambda, T) + \Delta^2(\Delta\lambda)$; only random errors being included in this expression for $\Delta^2 I$. Thus $\Delta^2 I = 225 + 9$ and $\Delta I = \pm 15$%.

From 4.2.1 we have that I^1 = 30 chart divisions (R_2). This is correct to $\pm$ 1 division thus $\Delta I^1 = \pm 3$%.

The random errors in K5000 are due to ΔI and ΔI^1 thus Δ^2 K5000 = 234 + 9 and Δ K5000 = $\pm$ 16%. However, this is small compared with the uncertainty in f which was not calculated very rigorously (4.2.7). f may be underestimated or overestimated by an unknown factor. The corrected value of K5000 is 6.7×10^{11} photons cc^{-1} sec^{-1} div^{-1}. Due to the uncertainty in f, K5000 may differ from 6.7×10^{11} photons $cc^{-1} sec^{-1} div^{-1}$. In view of the nature of f, it seems unlikely that it differs much from unity, and so the value of K5000 probably lies within the limits 2×10^{11} to $1.\times 10^{12}$ photons cc^{-1} sec^{-1} div^{-1}.

4.3 The Absolute Integrated Intensity of the Nitrogen Afterglow Bands, I_{N_2}.

In the experiment A described above (3.) the integrated intensity of the 5854 Å, 5804 Å and 5755 Å nitrogen afterglow bands was recorded. The monochromator entrance slit was set at a width of 0.5 mm, and the exit slit at a width of 0.6 mm, which

corresponds to a wavelength range of 300 Å.

$$\text{Let } K5755 = \frac{\left\{\begin{array}{l}\text{Intensity in photons cc}^{-1}\text{ sec}^{-1}\text{ in the discharge}\\ \text{tube corresponding to the wavelength range}\\ \text{5625 Å to 5905 Å.}\end{array}\right\}}{\left\{\begin{array}{l}\text{Corresponding deflection of Brown Recorder in}\\ \text{chart divisions } (R_2).\ \text{(Monochromator entrance}\\ \text{slit 0.05 cm, exit slit 0.06 cm).}\end{array}\right\}}$$

K5000 was measured with the monochromator entrance slit 0.005 cm wide and the exit slit 0.06 cm wide. Fig.4 shows that, when the entrance slit width was increased from 0.005 cm to 0.05 cm, the Brown Recorder deflection increased by a factor of 22. The sensitivity of the photomultiplier at 5755 Å = $\frac{1}{2.8}$ x sensitivity of the photomultiplier at 5000 Å from data published by E.M.I. Ltd. Thus $K5755 = \frac{2.8}{22} \times K5000 = 0.127 \times K5000$ photons $cc^{-1} sec^{-1} div^{-1}$.

Bayes and Kistiakowsky (1960) have measured the intensity of the visible and infra red nitrogen afterglow $B^3\Pi g \rightarrow A^3\Sigma_u^+$ and $Y \rightarrow B^3\Pi g$ bands. Using their intensity scale the total band intensity = 42.94 ; the intensity of the bands in the wavelength range 5755 Å - 5804 Å = 4.29, and the intensity of the bands in the wavelength range 5905 Å - 6127 Å = 0.77.

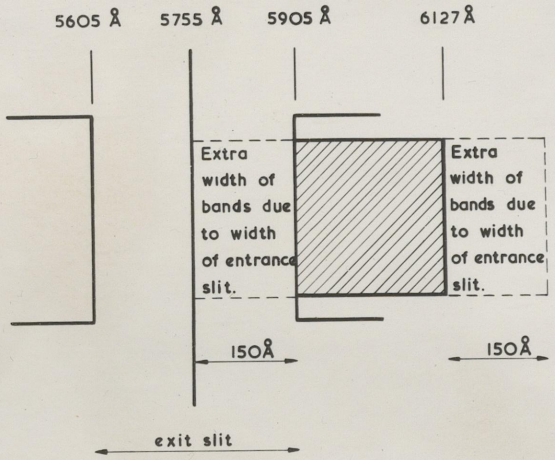

FIG. 28

Fig.28. Relative positions of the Monochromator Exit Slit and bands in the wavelength range 5905 Å - 6127 Å.

Fig.28 refers to the measurement of I5755 in experiment A. The dotted line shows the width of bands in the range 5905 Å - 6127 Å due to the finite width of the entrance slit. It appears that $\frac{1}{3}$ of the intensity of the bands in the range 5905 Å - 6127 Å would pass through the exit slit of the monochromator.

Using the data of Hayes and Kistiakowsky it can be seen that on their intensity scale $I_{5755} = 4.29 + \frac{0.77}{3} = 4.55$; and that $\frac{\text{Total Nitrogen Afterglow Intensity}}{I_{5755}} = \frac{42.9}{4.55} = 9.4$.

Since the nitrogen afterglow has a characteristic intensity distribution, it is assumed that the equality applies to the present experiments.

It is also assumed that the relative intensity of the nitrogen afterglow bands was unchanged by the addition of the small amounts of oxygen added to the system in the present experiments. Thus $I_{N_2} \propto I_{5755}$, and we can write

$$I_{N_2} = 9.4\ I_{5755}\ K_{5755}$$

$$= 1.2\ I_{5755}\ K_{5000} \text{ photons cc}^{-1}\text{sec}^{-1}.$$

4.4 The Absolute Integrated Intensity of the Nitric Oxide Afterglow Bands, I_{NO}.

The intensity I_{p2363} of the 2370 Å - 2363 Å γ (0,1) nitric oxide band was recorded in experiment A using a monochromator entrance slit of width 1 mm and an exit slit of width 1.6 mm.

$$\text{Let } K_{2363} = \left\{ \begin{array}{l} \text{Intensity in Photons cc}^{-1}\text{sec}^{-1} \text{ in the discharge} \\ \text{tube of the } \gamma \text{ (0,1) nitric oxide band.} \\ \hline \text{Corresponding deflection of Brown Recorder in chart} \\ \text{divisions } (R_2), \text{ (Monochromator entrance slit width 1mm)} \end{array} \right\}$$

The sensitivity of the Photomultiplier at 2363 Å = 2.1 x sensitivity at 5000 Å.

Fig.5 shows that when the entrance slit of the monochromator, was widened from 0.05 mm to 1 mm the Brown Recorder deflection

increased by a factor of 59. Thus $K_{2363} = \frac{1}{2.1 \times 59} K_{5000}$

$= 0.0081\ K_{5000}$ cc^{-1} sec^{-1} div^{-1}.

The spectroscopic measurements (2.4) made in the present investigation show that there is fair agreement between the measured density values of the NO β and γ bands and the visual estimates published by ~~Pierce~~ Pearse and Gaydon in 'The Identification of Molecular Spectra'. Robinson and Nicholls made photo-electric measurements of the intensity of some NO β and γ bands and also calculated theoretical intensities. When ~~Pierce~~ Pearse and Gaydon's values were compared with the more accurate intensity measurements of Robinson and Nicholls there was still fairly good agreement though the values differed by a factor of 2 in some cases.

TABLE 24. COMPARISON OF INTENSITY MEASUREMENTS OF NITRIC OXIDE BANDS.

Integrated Intensity of β Bands	Integrated Intensity of γ Bands	Reference
110	45.8	Robinson and Nicholls
114	56	'The Identification of Molecular Spectra'.

The sum of the intensities recorded by Robinson and Nicholls is shown in table 24, also the sum of the intensities for the corresponding bands published in 'The Identification of Molecular Spectra' (I.M.S.). It can be seen that the agreement was fairly good. Table 25 shows that individual intensities agree fairly well.

TABLE 25. COMPARISON OF MEASUREMENTS OF THE INTENSITY OF SOME NITRIC OXIDE BANDS.

Intensity of 2370 Å - 2363 Å γ (0,1) band	Intensity of 2890 Å - 2885 Å β (0,6) band	Intensity of 3206 Å - 3198 Å β (0,8) band	Reference
4	8.5	9.7	Robinson and Nicholls
10	10	10	I.M.S.

The assumption is now made that the measured densities listed in table 3 quantitatively describe the nitric oxide spectrum emitted by the afterglow in the present experiments. Reference to fig. 6a will show that this is reasonable. The following equality can then be written $I_{NO} = \frac{\Sigma}{i12363} \times I12363 \; K2363$;

where I_{NO} = the absolute integrated intensity of nitric oxide β and γ bands in photons $cc^{-1}sec^{-1}$; Σ =the integrated density of the nitric oxide β and γ bands in table 3, and i2363 = the measured density of the 2370 Å - 2363 Å γ (0,1) nitric oxide band on the same scale. From table 3 Σ = 17.6 and i2363 = 1.5.

Thus I_{NO} = 11.7 I2363 K2363

= 0.1 K5000 I2363

The above assumption may lead to an error of ± 25% in I_{NO} because the density values correspond to a scale proportional to log (intensity). This can be tested by comparing the ratio $\frac{a}{b + c + d + e + \ldots}$ with

$$\frac{\log a}{\log b + \log c + \log d + \log e + \ldots}$$ where a, b, c, d, e, ... are a set of about 20 numbers of the same magnitude as the density values in table 3.

The assumption that there is no change in the relative intensity distribution of nitric oxide β and γ bands with oxygen is implicit in $I_{NO} = 0.1\ K5000\ I2363$. From fig.12 it can be seen that there was no change in the relative intensity distribution of the observed nitric oxide β and γ bands with oxygen in experiment B.

The intensity Ip2890 of the 2892 Å - 2885 Å β (0,6) nitric oxide band was recorded in experiment A using a monochromator entrance slit width 1 mm, and the sensitivity of the recording system at 2890 Å = 1.86 x sensitivity at 5000 Å (E.M.I. Ltd. data). Thus $K2890 = \frac{1}{59} \times \frac{1}{1.86} K5000 = 0.0091\ K5000\ cc^{-1}sec^{-1}div^{-1}$. (Fig.5 shows that the Brown Recorder deflection increases by a factor of 59, when the slit width is increased from 0.05 mm, used for K5000 to 1 mm used to measure Ip2890). According to table 3, $I_{NO} = 13.5\ K2890\ I2890$, thus $I_{NO} = 0.12\ K5000\ I2890$.

The intensity Ip3200 of the 3206 Å - 3198 Å β (0,8) band of nitric oxide was measured using a monochromator entrance slit of width 0.5 mm. This corresponds to a factor of 22 increase in Brown Recorder deflection compared to that observed using a 0.05 mm slit (fig.5). The sensitivity of the recording system at 3200 Å = 2.08 x sensitivity at 5000 Å (E.M.I. Ltd. data). Thus

$K3200 = \frac{1}{22} \times \frac{1}{2.08} \times K5000 = 0.0219\ K5000\ cc^{-1}sec^{-1}div^{-1}$. According to table 3, $I_{NO} = 9.3\ K3200\ I3200$ thus $I_{NO} = 0.20\ K5000\ I3200$.

4.5 The Concentration of Nitrogen Atoms.

Berkowitz, Chupka, and Kistiakowsky (1956) using a mass spectrometer found that the intensity of the nitrogen afterglow is proportional to the square of the concentration of ground state nitrogen atoms (1.2.6). Also the nitrogen afterglow intensity I_{N_2} is proportional to the total number of molecules per cc, Mcc^{-1}. Thus $I_{N_2} = B_1 Mn_1^2$ where n_1 is the number of nitrogen atoms per cc and B_1 is the total rate constant for the production of the nitrogen afterglow photons by the processes

$$N + N + M \rightarrow N_2^{**} + M$$

$$N_2^{**} + M \rightarrow N_2^{*} + M$$

$$N_2^{*} \rightarrow N_2 + h\nu \quad \text{(Nitrogen afterglow band photon).}$$

From a rough calibration of the afterglow intensity and the concentration of nitrogen atoms, Berkowitz and Kistiakowsky determined B_1 as $2 \times 10^{-33}\ cc^2\ molecule^{-2}sec^{-1}$. However the infra red afterglow bands were not included in the measured radiation intensity, thus the rate constant B_1 was smaller than the total rate constant for production of photons by the above reactions.

Harteck et al (1958) measured the nitrogen atom concentration by titrating active nitrogen with nitric oxide (5.2) at a given point in a stream of active nitrogen. The rate of recombination

of nitrogen atoms was measured by the decrease of intensity of the afterglow along the tube the gas flow rate being known. According to their measurements $B_1 = (1.72 \pm 0.17) \times 10^{-32}$ cc^{2}mol^{-2}sec^{-1}.

In the present experiments the nitrogen used was at a pressure of 1.23 mm Hg and at a temperature of about 20°C. This corresponds to a total particle concentration $M = 4.06 \times 10^{16}$ molecules cc^{-1}, and to $B_1M = 7 \times 10^{-16}$ mol^{-1}cc sec^{-1}. We are assuming that the rate constant B_1M relates the total intensity of the bands observed by Bayes and Kistiakowsky (1960) to the nitrogen atom concentration, by $I_{N_2} = B_1Mn_1^2$. We have $I_{N_2} = 1.2$ K5000 I5755 from 4.3, thus

$$n_1^2 = \frac{I_{N_2}}{B_1M} = \frac{1.2 \text{ K5000 I5755}}{7 \times 10^{-16}} \text{ atoms}^2 \text{ cc}^2$$

$$= 1.72 \times 10^{15} \text{ K5000 I5755 atoms}^2 \text{ cc}^{-2}.$$

K5000 = 6.7×10^{11} from 4.2.7, and in experiment A a typical value of Ip5755 was 10 chart divisions (R_2). The corresponding value of n_1 is 1.1×10^{14} atoms cc^{-1}, i.e. about 0.1% of nitrogen molecules were dissociated into atoms. The corresponding value of B_1Mn_1 is $\pm$ 0.08 cc sec^{-1} $\sim$ 0.1 cc sec^{-1}. Owing to the uncertainty in K5000, n_1 lies between the limits 5×10^{13} to 2×10^{14} atoms cc^{-1}.

THE INTENSITY AND DECAY OF THE NITRIC OXIDE AND NITROGEN AFTERGLOWS IN TERMS OF GAS PHASE AND WALL PROCESSES.

5.1 Introduction to the Discussion.

TABLE 26. SYMBOLS USED IN CHAPTERS 5 AND 6.

I_{NO}	=	Integrated Intensity of Nitric Oxide Afterglow Bands in photons $cc^{-1} sec^{-1}$.
I_{N_2}	=	Integrated Intensity of Nitrogen Afterglow Bands in photons $cc^{-1} sec^{-1}$.
t	=	time in seconds.
I_{tNO}	=	Nitric Oxide Afterglow Intensity at time t.
I_{tN_2}	=	Nitrogen Afterglow Intensity at time t.
$I_{t\lambda}$	=	Afterglow Intensity at time t of band of wavelength λ Å.
R_{NO}	=	$\frac{-d \log I_{tNO}}{dt}$ sec^{-1}.
R_{N_2}	=	$\frac{-d \log I_{tN_2}}{dt}$ sec^{-1}.
n_1	=	Number of Nitrogen atoms cc^{-1}.
n_2	=	" " Oxygen " ".
n_3	=	" " " Molecules cc^{-1}.
n_4	=	" " Nitric Oxide Molecules cc^{-1}.
M	=	Number of Nitrogen Molecules cc^{-1} and also represents a molecule.
W	=	Wall of discharge tube.
S	=	Rate of generation of Nitrogen atoms in glow discharge in $cc^{-1} sec^{-1}$.
hv	=	Nitrogen Afterglow Band photon.
hv (β, γ)	=	Photon from Nitric Oxide Molecule due to $B^2\Pi \rightarrow X^2\Pi$ or $A^2\Sigma^+_v \rightarrow X^2\Pi$ transitions.

Berkowits, Chupka and Kistiakowsky (1956) observed that the intensity of the nitrogen afterglow $I_{N_2} = B_1 n_1^2$, where n_1 is the concentration of ground state nitrogen atoms and B_1 is a constant. The reactions which give rise to the nitrogen afterglow are described in (1.2.6). Effectively the overall process is $N + N + M \rightarrow N_2 + M + h\nu$.

According to Kaufman and Kelso (1957) the NO β and γ bands emitted when nitric oxide is added to active nitrogen are due to the reactions

$$NO + N \rightarrow N_2 + O$$
$$N + O + M \rightarrow NO^* + M$$
$$NO^* \rightarrow NO + h\nu\ (\beta, \gamma).$$

They deduced this by adding $N^{15}O$ to N_2^{14} containing N^{14} atoms, having previously noted the isotope wavelength shift between $N^{14}O$ and $N^{15}O$ spectra. They found that the NO bands were emitted by $N^{14}O$ only, supporting the reactions

$$N^{14} + N^{15}O \rightarrow N_2^{14,15} + O$$
$$N^{14} + O + M \rightarrow N^{14}O^* + M$$
$$N_{14}O^* \rightarrow NO + h\nu\ (\beta, \gamma).$$

If as Tanaka (1954) had proposed the mechanism of excitation was of the type

$$N + O + NO \rightarrow NO^* + NO$$
$$NO^* \rightarrow NO + h\nu\ (\beta, \gamma)$$

then some $N^{15}O$ bands should have been detected when $N^{15}O$ was added to N^{14}.

According to Kaufman (1958), if oxygen is present with active nitrogen, it is reasonable to suppose that oxygen atoms are produced by the reactions $N + O_2 \rightarrow NO + O$, $N + NO \rightarrow N_2 + O$. The oxygen atoms then combine with nitrogen atoms, and NO β and γ bands are emitted

$$N + O + M \rightarrow NO^{*} + M$$

$$NO^{*} \rightarrow NO + h\nu\ (\beta, \gamma)\ .$$

If the basic mechanism proposed by Kaufman and Kelso for the nitric oxide afterglow is correct then it would be expected that the nitric oxide afterglow intensity = $B_{12}Mn_1n_2$ where n_1 and n_2 are the concentrations of ground state nitrogen atoms and oxygen atoms respectively and B_{12} is a constant. The energies of the upper states of the nitric oxide afterglow transitions are about 6.49 ev above the ground state, and 6.49 ev is the dissociation energy of the nitric oxide molecule. Hence the nitrogen and oxygen atoms must be in the ground state before combination according to the above mechanism. The purpose of the discussion in chapters 5 and 6 is to relate the observed intensity of the nitric oxide afterglow bands quantitatively to the law $I_{NO} = B_{12}Mn_1n_2$, and also to calculate B_{12} the rate constant for combination of nitrogen and oxygen atoms. The reaction $N + O_2 \rightarrow NO + O$, and the effect of the walls are also discussed.

5.2 <u>The Glow Discharge.</u>

It is standard knowledge, Hinshelwood (1940), that in simple gas phase reactions of the type,

$$A + B \rightarrow AB$$

the reactants are removed at the rate

$$\frac{-dn_A}{dt} = \frac{-dn_B}{dt} = Kn_An_B\ ,$$

and that the product is formed at the rate $\frac{dn_{AB}}{dt} = Kn_An_B$ where n_A, n_B, and n_{AB} are the volume concentrations of A, B, and AB

respectively.

Let us consider the reaction

$$A + B + M \rightarrow AB + M$$

where A and B are atoms, M is a molecule, and AB is of-course a diatomic molecule. When two atoms approach to within an $\mathring{a}$ngstrom or so of each other, they form an unstable molecule; and they will rapidly fly apart, unless sufficient energy is removed to allow them to drop into a stable molecular state. Since the collision time is $\sim 10^{-13}$ secs, then radiation of the excess energy is not likely to occur, because the radiative lifetime of an excited state is $\sim 10^{-8}$ secs. However the excess energy can be removed, if the two atoms A and B collide at the same time with a molecule M which undergoes the necessary change in energy. Thus in a reaction of the type $A + B + M \rightarrow AB + M$ where A, B, are atoms and M is a molecule,

$$\frac{-dn_A}{dt} = \frac{-dn_B}{dt} = \frac{dn_{AB}}{dt} = K^1 M n_A n_B ,$$

where K^1 is a constant and M is the volume concentration of molecules.

The following reactions, (Table 26a), are likely to be predominant in the glow discharge of a nitrogen, oxygen mixture, according to the discussion of 5.1. No doubt some of the reactants will be in an ionised state but it is assumed that chamically the reactions would be the same. The rate constants, and the rate of removal of the reactants per cc are given for each reactant; the rate constants being equivalent to K and K^1 in the above discussion. The combination rate of oxygen atoms is very slow and is neglected.

TABLE 26 a. REACTIONS IN THE GLOW DISCHARGE.

Reaction	Rate Constant	Reaction Rate $cc^{-1} sec^{-1}$
$N + N + M \rightarrow N_2 + M + h\nu$	B_1 $cc^2 sec^{-1} mol^{-2}$	$B_1 n_1^2$
$N + O_2 \rightarrow NO + O$	B_{13} $cc\ sec^{-1} mol^{-1}$	$B_{13} n_1 n_3$
$N + NO \rightarrow N_2 + O$	B_{14} $cc\ sec^{-1} mol^{-1}$	$B_{14} n_1 n_4$
$O + Wall \rightarrow \frac{1}{2}O_2 + Wall$	B_{2W} sec^{-1}	$B_{2W} n_2$
$N + Wall \rightarrow \frac{1}{2}N_2 + Wall$	B_{1W} sec^{-1}	$B_{1W} n_1$
$N + O + M \rightarrow NO^* + M$ $NO^* \rightarrow NO + h\nu\ (\beta, \gamma)$	B_{12} $cc^2 sec^{-1} mol^{-2}$	$B_{12} n_1 n_2$
Rate of formation of nitrogen atoms		S

According to Berkowitz et al (1956) the nitrogen afterglow band intensity I_{N_2} is given by,

$$I_{N_2} \propto n_1^2$$

or $$I_{N_2} = B_1 n_1^2 \qquad (1)$$

Similarly we put

$$I_{NO} \propto n_1 n_2$$

$$I_{NO} = B_{12} n_1 n_2 \qquad (2)$$

At equilibrium in the R.F. discharge the rate of generation of each species of molecule and atom is balanced by the rate of loss. From table 26a we have the following equations.

Nitrogen Atoms.

$$-\frac{dn_1}{dt} = -S + B_{1W}n_1 + B_{13}n_1n_3 + B_{14}n_1n_4 + B_{12}Mn_1n_2 + B_1Mn_1^2 = 0 \quad (3)$$

Oxygen Atoms.

$$-\frac{dn_2}{dt} = -B_{13}n_1n_3 - B_{14}n_1n_4 + B_{2W}n_2 + B_{12}Mn_1n_2 = 0 \quad (4)$$

Nitric Oxide Molecules.

$$-\frac{dn_4}{dt} = -B_{13}n_1n_3 + B_{14}n_1n_4 = 0 \quad (5)$$

$$\therefore n_4 = \frac{B_{13}n_3}{B_{14}} \quad (6)$$

Substituting in eq.4 using eq.6 we have

$$2B_{13}n_1n_3 = B_{2W}n_2 + B_{12}Mn_1n_2 \quad (7)$$

$$\therefore \text{Oxygen Atom Concentration } n_2 = \frac{2B_{13}n_1n_3}{(B_{2W} + B_{12}Mn_1)}$$

From eq.3 and eq.6 we have that the nitrogen atom concentration n_1 is given by,

$$n_1 = \frac{S}{B_{1W} + 2B_{13}n_3 + B_{12}Mn_2 + B_1Mn_1} \quad (8)$$

From eq.2 and eq.7

$$I_{NO} = \frac{2B_{12}MB_{13}n_1^2n_3}{(B_{2W} + B_{12}Mn_1)} \quad (9)$$

Substituting from eq.8 in eq.9,

$$I_{NO} = \frac{2B_{12}\,B_{13}n_3\;S^2M}{(B_{2W} + B_{12}Mn_1)\,(B_{1W} + 2B_{13}n_3 + B_{12}Mn_2 + B_1Mn_1)^2} \qquad (10)$$

Assuming that $B_{12}Mn_1$ is small compared with B_{2W} and $(B_{12}Mn_2 + B_1Mn_1)$ is small compared with $(B_{1W} + 2B_{13}n_3)$, then

$$I_{NO} = \frac{2B_{12}B_{13}n_3S^2M}{B_{2W}\,(B_{1W} + 2B_{13}n_3)^2} \qquad (11)$$

The above assumptions are shown to be justified in section 6.4.

Let $P = 2B_{12}B_{13}S^2M$, (12)

then $$I_{NO} = \frac{Pn_3}{B_{2W}\,(B_{1W} + 2B_{13}n_3)^2} \qquad (13)$$

Eq.13 implies that as n_3, the concentration of oxygen molecules, increases, the intensity of the nitric oxide bands will decrease as was observed (3.6.1).

Simplifying eq.8 according to the assumption that $(B_{1W} + 2B_{13}n_3) \gg (B_{12}Mn_2 + B_1Mn_1)$, used to simplify eq.9 we have $n_1 = \frac{S}{(B_{1W} + 2B_{13}n_3)}$. Substituting this in eq.1 we have

$$I_{N_2} = \frac{B_1MS^2}{(B_{1W} + 2B_{13}n_3)^2} \qquad (13a)$$

This implies that $I_{N_2}^{-\frac{1}{2}} = E + F\,n_3$ where E and F are constants if B_{1W} and M are constants.

5.3 The Afterglow.

We will now consider the decay of the afterglow. It is assumed that the rate of removal of atoms by recombination of nitrogen atoms

$$N + N + M \rightarrow N_2^{**} + M$$
$$N_2^{**} + M \rightarrow N_2^{*} + M$$
$$N_2^{*} \rightarrow N_2 + h\nu$$

and also by combination of nitrogen and oxygen atoms

$$N + O + M \rightarrow NO^{*} + M$$
$$NO^{*} \rightarrow NO + h\nu \ (\beta, \gamma)$$

is small compared with the rate of attachment of atoms to the walls of the discharge tube,

$$N + \text{wall} \rightarrow \tfrac{1}{2}N_2 + \text{wall}$$
$$O + \text{wall} \rightarrow \tfrac{1}{2}O_2 + \text{wall}\ .$$

Thus in equations 3 and 4 the terms $B_{12}{}^{M}n_1n_2$ and $B_1{}^{M}n_1{}^2$ are considered negligible compared with $B_{1w}n_1$ and $B_{2w}n_2$. The production of oxygen atoms at the rate $2B_{13}n_1n_3$ in the afterglow is small but it is not neglected. In 6.2.3 it is shown that B_{13} is smaller in the afterglow than in the glow discharge.

From eqs.3, 4 and 6, deleting the terms $B_{12}{}^{M}n_1n_2$ and $B_1{}^{M}n_1{}^2$, and putting the rate of production of nitrogen atoms $S = 0$ we have,

$$-\frac{dn_1}{dt} = B_{1w}{}^{(N)}n_1 + 2B_{13}{}^{(N)(O_2)}n_1n_3 \qquad (14)$$

$$-\frac{dn_2}{dt} = B_{2w}{}^{(O)}n_2 - 2B_{13}{}^{(N)(O_2)}n_1n_3 \qquad (15)$$

$\frac{dn_1}{dt}$ and $\frac{dn_2}{dt}$ are not equal to zero in the afterglow, since the concentrations of the active species are decreasing. Thus adding eqs. 14 and 15 we have

$$-\frac{1}{n_1}\frac{dn_1}{dt} - \frac{1}{n_2}\frac{dn_2}{dt} = B_{1W} + B_{2W} + 2B_{13}n_3 - \frac{2B_{13}n_3n_1}{n_2}$$

$$\text{or } -\frac{d \log n_1}{dt} - \frac{d \log n_2}{dt} = B_{1W} + B_{2W} + 2B_{13}n_3 - \frac{2B_{13}n_3n_1}{n_2}$$

From eq. 7 , $n_2 = \frac{2B'_{13}n_1n_3}{B_{2W}}$ just after the glow discharge; B'_{13} indicates here B_{13} (glow).

Thus we have by substitution and integration,

$-(\log n_1 + \log n_2) = (B_{1W} + B_{2W}(1 - \frac{B_{13}}{B'_{13}}) + 2B_{13}n_3)\ t + \text{constant}$. Since B_{13} (afterglow) $\ll B_{13}$ (glow), (6.2.3), then the above equation is effectively

$$-\log n_1n_2 = (B_{1W} + B_{2W} + 2B_{13}n_3)\ t + \text{constant} \qquad (16)$$

Thus using eq. 2,

$$\log I_tN0 = -(B_{1W} + B_{2W} + 2B_{13}n_3)t + \text{constant} + \log B_{12}M, \qquad (17)$$

where M is a constant, when the total gas pressure is constant.

By differentiating the theoretical equation 17 we have

$$-\frac{d \log I_tN0}{dt} = (B_{1W} + B_{2W} + 2B_{13}n_3) \qquad (18)$$

Thus according to the theory ,

$$-\frac{d \log I_t\lambda}{dt} = (B_{1W} + B_{2W} + 2B_{13}n_3) \qquad (19)$$

where $I_t\lambda$ is the afterglow intensity of an individual band at time t. B_{1W} and B_{2W} in eq. 19 might differ slightly from B_{1W} and B_{2W} in eq. 18, assuming that the rate constants for attachment of atoms to the walls are dependent on the mean energy of the atoms; and that there are slight differences in the mean kinetic energy

of atoms giving rise to different upper vibrational levels of the nitric oxide molecule. Eq.19 is identical in form with the observed afterglow decay $R_{NO} = \frac{-d \log I_t \lambda}{dt}$, (3.2.2) and (3.6.3).

This law was obeyed from t = 0 to the maximum time observed; R_{NO} being a constant, independent of time.

Thus, according to this discussion,

$$R_{NO} = R_{1W} + R_{2W} + 2R_{13}n_3 \qquad (20)$$

and $$R_{N_2} = 2\,(R_{1W} + 2R_{13}n_3) \qquad (21).$$

DISCUSSION OF RESULTS

6.1 The Decay of the Afterglow.

6.1.1 Afterglow decay constants R_{NO} and R_{N_2}.

In both experiment A and experiment B the decay of individual afterglow bands obeyed laws of the form $R_{NO} = \frac{-d \log I_{t\lambda}}{dt}$ for nitric oxide afterglow bands, and $R_{N_2} = \frac{-d \log I_{t\lambda}}{dt}$ for nitrogen afterglow bands; where R_{NO} and R_{N_2} were independent of time.

Values of R_{NO} measured in experiment A are shown in table 27 for various nitric oxide bands. In the case of runs 8, 5 and 3 the observed values of R_{NO} vary by ± 5% with wavelength. In the case of runs 7 and 6 the variation is ≅ 35%.

The values of R_{NO} measured in experiment B are shown in tables 18 and 19. From table 19, R_{NO} for the $v^1 = 0$, δ nitric oxide bands is (15 ± 5)% greater than R_{NO} for the $v^1 = 0$, β nitric oxide bands. The values of R_{NO} vary more or less regularly with oxygen added as discussed in 3.6.3.

In general the R_{NO} values varied more erratically in experiment A than in experiment B.

The main difference between experiments A and B was that in experiment B the same nitrogen was used throughout the experiment. Also the cycle of R.F. discharge pulses was not interrupted between observations for a given oxygen percentage in experiment B.

Rayleigh (1942) has shown that the adsorbed layer on the walls of an afterglow tube has a marked influence on the characteristics of the discharge tube. Thus it is asserted that in experiment B the effect of the adsorbed layer on the afterglow decay rate varied little, but in experiment A there was some variation in the adsorbed layer. It is pertinent to note that each run lasted about 1 hour. The large variation of R_{NO} with wavelength in runs 7 and 6 is therefore explained by a change in the adsorbed layer in the time between observations. This is supported by the fact that in run 7 R_{NO} increases with wavelength and in run 6 it decreases.

TABLE 27. VALUES OF AFTERGLOW DECAY CONSTANTS IN EXPERIMENT A.

Run	Number of Oxygen Molecules Added cc^{-1}	$R_{NO} = \frac{-d \log I_{t2363}}{dt}$	$R_{NO} = \frac{-d \log I_{t2890}}{dt}$	$R_{NO} = \frac{-d \log I_{t3200}}{dt}$
7	3.7×10^{12}	0.66	0.9	0.9
8	3.7×10^{12}	0.63	0.58	0.6
5	7×10^{12}	0.35	0.32	0.32
6	3.6×10^{13}	0.75	0.52	0.45
3	3.7×10^{13}	0.96	1.1	0.91

The erratic variations of R_{NO} in experiment A, in run 7 and run 6, are thus assumed to be due to changes in the adsorbed layer on the walls of the afterglow tube during the experiment;

and are therefore rejected from further discussion. The apparent difference of 15% in the decay rates of β and γ bands in experiment B may be due to a regular cycle of change in the condition of the walls with time.

In both experiments A and B nitric oxide afterglow bands from levels above $v' = 0$ were rather weak. Thus the decay rate of these bands could not be measured. In view of the small difference observed between R_{NO} for $v' = 0$, β and γ bands, and the small energy differences between the vibrational energy levels of the $B^2\Pi g$ and $A^2\Sigma_u^+$ states of the nitric oxide molecule; it seems unlikely that the mean value of R_{NO}, corresponding to the decay of the integrated intensity of nitric oxide afterglow bands, differs by more than 20% from the values of R_{NO} for individual bands. Thus at various points in the discussion it is assumed that $R_{NO} = \frac{-d \log I_{tNO}}{dt}$, is given by the decay rate of an individual nitric oxide band. The value of R_{N_2} used in $R_{N_2} = \frac{-d \log I_{tN_2}}{dt}$ is the value corresponding to the decay of the integrated intensity of the (10,6), (11,7), (12,8) bands of the nitrogen afterglow.

6.1.2 <u>The Rate of Attachment of Oxygen and Nitrogen Atoms to the Walls.</u>

According to the discussion of 5.3, $R_{NO} = R_{1W} + R_{2W} + 2R_{13}n_3$ (eq.20) and $R_{N_2} = 2(R_{1W} + 2R_{13}n_3)$, (eq.21); where R_{1W} and R_{2W} are rate constants for the attachment of nitrogen, and oxygen atoms to the walls of the system respectively. The values of R_{1W}

and B_{2W} derived from the results of experiment A are shown in table 28. It should be noted that certain experimental values of R_{NO} have been rejected from the discussion as discussed in 6.1.1.

It is shown below (6.2.3) that the value of B_{13} in the afterglow is less than that of B_{13} in the glow discharge.

The values of B_{2W} in table 28 appear more or less independent of wavelength as they would be expected to be. B_{2W} was calculated using the equation $B_{2W} = R_{NO} - \frac{R_{N_2}}{2}$, derived from eqs.20 and 21. For the lower oxygen concentrations R_{NO} and R_{N_2} are an order of magnitude greater than B_{2W}; and so precision in the values of B_{2W} could not be expected. From table 28 it can be concluded that B_{2W} is proportional to the oxygen added to the system, in the range of oxygen concentrations used. A possible explanation of this is that B_{2W} is proportional to the concentration of oxygen atoms on the walls, and that the concentration of atoms on the walls was proportional to the oxygen added. Changes in the equilibrium concentration of atoms on the walls of the discharge tube could partly explain the erratic variation of R_{NO} evident in some cases in experiment A, (Table 27). Running the discharge cycle, without interruption, between afterglow band observations corresponding to a given oxygen concentration has a stabilising effect, as the values of R_{NO} measured in experiment B were less erratic. It can be deduced that the R.F. discharge has an influence on the

TABLE 28. VALUES OF WALL DECAY RATE CONSTANTS FOR NITROGEN AND OXYGEN ATOMS.

Run	$R_{N_2} = \frac{-d \log I_{\lambda 5755}}{dt}$	$\frac{R_{N_2}}{2} = B_{1W} + 2B_{13}n_3$	γ (0,1)		β (0,6)		β (0,8)		Number of Oxygen Molecules Added cc^{-1}
			R_{NO}	B_{2W}	R_{NO}	B_{2W}	R_{NO}	B_{2W}	
7	1.26	0.63	0.66	0.03					3.7×10^{12}
8	1.07	0.54	0.63	0.09	0.58	0.04	0.60	0.06	3.7×10^{12}
5	0.58	0.29	0.35	0.06	0.32	0.03	0.32	0.03	7×10^{12}
6	0.77	0.39	0.75	0.36					3.6×10^{13}
3	1.17	0.58	0.96	0.38	1.1	0.52	0.91	0.33	3.7×10^{13}

equilibrium between the oxygen concentration on the walls and the system.

We have from fig.19 that in experiment B, R_{NO} for the γ (0,3) and β (0,6) nitric oxide bands increases on average by 10% when 5×10^{13} oxygen molecules cc^{-1} are added to the system.

6.2 The Intensity of the Nitric Oxide and Nitrogen Afterglows.

6.2.1 The Relationship between the Nitric Oxide and Nitrogen Afterglow Intensities. Experiment A.

According to the discussion in 5., the integrated intensity of nitric oxide β and γ afterglow bands is given by

$$I_{NO} = \frac{2B_{12}MB_{13}n_1{}^2n_3}{(B_{2W} + B_{12}Mn_1)} \quad , \text{(eq.9)} \; ; \text{ where } B_{12}n_1 \text{ is assumed to be}$$

small compared with B_{2W}. Thus substituting from eq.1 in eq.9 we have

$$I_{NO} = \frac{2B_{12}B_{13}I_{N_2}n_3}{B_{2W}\,B_1} \qquad (22)$$

Thus $$I_{NO} \propto \frac{I_{N_2}n_3}{B_{2W}} \quad \text{or} \quad \frac{I_{NO}B_{2W}}{I_{N_2}\,n_3} = \text{constant.} \qquad (23)$$

Assuming $I_{NO} \propto I_{2363} = Ip_{2363}$ and $I_{N_2} \propto I_{5755} = Ip_{5755}$ (4.3 and 4.4) we have

$$\frac{10^{13}Ip_{2363}\,B_{2W}}{Ip_{5755}\,n_3} = B_{2363} = \text{constant} \qquad (24)$$

Values of B_{2363}, B_{2890} and B_{3200} have been calculated using the intensities and values of B_{2W} corresponding to the γ (0,1), β (0,6), and β (0,8) nitric oxide bands respectively, (Table 29). These data were measured in experiment A.

According to the discussion in this section the values of

TABLE 29. B_{2363}, B_{2890} AND B_{3200} VS. OXYGEN ADDED.

Run	Number of Oxygen Molecules Added cc^{-1}	Ip_{5755} Chart Divs. (R_2)	Ip_{2363} Chart Divs. (R_2)	$\frac{10^{13} Ip_{2363} B_{2E}}{2 Ip_{5755} n_3} = B_{2363}$	Ip_{2890} Chart Divs. (R_2)	$\frac{10^{13} Ip_{2890} B_{2E}}{2 Ip_{5755} n_3} = B_{2890}$	Ip_{3200} Chart Divs. (R_2)	$\frac{10^{13} Ip_{3200}}{2 Ip_{5755} n_3} = B_{3200}$	$\frac{B_{2363} + B_{2890} + B_{3200}}{n}$
7	3.7×10^{12}	9.3	27.8	0.12					0.12
8	3.7×10^{12}	9.5	29.8	0.38	14	0.08	8.1	0.07	0.18
5	7.0×10^{12}	19.2	26.7	0.06	26.5	0.03	15.5	0.02	0.04
6	3.6×10^{13}	18.3	44.8	0.12					0.12
3	3.7×10^{13}	11.7	29.1	0.13	32.9	0.2	18.5	0.07	0.13
				Mean B_{2363} = 0.16		Mean B_{2890} = 0.1		Mean B_{3200} = 0.05	n = 1, runs 7 and 6 n = 3, runs 8,5,3.

Notes 1. Monochromator Entrance slit width = 1mm for Ip_{2363} and 0.5 mm for Ip_{2890} and Ip_{3200}.

B_{2363} etc. should be independent of the oxygen added. There is some scatter in the values in table 29 but they vary far less than $B_{2\prime\prime}$ or the oxygen added. Thus equation (24) is supported by these results.

Variations in the concentration of oxygen adsorbed on the walls of the system might be the reason for the remaining scatter in the values of B_{2363}, B_{2890} and B_{3200}. The mean values of B_{2363}, B_{2890} and B_{3200} are not equal, partly because different monochromator exit slit widths were used (Table 29), and because of variations in the sensitivity of the photomultiplier with wavelength, (4.4). The mean values for each oxygen concentration are reasonably constant.

TABLE 30. COMPARISON OF INTENSITY OF 2370 Å - 2363 Å δ (0,1) NITRIC OXIDE AFTERGLOW BAND WITH INTEGRATED INTENSITY OF 5854 Å (10,6), 5804 Å (11,7) AND 5755 Å (12,8) NITROGEN 1st POSITIVE BANDS.

I_{P2363} Chart Divs.(R_2)	I_{P5755} Chart Divs.(R_2)	$\frac{I_{P2363}}{I_{P5755}}$	Number of Oxygen Molecules Added cc^{-1}
27.8	9.3	3	3.7×10^{12}
29.8	9.5	3.1	3.7×10^{12}
26.7	19.2	1.4	7×10^{12}
44.8	18.3	2.5	3.6×10^{13}
29.1	11.7	2.5	3.7×10^{13}

It can be seen from table 30 that the variation of $\frac{I_{P2363}}{I_{P5755}}$ with oxygen is comparatively small. This would be expected as it has been shown that $\frac{I_{P2363} \times n_3}{I_{P5755} \quad B_{2W}}$ = constant, and that B_{2W} is proportional to n_3 (6.1.2). It can also be seen from the results of Kurzweg, Bass and Broida (1957) that the intensity of the nitrogen afterglow, and that of the nitric afterglow, decrease at about the same rate with oxygen added.

6.2.2. The Variation of the Nitric Oxide Afterglow Intensity with Oxygen. Experiment B.

According to figs.13 to 16 the mean variation of the afterglow intensities of the $\gamma(0,2)$, $\gamma(0,3)$, $\beta(0,6)$ and $\beta(0,7)$ bands of nitric oxide with added oxygen can be represented by

$$I_P^{-\frac{1}{2}} = E + F n_3 \qquad (25)$$

where Ip is the afterglow intensity of an individual nitric oxide band, and E and F are independent of n_3 the oxygen added per cc of nitrogen. Rearranging eq.25 we have

$$I_P = \frac{\text{constant}}{(E + F n_3)^2} \qquad (26)$$

According to the theoretical eq.13

$I_{NO} = \frac{P n_3}{B_{2W} (B_{1W} + 2B_{13} n_3)^2}$, where P is a constant at constant total pressure; and according to experiment A (table 28), B_{2W} is proportional to n_3. Assuming that Ip the afterglow intensity of an individual nitric oxide band varies with oxygen in the same way as I_{NO}, we can modify eq.13 to

$$Ip = \frac{P_1}{(B_{1W} + 2B_{13}n_3)^2} \qquad (27)$$

when P_1 is a constant. This equation is identical in form with the empirical equation 26.

According to table 17, $Iop^{\frac{1}{2}} \cdot \frac{dIp^{-\frac{1}{2}}}{dn_3}$ is within experimental error independent of wavelength, where $Iop^{\frac{1}{2}}$ is the value of $Ip^{\frac{1}{2}}$ where $n_3 = 0$. This can be explained as follows. Rearranging eq.27 we have $Ip^{-\frac{1}{2}} = P_1^{-\frac{1}{2}} (B_{1W} + 2B_{13}n_3)$ (28)

Thus $\frac{dIp^{-\frac{1}{2}}}{dn_3} = P_1^{-\frac{1}{2}} (2B_{13})$. From eq.27 we have $Iop^{\frac{1}{2}} = \frac{P_1^{\frac{1}{2}}}{B_{1W}}$,

and therefore

$$Iop^{\frac{1}{2}} \cdot \frac{dIp^{-\frac{1}{2}}}{dn_3} = \frac{2B_{13}}{B_{1W}} . \qquad (29)$$

According to our experiment and theory $Iop^{\frac{1}{2}} \cdot \frac{dIp^{-\frac{1}{2}}}{dn_3}$ = constant. According to table 17 the mean value of $Iop^{\frac{1}{2}} \cdot \frac{dIp^{-\frac{1}{2}}}{dn_3} = 4 \times 10^{14}$ mol^{-1}cc. Taking the value of B_{1W} as $\frac{RNO}{2}$, then $B_{1W} = 0.21$ sec^{-1} from table 19; and so according to eq.29 $B_{13} = 4.2 \times 10^{15}$ molecule^{-1}cc sec^{-1}. Using the equation $Ip^{-\frac{1}{2}}_{2590} = \text{constant} \times (B_{1W} + 2B_{13}n_3)$ (30) a set of values of B_{13} is now calculated. The value of B_{1W} will be taken as $\frac{RNO}{2}$ since a more accurate value is not available. The method of calculation is self evident.

TABLE 31. EQUATIONS FOR CALCULATING B_{13}.

Equation Number	Ip_{2590} Chart Divs. (R_2)	$B_{1W} = \frac{R_{NO}}{2}$ sec^{-1}	Oxygen Added Molecules cc^{-1}	$Ip^{-\frac{1}{2}}_{2590} = K(B_{1W} + 2B_{13}n_3)$
a	34.5	0.22	0	$0.17 = K\ (0.22)$
b	15.3	0.23	10^{13}	$0.26 = K\ (0.23 + 2 \times 10^{13}B_{13})$
c	9.3	0.24	2×10^{13}	$0.33 = K(0.24 + 4 \times 10^{13}B_{13})$
d	6.7	0.26	3.1×10^{13}	$0.39 = K(0.26 + 6.2 \times 10^{13}B_{13})$
e	5.5	0.26	4.1×10^{13}	$0.43 = K(0.26 + 8.2 \times 10^{13}B_{13})$
f	4.4	0.27	5.1×10^{13}	$0.48 = K(0.27 + 10.2 \times 10^{13}B_{13})$

$$b \div a \qquad \frac{0.26}{0.17} = \frac{(0.23 + 2 \times 10^{13}B_{13})}{0.22}$$

i.e. $0.336 = 0.23 \times 2 \times 10^{13}B_{13}$

$B_{13} = 5.3 \times 10^{-15}\ mol^{-1}\ cc\ sec^{-1}$.

$$c \div b \qquad \frac{0.33}{0.26} = \frac{(0.24 + 4 \times 10^{13}B_{13})}{(0.23 + 2 \times 10^{13}B_{13})}$$

Cross multiplying $0.292 + 2.54 \times 10^{13}B_{13} = 0.24 + 4 \times 10^{13}B_{13}$

$B_{13} = 3.56 \times 10^{-15}\ mol^{-1}\ cc\ sec^{-1}$.

$d \div c \quad \frac{0.39}{0.33} = \frac{(0.26 + 6.2 \times 10^{13} B_{13})}{(0.24 + 4 \times 10^{13} B_{13})}$

Cross multiplying $0.284 + 4.72 \times 10^{13} B_{13} = 0.26 + 6.2 \times 10^{13} B_{13}$

$B_{13} = 1.6 \times 10^{-15}$ mol^{-1}cc sec^{-1}.

$e \div d \quad \frac{0.43}{0.39} = \frac{(0.26 + 8.2 \times 10^{13} B_{13})}{(0.26 + 6.2 \times 10^{13} B_{13})}$

$0.286 + 6.85 \times 10^{13} B_{13} = 0.26 + 8.2 \times 10^{13} B_{13}$

$B_{13} = 1.9 \times 10^{-15}$ mol^{-1}cc sec^{-1}.

$f \div e \quad \frac{0.48}{0.43} \quad \frac{(0.27 + 10.2 \times 10^{13} B_{13})}{(0.26 + 8.2 \times 10^{13} B_{13})}$

$0.29 + 9.15 \times 10^{13} B_{13} = 0.27 + 10.2 \times 10^{13} B_{13}$

$B_{13} = 1.9 \times 10^{-15}$ mol^{-1} cc sec^{-1}.

TABLE 32. APPARENT VARIATION OF B_{13} WITH OXYGEN ADDED.

B_{13} mol^{-1}cc sec^{-1}	Oxygen Added Molecules cc^{-1}	Percentage Oxygen Added
5.3×10^{-15}	10^{13}	0.025
3.6×10^{-15}	2×10^{13}	0.05
1.6×10^{-15}	3.1×10^{13}	0.075
1.9×10^{-15}	4.1×10^{13}	0.1
1.9×10^{-15}	5.1×10^{13}	0.125

The mean of the values of B_{13} in table 32 is 2.9×10^{-15} mol^{-1} cc sec^{-1} which is about 75% of the value calculated from $Iop^{\frac{1}{2}} \times \frac{dIp^{-\frac{1}{2}}}{dn_3}$.

According to table 32 B_{13} appears to vary in a definite manner with added oxygen, reflecting the oscillation of the $Ip^{-\frac{1}{2}}$ vs. n_3 curves about the mean linear variation. However the rate constant for the reaction $N + O_2 \rightarrow NO + O$ by definition does not vary with added oxygen. The apparent decrease in B_{13} is probably due to the recombination rate of nitrogen atoms decreasing with the nitrogen atom concentration, as oxygen was added. According to eq.10 (5.2) the initial intensity of the afterglow is given by

$$I_{NO} = \frac{2B_{12}B_{13}n_3S^2M}{(B_{2W} + B_{12}Mn_1)(B_{1W} + 2B_{13}n_3 + B_{12}Mn_2 + B_1Mn_1)^2}$$

$$= \frac{2B_{12}B_{13}n_3S^2M}{(B_{2W})(B_{1W} + n_3 \quad 2B_{13} + \frac{B_{12}Mn_2}{n_3} + \frac{B_1Mn_1}{n_3} \quad)^2},$$

since $B_{2W} > B_{12}Mn_1$ from table 35. It was assumed in calculating B_{13} that the denominator of I_{NO} was of the form $B_{2W}(B_{1W} + 2B_{13}n_3)^2$. Identifying this with the more general denominator in eq.10 it can be seen that the calculated values of B_{13} are in fact values of $B_{13} + \frac{B_{12}Mn_2}{2n_3} + \frac{B_1Mn_1}{2n_3}$. The last term would certainly decrease with added oxygen. In 6.4, where the removal rates of atoms by various processes are compared; it is shown that the removal of nitrogen atoms by recombination, corresponding to the

term $\frac{B_1 M n_1}{2n_3}$, could account for the decrease in the calculated values of B_{13}.

The subsequent increase in the last two values of B_{13} is not accounted for. The mean value of B_{13} calculated above may be 3 times the true value since $\frac{B_1 M n_1}{n_3}$ is comparable with B_{13} at the lower oxygen concentrations. This is discussed in 6.4, and it is concluded that $B_{13} = (1.4 \pm 0.3) \times 10^{-15}$ mol^{-1}cc sec^{-1}.

6.2.3 Rate of reaction of Nitrogen Atoms and Oxygen Molecules in the Afterglow.

B_{13} is the rate constant for the reaction $N + O_2 \rightarrow NO + O$, and according to eq.20 (5.3) $R_{NO} = B_{1W} + B_{2W} + 2B_{13}n_3$.

Thus $$\frac{dR_{NO}}{dn_3} = \frac{d(B_{1W} + B_{2W})}{dn_3} + 2B_{13} \qquad (31).$$

It is known from the results of experiment A, that B_{2W} increases with added oxygen (6.1.2); and from fig.19 that $\frac{1}{2}\frac{dR_{NO}}{dn_3} \sim 4 \times 10^{-16}$ cc sec^{-1}mol^{-1}. Assuming that $\frac{d(B_{1W} + B_{2W})}{dn_3} \sim 2B_{13}$ then we have that in the afterglow $B_{13} \sim 2 \times 10^{-16}$ cc sec^{-1}mol^{-1}. This is in good agreement with Kistiakowsky's value (1957) of 2×10^{-16} cc sec^{-1} mol^{-1} for B_{13} at room temperature, deduced from his formula $B_{13} = 3 \times 10^{12} \exp.\left(\frac{-6200}{RT}\right)$ cc sec^{-1}mol^{-1}. The larger value of B_{13} in the glow is probably due to the greater energy available in the discharge to provide the activation energy for

the reaction $N + O_2 \rightarrow NO + O$.

6.2.4 The Variation of the Nitrogen Afterglow Intensity with Oxygen. Experiment A.

From eqs. 1 and 8 the integrated nitrogen afterglow intensity

$$I_{N_2} = \frac{B_1 M^2}{(B_{1W} + 2B_{13}n_3 + B_1 M n_1)^2} \qquad (32).$$

The term $B_{12}Mn_2$ is ignored, because from the discussion of 6.4 it appears that $B_1 M n_1 \sim 2B_{13}n_3$ but $B_{12}Mn_1 << 2B_{13}n_3$. Assuming that I_{N_2} is proportional to Ip_{5755}; and since M is proportional to the total gas pressure p mm Hg, we have

$(Ip_{5755})^{\frac{1}{2}} (B_{1W} + 2B_{13}n_3 + B_1 M n_1) p^{-\frac{1}{2}} = G$.

Values of G, shown in table 33, have been calculated using the values of Ip_{5755} measured in experiment A, and $B_{13} = 10^{-15}$ mol^{-1} cc sec^{-1} which is the lower limit of the true value of B_{13} according to the discussion of 6.4.

$n_1^2 = 1.72 \times 10^{15}$ K5000 I_{5755} from 4.5.

$B_1 = 1.72 \times 10^{-32}$ cc^2 mol^{-2} sec^{-1} according to Harteck et al (1958) and $B_{1W} = 7 \times 10^{-16}$ mol^{-1}cc sec^{-1} from 4.5.

The values of G are within $\pm$ 13% of each other excluding that corresponding to run 5. This shows that the variation of the nitric oxide afterglow intensity in experiment B, and the nitrogen afterglow intensity in experiment A was determined by the same parameters; even though the form of the variation was obscured in experiment A by the erratic variation of B_{1W} from one run to another. This is in agreement with the theory.

TABLE 33. G VS. OXYGEN ADDED.

Run	Number of Oxygen Molecules Added cc^{-1}	$I_{p_{5755}}$ Chart Divs.(R_2)	$\sqrt{I_{p_{5755}}}$	$B_{1W} = \frac{1}{2}B_{N_2}$ sec^{-1}	$2B_{13}n_3$ sec^{-1}	B_1Mn_1 sec^{-1}	$B_{1W} + 2B_{13}n_3 + B_1Mn_1$ sec^{-1}	P mm Hg.	$(B_{1W} + 2B_{13}n_3 + B_1Mn_1) \times \sqrt{I_{p_{5755}}} \times p^{-\frac{1}{2}}$
7	3.7×10^{12}	9.3	3.05	0.63	0.0074	0.07	0.707	0.875	1.9
8	3.7×10^{12}	9.5	3.08	0.54	0.0074	0.071	0.618	0.9	1.7
5	7.0×10^{12}	19.2	4.38	0.29	0.014	0.1	0.391	0.868	1.5
6	3.6×10^{13}	18.3	4.28	0.39	0.072	0.093	0.56	0.875	2.1
3	3.7×10^{13}	11.7	3.42	0.58	0.074	0.079	0.733	0.855	2.1

Experimental errors in the measurement of n_3 in the two experiments may account for the remaining variation in C.

6.2.5 Comparison with Previous Afterglow Intensity Measurements.

Anderson, Kavadas and McKay (1957) carried out experiments similar to the present experiments (1.3.2) using a non flow discharge tube system and oxygen-nitrogen mixtures. They did not, however, study individual bands in the spectrum of the afterglow. Although they were not concerned with measurement of the nitrogen afterglow intensity, the intensity values shown in table 34 can be deduced from fig.7 in their paper.

TABLE 34. AFTERGLOW INTENSITY I VS. OXYGEN. ANDERSON, KAVADAS AND McKAY.

$I^{-\frac{1}{2}}$ t = 0	I t = 0	Percentage Oxygen Added
0.01	100	0.01
0.03	33.3	0.03
0.06	16.7	0.05
0.08	12.5	0.12
0.11	9.1	0.2
0.16	6.3	0.30

In table 34, I = total afterglow intensity in arbitary units and t = time in seconds, the zero of time corresponding to the switching off of the discharge. From the values of I,

it can be seen that the percentage of oxygen needed to lower the afterglow intensity by a factor of ten is of the order of 0.1%. In the present experiments about the same amount of oxygen was needed to lower the intensity of individual afterglow bands by a factor of ten. It is of interest to note that, where a continuous flow of oxygen and nitrogen through a discharge is employed, up to 5% of oxygen is needed to reduce the afterglow intensity by a factor of ten, Berkowitz et al (1956) and Kuraweg et al (1957).

It can be seen from table 34 that $I^{-\frac{1}{2}}$ increases less rapidly with added oxygen than the $(\text{nitric oxide afterglow intensity})^{-\frac{1}{2}}$ in the present experiments (Table 31). However, in Anderson's experiment the decay of the afterglow intensity with time was mainly due to the recombination of nitrogen atoms for the first 20 seconds or so; also the logarithmic decay constant (corresponding to $B_{N_2} = 2B_{1W}$ in the present experiments) decreased slightly with added oxygen. Thus the slower decrease of $I^{-\frac{1}{2}}$ with oxygen can readily be explained in terms of eq.32 $I_{N_2} = \dfrac{B_1 MS^2}{(B_{1W} + 2B_{13}n_3 + B_1 Mn_1)^2}$

Although the term $2B_{13}n_3$ was increasing, B_{1W} and $B_1 Mn_1$ were decreasing; and so $I^{-\frac{1}{2}} \equiv I_{N_2}^{-\frac{1}{2}}$ increased more slowly.

6.3 Rate of Combination of Nitrogen and Oxygen Atoms.

B_{12} is the total rate constant for the reactions $N + O + M \rightarrow NO^* + M$ and $NO^* \rightarrow NO + h\nu$ (β, γ). According to eq.22 (6.2.1)

$I_{NO} = \dfrac{2B_{12}B_{13}I_{N_2}n_3}{B_{2W}B_1}$ and since $I_{N_2} = B_1 Mn_1^2$ (eq.1) then

$$I_{NO} = \frac{2B_{12}MB_{13}n_1^2 n_3}{B_{2W}} . \qquad \text{Thus } B_{12} = \frac{I_{NO}B_{2W}}{2MB_{13}n_1^2 n_3} . \tag{33}$$

Also from 4.4 we have $I_{NO} = 0.1\ K_{5000}\ I_{2363}$, and from 4.5 we have $n_1^2 = 1.72 \times 10^{15}\ K_{5000}\ I_{5755}$ atom^{2}cc^{-2}.

Substituting in eq.33 we have

$$B_{12} = \frac{0.1\ I_{2363}\ B_{2W}}{1.72 \times 10^{15} MB_{13}^2\ I_{5755} n_3}$$

$$= \frac{10^{13}\ I_{2363}\ B_{2W}}{2\ I_{5755}\ n_3} \times \frac{0.1}{1.72 \times 10^{28}\ MB_{13}} \tag{34}$$

Values of $B_{2363} = \frac{10^{13}\ Ip_{2363}\ B_{2W}}{2\ Ip_{5755}\ n_3}$ (eq.24)

are shown in table 29. According to the theory (6.2.1), B_{2363} is independent of the amount of oxygen added to the system, and this is supported by the values of B_{2363} in table 29. Since we are assuming that $Ip_{2363} = I_{2363}$ in this discussion, we have from eq.24 and eq.34

$$B_{12} = \frac{B_{2363} \times 0.1}{MB_{13} \times 1.72 \times 10^{28}} \qquad cc^2 mol^{-2} sec^{-1}$$

$\overline{B}_{2363} = 0.16$ (Table 29)

$B_{13} = 1.4 \times 10^{-15}$ mol^{-1}cc sec^{-1} (6.4)

$M = 4.06 \times 10^{16}$ molecules cc^{-1} (4.5)

Thus

$$B_{12} = \frac{0.16 \times 0.1}{4.06 \times 10^{16} \times 1.4 \times 10^{-15} \times 1.32 \times 10^{28}}$$

$$B_{12} = 1.58 \times 10^{-32}\ cc^2\ mol^{-2} sec^{-1}$$

We have from (4.4) that

$$I_{NO} = 0.12\, K_{5000}\, I_{2890}$$

$$\bar{B}_{2890} = 0.1 \qquad \text{(Table 29)}$$

Substituting in (33) for I_{NO} in terms of I_{2890}.

$$B_{12} = \frac{B_{2890} \times 0.12}{MB_{13} \times 1.72 \times 10^{28}}$$

$$= \frac{B_{2363} \times 0.1}{MB_{13} \times 1.72 \times 10^{28}} \times \frac{B_{2890}}{B_{2363}} \times \frac{0.12}{0.1}$$

$$= 1.58 \times 10^{-32} \times \frac{0.1}{0.16} \times \frac{0.12}{0.1}$$

$$= \underline{1.28 \times 10^{-32}\ cc^2 mol^{-2} sec^{-1}}.$$

We have from (4.4) that

$$I_{NO} = 0.2\ K_{5000}\ I_{3200}$$

$$\bar{B}_{3200} = 0.05 \qquad \text{(Table 29)}$$

Thus adjusting the value of R.H.S. of (34) as above

$$B_{12} = 1.58 \times 10^{-32} \times \frac{0.05}{0.16} \times \frac{0.2}{0.1}$$

$$= \underline{1.06 \times 10^{-32}\ cc^2 mol^{-2} sec^{-1}}.$$

The mean value of $B_{12} = 1.3 \times 10^{-32}\ cc^2 mol^{-2} sec^{-1}$.

According to P. Harteck, R. Reeves and G. Mannella (1958), $B_{12} = 3 \times 10^{-32}\ cc^2 molecules^{-2} sec^{-1}$, no details being given. However according to Kaufman (p.30 'Progress in Reaction Kinetics', Pergamon Press, 1961) the same authors have since measured a value $5 \times 10^{-33}\ cc^2 mol^{-2} sec^{-1}$ for B_{12}. The mean value of B_{12} calculated above is in fair agreement with the values of Harteck et al.

6.4 Comparison of the Rates of Gas Phase and Wall Processes.

It has been assumed in the foregoing discussion, that the dominant processes of removal of atoms in the present experiment were attachment of nitrogen and oxygen atoms to the walls of the system

	Atom Removal Rate Atoms $cc^{-1} sec^{-1}$
$N + Wall \rightarrow \frac{1}{2}N_2 + Wall$	$B_{1W} n_1$
$O + Wall \rightarrow \frac{1}{2}O_2 + Wall$	$B_{2W} n_2$;

and also removal of nitrogen atoms by reaction with oxygen molecules, and nitric oxide molecules

	Atom Removal Rate Atoms $cc^{-1} sec^{-1}$
$N + O_2 \rightarrow NO + O$ $N + NO \rightarrow N_2 + O$	$2B_{13} n_1 n_3$

The effect of recombination of nitrogen atoms

	Atom Removal Rate Atoms $cc^{-1} sec^{-1}$
$N + N + M \rightarrow N_2^{**} + M$ $N_2^{**} + M \rightarrow N_2^{*} + M$ $N_2^{*} \rightarrow N_2 + h\nu$	$B_1 n_1^2$

and combination of nitrogen and oxygen atoms

	Atom Removal Rate Atoms $cc^{-1} sec^{-1}$
$N + O + M \rightarrow NO^{*} + M$ $NO^{*} \rightarrow NO + h\nu \ (\beta, \gamma)$	$B_{12} n_1 n_2$

was neglected.

When all the above processes are assumed to be important, the initial integrated intensity of the nitric oxide afterglow is according to eq.10

$$I_{NO} = \frac{2B_{12}B_{13}n_3\delta^2_M}{(B_{2W} + B_{12}M n_1)\,(B_{1W} + 2B_{13}n_3 + B_{12}M n_2 + B_1 M n_1)^2}$$

If the processes of atomic recombination and combination are neglected, i.e. if it is assumed that $B_{2W} >> B_{12}M n_1$ and $(B_{1W} + 2B_{13}n_3) >> B_{12}M n_2 + B_1 M n_1$, then

$$I_{NO} = \frac{2B_{12}B_{13}n_3\delta^2_M}{B_{2W}\,(B_{1W} + 2B_{13}n_3)^2} \qquad \text{(eq.11)}.$$

We now consider the ratio of B_{2W} to $B_{12}M n_1$ and $(B_{1W} + 2B_{13}n_3)$ to $(B_{12}M n_2 + B_1 M n_1)$. It is necessary to calculate the value of n_2 first of all.

The data in table 35 are typical values of the quantities measured in the present experiments. According to eq.7 the oxygen atom concentration is given by $n_2 = \frac{2B_{13}n_3n_1}{(B_{2W} + B_{12}M n_1)}$

and this is simplified to $n_2 = \frac{2B_{13}n_3n_1}{B_{2W}}$

according to the approximations mentioned above. Thus using the data in table 35 and 36

$$n_2 = \frac{2 \times 1.75 \times 10^{-15} \times 3 \times 10^{13} \times 10^{14}}{0.4} = 2.6 \times 10^{13}\ cc^{-1}$$

and $B_{12}M n_2 \sim 0.014\ sec^{-1}$.

TABLE 35. CORRESPONDING VALUES OF VARIOUS PARAMETERS.

Number of Oxygen Molecules Added $cc^{-1} = n_3$	I_{p5755} Chart Divs. (R_2)	Nitrogen atom concentration n_1 atoms cc^{-1}	Oxygen Atom Wall decay Rate constant B_{2W} sec^{-1}	$B_{13} mol^{-1} cc\ sec^{-1}$
3×10^{13}	~ 10	$\sim 10^{14}$	~ 0.4	Mean value 1.75×10^{-15} for $n_3 = 3 \times 10^{13}$, 4×10^{13} cc^{-1}
Reference	TABLE 5	(4.5)	TABLE 28	TABLE 32

From table 36, $B_{12}Mn_1 \sim 0.035$ sec^{-1}. This value is of the order of magnitude of the smallest values of B_{2W}, but is small compared with the total decay constant B_{NO} of the nitric oxide afterglow bands; and would not introduce appreciable curvature into the log (afterglow intensity) versus time curves. The values of B_{2W} and $B_{12}Mn_1$ are thus consistent with the assumption used in the discussion in chapters 5 and 6. The measured values of B_{2W} (Table 28) are a measure of the rate constant for removal of oxygen atoms by all contributing processes, so that these values of B_{2W} would include the term $B_{12}Mn_1$ averaged over the duration of the afterglow.

We now consider the ratio of $(B_{1W} + 2B_{13}n_3)$ to $(B_{12}Mn_2 + B_1Mn_1)$. From table 36 we have $B_{12}Mn_2 + B_1Mn_1 = 0.11$ sec^{-1}. Also we have $B_{1W} + 2B_{13}n_3 \sim 0.5$ sec^{-1}. These values are also consistent with the assumption made in chapters 5 and 6. In (6.2.2) values of B_{13} were calculated and it was found that B_{13} appeared to vary with oxygen

TABLE 36. CORRESPONDING VALUES OF VARIOUS PARAMETERS.

	B_{12} $cc^2 mol^{-2} sec^{-1}$	Nitrogen Molecule Concentration M cc^{-1}	Nitrogen Atom Concentration n_1 cc^{-1}	$B_{12}Mn_1$ sec^{-1}	$B_{12}Mn_2$ sec^{-1}	B_1Mn_1 sec^{-1}	B_{13} $mol^{-1} cc\ sec^{-1}$	$2B_{13}n_3$ sec^{-1}	B_{1W} sec^{-1}	B_{2W} sec^{-1}	Number of Oxygen Molecules Added cc^{-1}
	1.3×10^{-32}	4.06×10^{16}	5×10^{13} to 2×10^{14}	$\sim$ 0.035	0.014	0.1	1.75×10^{-15}	0.105	$\sim$ 0.4	$\sim$ 0.4	3×10^{13}
Reference	6.3	4.5	4.5			4.5	TABLE 32 and 6.2.4		TABLE 27	TABLE 27	

added. It is consistent with the theory to postulate that, since the denominator of I_{NO} was simplified from $B_{2W}(B_{1W} + 2B_{13}n_3 + B_{12}Mn_2 + B_1Mn_1)^2$ to $B_{2W}(B_{1W} + 2B_{13}n_3)^2$, the apparent values of B_{13} are equal to $\left(B_{13} + \frac{B_{12}Mn_2 + B_1Mn_1}{2n_3}\right)$.

Using the data in table 36 and the lower limit for n_1 $\frac{B_{12}Mn_2 + B_1Mn_1}{2n_3} \sim 10^{-15}$. This is about half the value of B_{13} calculated for an oxygen concentration of 3×10^{13} molecules cc^{-1} sec^{-1}. This supports the view that the term $\frac{B_1Mn_1}{2n_3}$ contributed to the apparent values of B_{13} shown in table 32, and that the true value of B_{13} in the glow discharge lies between 1.75×10^{-15} mol^{-1} cc sec^{-1} and 10^{-15} mol^{-1} cc sec^{-1}. Thus $B_{13} = (1.4 \pm 0.3) \times 10^{-15}$ mol^{-1} cc sec^{-1}. That is the rate of removal of nitrogen atoms by three body recombinations $N + N + M \rightarrow N_2^{**} + M$ was comparable with the rate of removal of nitrogen atoms by $N + O_2 \rightarrow NO + O$ for oxygen concentrations $\simeq$ 3×10^{13} molecules cc^{-1}.

6.5 The Accuracy of the Rate Constant for Combination of Nitrogen and Oxygen Atoms.

B_{12} is the rate constant for combination of nitrogen and oxygen atoms calculated in 6.3. Substituting $I_{NO} = 0.2\ K_{5000}\ I_{3200}$ (4.4) and $n_1^2 = 1.72 \times 10^{15}\ K_{5000}\ I_{5755}$ (4.5) in eq.33 we have

$$B_{12} = \frac{0.2\ I_{3200}\ B_{2W}}{1.72 \times 10^{15}\ I_{5755}\ 2MB_{13}n_3} \qquad (35)$$

According to H.J.J. Braddick 'The Physics of Experimental Method', p.21, the square of the percentage error of a product is the sum of the squares of the percentage errors of the factors, where the errors are random errors. Let the percentage error in B_{12} = ΔB_{12}. We now consider the errors in the individual factors in the expression 35.

ΔI_{3200}

The values of I_{p3200} used in calculating B_{12} were ~15 chart divisions (R_2). According to the discussion of 4.1, I_{p3200} ~10% less than I_{3200}.

Δ 0.2

The error in the factor 0.2 from I_{NO} = 0.2 K_{5000} I_{3200} is from (4.4) ~ ± 25%.

ΔB_{2W}

B_{2W} was measured from the gradients of straight line graphs. Since B_{2W} was included in B_{3200}, and the mean value of B_{3200} was used (Table 30) to calculate B_{12}, then effectively the mean of three values of B_{2W} was used. The error in this quantity is probably not more than ± 15%.

Δ M

The total pressure in the vacuum system could be read to about ± 5%, thus the error in M is ± 5%.

ΔB_{13}

The value of B_{13} used to calculate B_{12} was the value 1.4×10^{-15} mol^{-1} cc sec^{-1} .

According to the discussion of 6.4 the true value of B_{13} is probably about $(1.4 \pm 0.3) \times 10^{-15}$ $mol^{-1} cc\ sec^{-1}$, i.e. there is a $\pm$ 20% uncertainty in B_{13}.

ΔI_{5755}

As in the case of I_{3200} the value of Ip_{5755} used to calculate B_{12} may be 10% less than I_{5755}.

$\Delta 1.72$

According to Harteck et al (1958) there is a 10% error in the value of B_1 which gives a 10% error in the factor 1.72×10^{15} (see 4.5).

Any further error in 1.72×10^{15} cannot be estimated but is not likely to be large.

Δn_3

The mean of 3 values of n_3 was used to calculate B_{12}. The error in n_3 is not likely to be more than $\pm$ 10%.

Using the information from 'The Physics of Experimental Method' we have,

$$\Delta^2 B_{12} = \Delta^2 0.2 + \Delta^2 B_{2W} + \Delta^2 M + \Delta^2 B_{13} + \Delta^2 1.72 + \Delta^2 n_3$$

Substituting in the percentage errors of the individual quantities involved in B_{12} we have $\Delta^2 B_{12} = 625 + 225 + 25 + 400 + 100 + 100$. The errors in I_{3200} and I_{5755} should cancel out. Thus $\Delta B_{12} = \pm 40\%$.

Since $\bar{B}_{12} = 1.3 \times 10^{-32}$ $cc^2\ mol^{-2}\ sec^{-1}$,

$B_{12} = (1.3 \pm 0.5) \times 10^{-32}$ $cc^2 mol^{-2} sec^{-1}$.

CONCLUSIONS

The afterglow of an R.F. discharge through nitrogen at a pressure of about 1 mm Hg has been investigated. Up to 0.15% of oxygen was added to the nitrogen; and the effect on the nitric oxide afterglow β and γ bands and nitrogen afterglow 1st positive bands studied.

It is concluded that there is no change in the relative afterglow intensities of the $v^1 = 0$, β and γ bands of nitric oxide, when up to 0.15% of oxygen is added to the nitrogen.

For a given percentage of oxygen, the afterglow intensities of the $v^1 = 0$, β and γ nitric oxidebands decay with time in the same manner. $-\frac{d \log I_t}{dt}$ is (15 ± 5)% greater for $v^1=0$, γ nitric oxide bands than for $v^1 = 0$, β nitric oxide bands, where I_t is the afterglow intensity at time t, though it is possible that the observed difference was due to a change in the condition of the discharge tube walls between one measurement and another, e.g. adsorption or desorption of oxygen by the walls. Scatter ~ 5% in the observed values of $-\frac{d \log I_t}{dt}$ for the γ (0,1), β (0,6) and β (0,8) nitric oxide bands in two particular runs may have been due to a more erratic variation in the condition of the discharge tube walls. In general the decay rate of the intensity of the nitric oxide afterglow bands differs from that of the nitrogen afterglow bands. $-\frac{d \log I_t}{dt}$ = constant independent of time for all observed bands in these experiments, thus it is concluded that the active particles giving rise to the afterglow were removed mainly by attachment to the walls.

Two sources of excitation of nitric oxide β and γ bands were considered to be present in the R.F. glow discharge; electronic excitation of nitric oxide molecules, and the excitation which gave rise to the nitric oxide afterglow. It is concluded from the relationship of the initial intensity of a β or γ afterglow band of nitric oxide, to; the initial intensity of a nitrogen 1st positive afterglow band, the decay rate of the given nitric oxide band, the decay rate of the nitrogen 1st positive band, and the amount of oxygen added that the source of the nitric oxide afterglow is a combination of nitrogen and oxygen atoms in collision with a third inactive particle,

$$N + O + M \rightarrow NO^{*} + M$$

$$NO^{*} \rightarrow NO + h\nu \quad (\beta, \gamma)$$

in agreement with the currently accepted mechanism. The rate constant for the combination of oxygen and nitrogen atoms

$B_{12} = (1.3 \pm 0.5) \times 10^{-32}$ cc^{2}mol^{-2}sec^{-1}. This is in fair agreement with the value 5×10^{-33} cc^{2}mol^{-2}sec^{-1} obtained by P. Harteck et al (Progress in Reaction Kinetics, Pergamon Press, 1961). Nitrogen atoms were produced by dissociation of nitrogen molecules in the glow discharge about 0.1% of the molecules being dissociated according to a calibration of the recording system; and oxygen atoms were produced in the glow discharge, and the afterglow by the reactions

$$N + O_2 \rightarrow NO + O$$

$$N + NO \rightarrow N_2 + O$$

as proposed by Kaufman (1958). The removal of nitrogen atoms by the above reactions is the cause of the decrease of the initial intensity

of the nitric oxide and nitrogen afterglows, when the oxygen percentage is increased. The rate constant B_{13} for the reaction $N + O_2 \rightarrow NO + O$ was $(1.4 \pm 0.3) \times 10^{-15}$ $mol^{-1}cc\ sec^{-1}$ in the glow discharge.

In the afterglow $B_{13} \sim 2 \times 10^{-16}$ $mol^{-1}cc\ sec^{-1}$, which agrees with the value of 2×10^{-16} $mol^{-1}cc\ sec^{-1}$ calculated for a temperature of about 20°C from the formula given by Kistiakowsky (1957).

On the basis of the currently accepted mechanism of the nitric oxide afterglow, and other reactions and wall processes; it is concluded that the integrated intensity of the nitric oxide afterglow is given by

$$I_{NO} = \frac{2B_{12}B_{13}n_3S^2M}{(B_{2W} + B_{12}Mn_1)(B_{1W} + 2B_{13}n_3 + B_{12}Mn_2 + B_1Mn_1)^2}$$

I_{NO} is the integrated intensity of the nitric oxide afterglow, when the electronic excitation of nitric oxide bands has just decayed to zero, which it does in less than 0.1 seconds. n_3 = number of oxygen molecules per cc, n_1 = number of nitrogen atoms per cc, n_2 = number of oxygen atoms per cc; M is the total number of particles per cc and S is the rate of production of nitrogen atoms per cc in the preceding discharge. B_{2W} and B_{1W} are the rate constants for monoatomic wall attachment of oxygen and nitrogen atoms respectively and B_1 is the rate constant for the three body combination of nitrogen atoms. This equation is useful, where removal of atoms by attachment to the walls dominates removal by combination.

In the present experiments it was found that B_{2W} was proportional to n_3 the amount of oxygen added to the system. This suggests that

a proportion of the oxygen molecules adsorbed on the glass walls of the system was dissociated into atoms; and that the rate of attachment of oxygen atoms to the walls of the system was proportional to the concentration of oxygen atoms on the wall.

REFERENCES

Anderson J.M., Kavadas A.D., McKay R.W., Proc.Phys.Soc., 70A, 877, (1957).

Barth C.A., Schade W.J., Kaplan J., J.Chem.Phys., 30, 347, (1959).

Bayes K.D., and Kistiakowsky G.B., J.Chem.Phys., 32, 992, (1960).

Benson J.M., J.App.Phys., 23, 757, (1952).

Berkowitz J., Chupka W.A., Kistiakowsky G.B., J.Chem.Phys., 25, 457,(1956).

Bichowsky F.R., and Rossini F.D., Thermochemistry of chemical substances.

Bonhoeffer K.F., and Kaminsky G., Zeits.Electrochem., 32, 536, (1926).

Bromer H.H., Zeits.f.Physik., 158, 1, (1960).

Carlo G., and Kaplan J., Zeits.f.Physik, 58, 769, (1929).

Carlo G., and Reineke L.H., Abhandl. Braunschweig.Wiss.Gessel-schaften., 1, 8, (1949).

Easson L.H., and Armour R.W., Proc.Roy.Soc. Edinburgh., 48, 1, (1927-28).

Gaydon A.G., Proc.Phys.Soc., 56A, 160, (1944).

Gaydon A.G., Nature, 153, 407, (1944).

Gaydon A.G., Dissociation Energies, Chapman and Hall, London, (1953).

Harteck P., Reeves R., Mannella G., J.Chem.Phys., 29, 608, (1958).

Herbert W.S., Herzberg G., Mills G.A., J.Canad.Research, 15A, 35, (1937).

Hinshelwood C.N., Kinetics of chemical change, O.U.P., (1940).

Jackson D.S., and Schiff H.I., J.Chem.Phys., 23, 2333, (1955).

Kaplan J., Phys.Rev., 33, 189, (1929).

Kaplan J., Phys.Rev., 73, 494, (1948).

Kaufman F. and Kelso J.R., J.Chem.Phys., 27, 1209, (1957).

Kaufman F., J.Chem.Phys., 28, 992, (1958).

Kaufman F., and Kelso J.R., J.Chem.Phys., 32, 301, (1960).

Kistiakowsky G.B., and Volpi G.G., J.Chem.Phys., 27, 1141, (1957).

Knauss H.P., Phys.Rev., 32, 417, (1928).

Kneser H.O., Ann.d.Physik, 87.5, 717, (1928).

Kurzweg U.H., Bass A.M., Broida H.P., J.Mol.Spectroscopy., 1, 184, (1957).

Lewis P., J.Astrophys., 12, 8, (1900).

Mitra S.K., Active Nitrogen - a new theory, Assoc. for the Cult. of Science, Calcutta, (1945).

Morren, Ann.Chim.et Phys., 4, 293, (1865).

Pearse
~~Pierce~~ R.W.B., and Gaydon A.G., The Identification of Molecular Spectra.

Rayleigh,(Lord), Proc.Roy.Soc., 151A, 567, (1935).

Rayleigh,(Lord), Proc.Roy.Soc., 176A, 1, (1940).

Rayleigh,(Lord), Proc.Roy.Soc., 180A, 123, (1942).

Robinson D., and Nicholls R.W., The University of Western Ontario, Contract No.AF.19 (604) - 1718.

Strutt R.J., Proc.Roy.Soc., 85A, 219, (1911).

Strutt R.J., Proc.Roy.Soc., 86A, 105, (1912).

Strutt R.J., Proc.Roy.Soc., 91A, 303, (1915).

Strutt R.J., Proc.Roy.Soc., 93A, 254, (1917).

Tanaka Y., J.Chem.Phys., 22, 2045, (1954).

Tanaka Y., Planetary and Space Science, 1, 7.13, (1959).

Tiede E., and Domke E., Ber Deutsch.Chem.Gessell., 46, 4095, (1913).

Tiede E., and Domke E., Ber.Deutsch.Chem.Gessell., 47, 420, (1914).

Vanderslice J.T., Mason E.A., Maisch W.G., J.Chem.Phys., 31, 738, (1959).

Van Der Zeil, Physica, 4, 373, (1937).

Willey R.J.B., Proc.Roy.Soc., 159A, 247, (1937).

Worley R.E., Phys.Rev., 73, 531, (1948).